

**Contribution of Particle Size and Moisture Content to Flowability of Fractionated  
Ground Loblolly Pine**

by

Oluwatosin Jerry Oginni

A thesis submitted to the Graduate Faculty of  
Auburn University  
in partial fulfillment of the  
requirements for the Degree of  
Master of Science

Auburn, Alabama  
August 2, 2014

Keywords: Loblolly pine, particle size, moisture content, physical and flow properties, fraction

Copyright 2014 by Oluwatosin Jerry Oginni

Approved by

Oladiran Fasina, Chair, Professor of Biosystems Engineering  
Sushil Adhikari, Associate Professor of Biosystems Engineering  
John Fulton, Associate Professor of Biosystems Engineering

## **Abstract**

The use of woody biomass requires feedstock materials in particulate form; therefore there is a need for size reduction of the feedstock materials. Ground biomass typically has a non-uniform particle size and as a biological material, biomass will exchange moisture with the environment. Thus, ground biomass feedstock will have typical flow problems associated with bulk materials during storage. The objective of this research is to investigate the contribution of particle size and moisture content to flowability of fractionated ground loblolly pine. In this study, ground loblolly pines were fractionated into six size classes at five moisture content levels. The physical and flow characteristics of the fractionated samples that are related to flowability and design of the storage vessels were quantified. The geometric mean diameters for the fractions were in the range 0.10 - 2.38 mm. Bulk and tap densities of the fractions increased with fraction size but particle density was not affected by fraction size. The densities (bulk, particle and tap) decreased with increase in moisture content. Porosity, Hausner ratio and compressibility increased with increase in moisture content and reduction in fraction size. The flowability of the fractions decreased with decrease in fraction size and increase in moisture content. Flow index values of 4.11, 4.17 and 4.29 were recorded for 1.40 mm fractions at moisture levels of 4.78%, 8.69% and 16.53%, respectively which implies easy flowing. However, a reduction in flowability from easy flowing to cohesive flowing was observed when 1.40 mm fractions were dosed with 0.50 mm fractions at 10:1, 10:2 and 10:3 mass ratio respectively. Cohesive strength and angle of internal friction decreased with increase in fraction size. Moisture content caused an increase in angle of internal friction but had no significant

effect on the cohesive strength of the fractions. Particle size and moisture content had a significant effect on the angle of wall friction of the fractions. There was a reduction in wall friction angle with increase in fraction size. Lower wall friction angles were obtained at lower moisture content when stainless and mild steel surfaces were used while Tivar 88 surface had a consistent low angle of wall friction at all moisture levels. The adjusted hopper outlet size varied between 1.20 and 28.56 mm with 1.40mm fraction having the highest minimum hopper outlet size. The wall normal and vertical pressure acting on the cylindrical section of the silo increased from 9.35 to 45.42 kPa and 15.34 to 48.91 kPa, respectively with increase in fraction size and decrease in moisture content. The initial fill and flow induced pressures acting on the hopper section of the silo increased from 15.34 to 48.91 kPa and 24.71 to 78.79 kPa, respectively with increase in fraction size and decrease in moisture content. The heating values (18-19 MJ/kg) and volatile matter (84.91 - 87.48% d.b) were not affected by the fraction size while ash content was found to increase with reduction in the fraction size.

## **Acknowledgments**

First of all, I thank God for his strength and grace on my life to successfully complete this research work. I would like to express my sincere gratitude to my academic advisor, Dr Oladiran Fasina for the opportunity he gave me to learn from his vast wealth of knowledge and experience in this research area and to earn my degree. I appreciate his patience and professional advice during the course of the program. My appreciation also goes to my committee members, Dr Sushil Adhikari and Dr John Fulton for the professional support and knowledge they gave during the research work. I would like to acknowledge Alabama Agricultural Experiment Station, Department of Energy (DOE), Southeastern Partnership for Integrated Biomass Supply Systems (IBSS) and National Institute of Food and Agriculture for the provision of research fund. In addition, I would like to appreciate Dr. Sunday Ogunsina and Mr Gbenga Olatunde for all their academic and moral supports.

My appreciation goes to my parents, Mr and Mrs Oginni for all the encouragement and prayers they offered throughout the course of my master's program. Many thanks to my siblings Ayo and his wife Bukola, Titi, Mayowa, Tolulope for the moral supports I got from them. To all my families and friends back in Nigeria, thank you all.

To all the group members under Dr Fasina; Anshu, Gurdeep, Jaskaran, Gbenga, Ujjain and Oluwafemi, I appreciate the time we spent working together. Thanks to all my Auburn friends and family for the time we had together.

## Table of Contents

Abstract .....	ii
Acknowledgments .....	iv
List of Figures .....	viii
List of Tables .....	x
Chapter 1 Introduction.....	1
Chapter 2 Literature review .....	4
2.1 Biomass: A Source of Renewable Energy.....	4
2.2 Biomass Supply Logistics .....	6
2.3 Size reduction and particle size .....	7
2.4 Flow patterns and flow problems.....	10
2.5 Physical Properties .....	14
2.5.1 Bulk density .....	14
2.5.2 Particle density .....	16
2.5.3 Porosity .....	18
2.5.4 Compressibility .....	19
2.5.5 Hausner ratio .....	21
2.6 Flow Properties .....	23
2.6.1 Cohesion .....	25
2.6.2 Angle of wall friction .....	27
2.6.3 Flow function and index .....	28
2.6.4 Design of hopper for flow .....	30
Summary .....	33
Chapter 3 Particle Size and Moisture Effect on Physical of Fractionated Ground Loblolly Pine	34
3.1. Abstract .....	34
3.2. Introduction .....	35
3.3. Materials and Methods .....	37

3.3.1	Sample preparation and fractionation .....	37
3.3.2	Particle size distribution .....	38
3.3.3	Bulk density .....	39
3.3.4	Particle density .....	39
3.3.5	Tap density, compressibility and hausner ratio .....	40
3.3.6	Composition and energy determination .....	41
3.3.6.1	Sample preparation .....	41
3.3.6.2	Energy content .....	41
3.3.6.3	Ash content .....	41
3.3.6.4	Volatile matter .....	42
3.3.7	Experimental design and statistical analysis .....	43
3.4	Results and Discussion .....	43
3.4.1	Particle size distribution .....	43
3.4.2	Bulk density .....	49
3.4.3	Tap density.....	51
3.4.4	Hausner ratio.....	53
3.4.5	Compressibility .....	54
3.4.6	Particle density .....	56
3.4.7	Porosity.....	57
3.4.8	Compositional analysis.....	59
3.4.8.1	Energy content.....	59
3.4.8.2	Ash content .....	60
3.4.8.3	Volatile matter .....	61
3.5	Conclusion .....	62
Chapter 4 Sensitivity of Hopper Design Paramter to Measured Physical and Flow Properties of Fractionated Ground Loblolly Pine .....		64
4.1	Abstract.....	65
4.2	Introduction .....	65
4.3	Materials and Methods .....	67
4.3.1	Sample preparation.....	67
4.3.2	Flow properties .....	67

4.3.3	Wall friction properties .....	69
4.3.4	Hopper design calculation .....	69
4.3.4.1	Hopper half angle .....	69
4.3.4.2	Minimum hopper outlet size .....	69
4.3.4.3	Silo wall loads .....	70
4.3.5	Experimental design and statistical analysis .....	72
4.4	Results and Discussion .....	73
4.4.1	Flow classification of fractionated ground loblolly pine .....	71
4.4.2	Angle of internal friction .....	78
4.4.3	Cohesive strength.....	79
4.4.4	Wall friction properties.....	80
4.4.5	Hopper half angle and minimum discharge outlet size .....	85
4.4.6	Silo wall loads .....	90
4.5	Conclusion .....	95
Chapter 5	Summary and Recommendation .....	96
5.1	Summary .....	96
5.2	Recommendation .....	97
References.	.....	99
Appendix A.....	.....	112
Appendix B: SAS codes for statistical analysis.....	.....	123

## List of Figures

Figure 1.1 Hammer rash on bins with flow problems.....	2
Figure 2.1 Flow chart of biomass supply logistics .....	7
Figure 2.2 Types of flow patterns in storage vessel: (a) Funnel flow; (b) Mass flow .....	11
Figure 2.3 Typical flow problems associated with bulk solids.....	12
Figure 2.4 Jenike shear cell.....	24
Figure 2.5 Typical plot of yield locus .....	25
Figure 2.6 Flow function: easy versus difficult flow .....	29
Figure 2.7 Hopper design chart for a conical hopper based on the Jenike's theory .....	32
Figure 2.8 Evaluation of critical applied stress.....	32
Figure 3.1 Particle size distribution of unfractionated loblolly pine fractions .....	44
Figure 3.2a Particle size distribution of fractionated loblolly pine at 4.78% moisture level.....	45
Figure 3.2b Particle size distribution of fractionated loblolly pine at 8.69% moisture level .....	45
Figure 3.2c Particle size distribution of fractionated loblolly pine at 16.53% moisture level.....	46
Figure 3.2d Particle size distribution of fractionated loblolly pine at 22.21% moisture level .....	46
Figure 3.2e Particle size distribution of fractionated loblolly pine at 25.53% moisture level.....	47
Figure 3.2f Particle size distribution of fractions retained on screen size 0.05mm .....	47
Figure 3.3 Particle size effect on energy content of fractionated loblolly pine .....	60
Figure 3.4 Particle size effect on ash content of fractionated loblolly pine.....	61
Figure 3.5 Particle size effect on volatile matter of fractionated loblolly pine.....	62
Figure 4.1 Typical flow problems associated with bulk solids.....	65
Figure 4.2: Powder flow tester and accessories .....	68
Figure 4.3 Silo subdivision into vertical and hopper section.....	71
Figure 4.4 Initial fill and flow induced pressure on hopper section of a silo .....	72
Figure 4.5a Flow function of fractionated loblolly pine at 4.78% moisture content.....	73



Figure 4.5b Flow function of fractionated loblolly pine at 8.69% moisture content.....	74
Figure 4.5c Flow function of fractionated loblolly pine at 16.53% moisture content.....	74
Figure 4.5d Flow function of fractionated loblolly pine at 22.21% moisture content.....	75
Figure 4.5e Flow function of fractionated loblolly pine at 25.53% moisture content .....	75
Figure 4.6 SEM images of stainless steel, mild steel and tivar 88 wall surfaces .....	84
Figure 4.7 Effect of moisture content on hopper angle of 0.25mm fraction.....	87
Figure 4.8 Effect of fraction size on hopper half angle at 4.78% moisture level.....	87
Figure 4.9 Plot of wall friction angles and hopper half angle of ground loblolly pine.....	88
Figure 4.10 Flow function and flow factor of fraction size 0.25mm at 8.69 % moisture content..	89
Figure 4.11 Effect of moisture content on pressures acting on silo wall for 0.25 mm fraction .....	92
Figure 4.12 Effect of particle size on pressures acting on the cylindrical and hopper section of the silo wall .....	92
Figure 4.13 Plot of vertical and wall pressure against cylindrical height for 0.05 mm fraction at 4.78 % moisture level .....	93
Figure 4.14 Plot of initial and flow induced loads against hopper height for 0.05 mm fraction at 4.78 % moisture level.....	93

## List of Tables

Table 2.1 Flowability classification of bulk solids based on mechanical compressibility.....	20
Table 2.2 Flowability classification using Hausner ratio .....	22
Table 2.3 Jenike classification of powder flowability by flow index (ffc) .....	28
Table 3.1 Geometric mean diameters of fractionated ground loblolly pine .....	49
Table 3.2 Bulk density ( $\text{kg/m}^3$ ) of fractionated ground loblolly pine .....	50
Table 3.3 Tap density ( $\text{kg/m}^3$ ) of fractionated ground loblolly pine .....	52
Table 3.4 Hausner ratio of fractionated ground loblolly pine .....	54
Table 3.5 Compressibility of fractionated ground loblolly pine .....	55
Table 3.6 Particle density ( $\text{kg/m}^3$ ) of fractionated ground loblolly pine .....	57
Table 3.7 Porosity of fractionated ground loblolly pine .....	59
Table 4.1 Jenike classification of powder flowability by flow index (ffc).....	76
Table 4.2 Flow classification of fractionated ground loblolly pine.....	76
Table 4.3 Flow indices of mixture of 1.40mm and 0.50mm fractions.....	77
Table 4.4 Angle of internal friction of fractionated loblolly pine.....	78
Table 4.5 Cohesive strength (kPa) of fractionated ground loblolly pine.....	80
Table 4.6 Angle of wall friction of fractionated ground loblolly pine using stainless steel wall...81	
Table 4.7 Angle of wall friction of fractionated ground loblolly pine using mild steel wall.....82	
Table 4.8 Angle of wall friction of fractionated ground loblolly pine using Tivar 88 wall .....	83
Table 4.9 Evaluation of hopper half angle, flow factor and hopper opening diameter ( $D_{\min}$ ) for a cylindrical hopper using Jenike's method .....	86
Table 4.10 Silo wall loads of fractionated ground loblolly pine.....	91
Table A.1 Symbols and Nomenclatures .....	112
Table B.1: ANOVA result of particle size and moisture effect on particle density of fractionated ground loblolly pine.....	113
Table B.2: ANOVA result of particle size and moisture effect on bulk density of fractionated ground loblolly pine .....	113
Table B.3: ANOVA result of particle size and moisture effect on tap density of fractionated ground loblolly pine.....	114

Table B.4: ANOVA result of particle size and moisture effect on compressibility of fractionated ground loblolly pine .....	114
Table B.5: ANOVA result of particle size and moisture effect on Hausner ratio of fractionated ground loblolly pine .....	115
Table B.6: ANOVA result of particle size and moisture effect on porosity of fractionated ground loblolly pine .....	115
Table B.7: ANOVA result of particle size and moisture effect on angle of internal friction of fractionated ground loblolly pine .....	116
Table B.8: ANOVA result of particle size and moisture effect on cohesion of fractionated ground loblolly pine .....	116
Table B.9-1: ANOVA result of particle size and moisture effect on angle of wall friction of fractionated ground loblolly pine using stainless steel .....	117
Table B.9-2: ANOVA result of particle size and moisture effect on angle of wall friction of fractionated ground loblolly pine using mild steel .....	117
Table B.9-3: ANOVA result of particle size and moisture effect on angle of wall friction of fractionated ground loblolly pine using Tivar 88 surface .....	118
Table B.10: ANOVA result of particle size effect on volatile matter (% db) of fractionated ground loblolly pine .....	118
Table B.11: ANOVA result of particle size effect on energy content of fractionated ground loblolly pine .....	119
Table B.12: ANOVA result of particle size effect on ash content (% db) of fractionated ground loblolly pine .....	119
Table B.13 Effect of wall surface on angle of wall friction at 4.78% moisture level .....	120
Table B.14 Effect of wall surface on angle of wall friction at 8.69% moisture level.....	120
Table B.15 Effect of wall surface on angle of wall friction at 16.53% moisture level.....	121
Table B.16 Effect of wall surface on angle of wall friction at 22.21% moisture level.....	121
Table B.17 Effect of wall surface on angle of wall friction at 25.53% moisture level.....	122

## **Chapter 1**

### **Introduction**

Almost every manufactured product passes through a powder, granular or particulate phase in its manufacturing cycle which means that a large quantity of these materials are processed, handled, stored and conveyed in bulk. The size range of these bulk materials varies from sub-micron sizes to sizes as large as 3 – 6 mm diameter. The selection and implementation of suitable handling systems for these materials is therefore important and crucial to efficiency and cost of processing. Low cost automation, efficiency of handling, reliability of equipment, installed and operating costs, clean operating environment, suitability of equipment to handle the required materials and best available technology are factors that influence the design and selection of storage and handling equipment (Velan, 2012).

Ineffective and unreliable handling systems contribute to processing plant startup delays, process inefficiencies and equipment downtime. The extent of this was confirmed in a six-year study by the Rand Corp. of 40 solids processing plants in the U.S. and Canada (Morrow, 1988). The findings revealed that 80% of all plants studied experienced bulk solids handling problems. Also, the affected facilities were slow in coming up to speed, with an average startup time for some types (raw, unprocessed solids feedstock) approaching 18 months. Once startup began, poor performance continued to affect these operations with capacity ranging between 40% and 50% of design values (Purutyan et al., 2001).

Inconsistent or no flow of bulk materials from storage equipment is one of the problems associated with bulk solid handling. Bulk materials form an arch or rat-hole inside the storage

vessel, preventing discharge and requiring the action of hammering, vibration, aeration or other methods to promote flow. This results in hopper damage from hammering, popularly known as hammer rash (Figure 1.1). The flow interruptions give rise to production difficulties and inefficiencies, including operators diverting from the main tasks to hammering of storage vessels. Hammering leads to safety and health issues such as noise, hand injuries and back strain (Bradley et al., 2011).



**Figure 1.1: Hammer rash on bins with flow problems (Source: Bradley et al., 2011).**

Therefore to ensure successful processing operations and enhance production rate in these industries, a consistent and reliable flow of bulk materials from storage equipment without flow obstruction, excessive spillage or dust generation is required (Fitzpatrick et al., 2004). The design of storage hoppers and bins for reliable flow requires information on flow properties of the stored material. The flow properties are also needed in handling and processing operations (Knowlton et al., 1994; Peleg, 1977). Bulk material properties that influence flow or flowability are termed flow properties. Some key factors that influence flow properties include moisture, particle size and shape (Fasina, 2006).

According to EISA (2007), over 1 billion dry tons of biomass is estimated to be produced annually from the abundant biomass resources in the United States. The biomass can be converted to liquid fuel - a sustainable replacement for fossil fuel. Biomass logistics often requires the use of storage equipment to hold feedstock for certain amount of time. Also, the use of biomass requires feedstock in particulate form. As a biological material, biomass will exchange moisture with the environment. These changes in particle size and moisture content of biomass will influence biomass flow behavior during discharge out of storage equipment and structures. Thus, biomass feedstock will have typical flow problems associated with bulk solid materials. Therefore, the use of this large quantity of biomass resources requires an effective design and selection of storage and handling system which will ensure consistent flow of the feedstock material for its intended use. Improper designs can results in biomass degradation, material loss, flow blockage and/or safety problems (Gil et al., 2013).

To our knowledge at the time of conducting this research, there is no reported study on the contribution of particle size and moisture to the flowability of fractionated ground loblolly pine. Therefore, the main objective of this study was to investigate the contribution of particle size and moisture content to flowability of fractionated ground loblolly pine. The specific objectives of this study were to:

1. quantify the physical properties of fractionated ground loblolly pine and the effect of moisture content on these properties.
2. quantify the flow properties of fractionated ground loblolly pine and perform sensitivity analyses on the physical and flow properties in relation to silo design.

## **Chapter 2 Literature Review**

### **2.1 Biomass: A Source of Renewable Energy**

In recent years, there has been a continuous increase in energy demand due to technological development and industrialization but development of energy sources is not keeping pace with the spiraling consumption. The major energy supply is obtained from fossil fuels which, according to the US Energy Information Administration (2014), meet around 72% of U.S. energy demand and 87% of world energy demand. Fossil fuels are fuels formed by natural processes such as anaerobic decomposition of buried dead organisms and it primarily consist of coal, natural gas and petroleum (Saxena et al., 2009).

Due to the adverse environmental impacts, non-renewable and finite nature of fossil fuels, it becomes imperative to develop sustainable and environmental friendly energy sources which will reduce world's dependency on fossil fuels (Kirtay, 2011; Moriarty and Honnery, 2008; Guo et al., 2012). These energy sources are termed renewable energy sources (e.g. biomass, wind, solar and geothermal) because they are continuously replenished and therefore are abundant on earth. About 9% of the energy consumed (total of 97 quadrillion Btu energy) in United States was obtained from renewable resources in 2011 (EIA, 2013). In the spectrum of renewable energy sources, biomass is the only renewable carbon source which can be converted into carbon-based fuels that can then be substituted for fossil fuel (EIA, 2008; Ozbay et al., 2001). Biomass can be transformed into heat, power, transportation fuels and chemicals by two main pathways; thermochemical and biochemical conversion. The choice of the conversion technique depends on

factors such as amount and type of feedstock, desired form of energy, economic and environmental conditions (McKendry, 2002).

Biomass are organic materials that are plant or animal based including but not limited to dedicated energy crops, agricultural crops and trees, food, feed and fiber crop residues, aquatic plants, forestry and wood residues, agricultural wastes, bio-based segments of industrial and municipal wastes, processing by-products and other non-fossil organic materials (ASABE, 2011). It accounts for 10% of global primary energy consumption making it the largest primary source of renewable energy (OECD/IEA, 2010). In the United States, biomass contributes nearly 3.9 quads and accounts for more than 4% of total U.S. primary energy consumption (EIA, 2010).

The United States has abundant biomass resources and has continued to increase bioenergy production in order to reduce energy insecurity and environmental problems posed by the use of fossil fuel. Perlack and Stokes (2011) stated that the United States has the resources to produce over 1 billion dry tons of biomass annually which can be converted into 90 billion gallons of liquid fuels. This quantity can replace about 30% of the nation's current annual petroleum consumption. According to the Energy Independence and Security Act (2007), the goal is to increase the amount of renewable fuels used in the United States transportation sector from 2012 level of 15 billion gallons to 36 billion gallons by 2022. The mandate further stipulates that, of the 36 billion gallons of renewable fuel, the goal is to produce 21 billion gallons of advanced biofuels derived mainly from cellulosic feedstock. The cellulosic feedstock will be from forest resources and dedicated energy crops.

Woody biomass has been identified as a reliable and viable biomass source due to the abundant quantity of forest trees in United States. Forest trees are grown approximately on one third (749 million hectare) of the nation's total land (Simmons et al., 2008). On a national basis,



forest lands in the contiguous United States are estimated to produce 370 million dry tons of woody biomass annually on a sustainable basis. The current discussion of using woody biomass continues a long history of relying on wood for energy production, both in the United States and in the world (White, 2010; Perlack and Stokes, 2011). Loblolly pine is an example of a potential significant source of woody biomass in the southeast United States.

Loblolly pine is a commercially important species in the southeast United States. This is due to its rapid growth and ease of establishment making it dominant on about 11.7 million ha (29 million acres) and makes up over one-half of the standing pine volume (Baker and Langdon, 2013; Cunningham et al., 2008). According to Williams and Gresham (2006), 15.2 Mg/ha of total biomass can be produced every year from loblolly pine tree by intensive management. This means that about 177.84 million tons of loblolly pine per year is potentially available for bioenergy.

## **2.2 Biomass Supply Logistics**

Biomass supply logistics involves the unit operations that are used to prepare biomass feedstock for the bio-refinery process (Figure 2.1). These unit operations include biomass harvesting and collection, storage, pre-processing, transportation and handling. Without assurance of efficient feedstock flow from point of origin to the throat of bio-refinery conversion, biofuel production can be limited by capacity and cost-prohibitive factors (BRDB, 2010). Biomass supply logistics represent one of the major challenges for cost effective production in the emerging lingo-cellulosic bio-refining industries (Sokhansanj and Hess, 2009).

The low density and high moisture content of woody biomass make biomass supply logistics cost intensive. For example, the bulk density of switchgrass was reported to vary between 49.4 to 266.5 kg/m<sup>3</sup> within the moisture content range of 8 to 60% (wb). A similar trend was also observed for wheat straw in which the bulk density ranged from 24.2 to 111.1 kg/m<sup>3</sup> within the

same moisture content range (Lam et al., 2007). This limits the amount of biomass that can be handled, transported and delivered to the bio-refinery. Also, there exist flowability problems due to irregular particle size and high moisture content of woody biomass. This is the focus of this research which is to quantify the influence of particle size and moisture content on the flowability of ground loblolly pine.

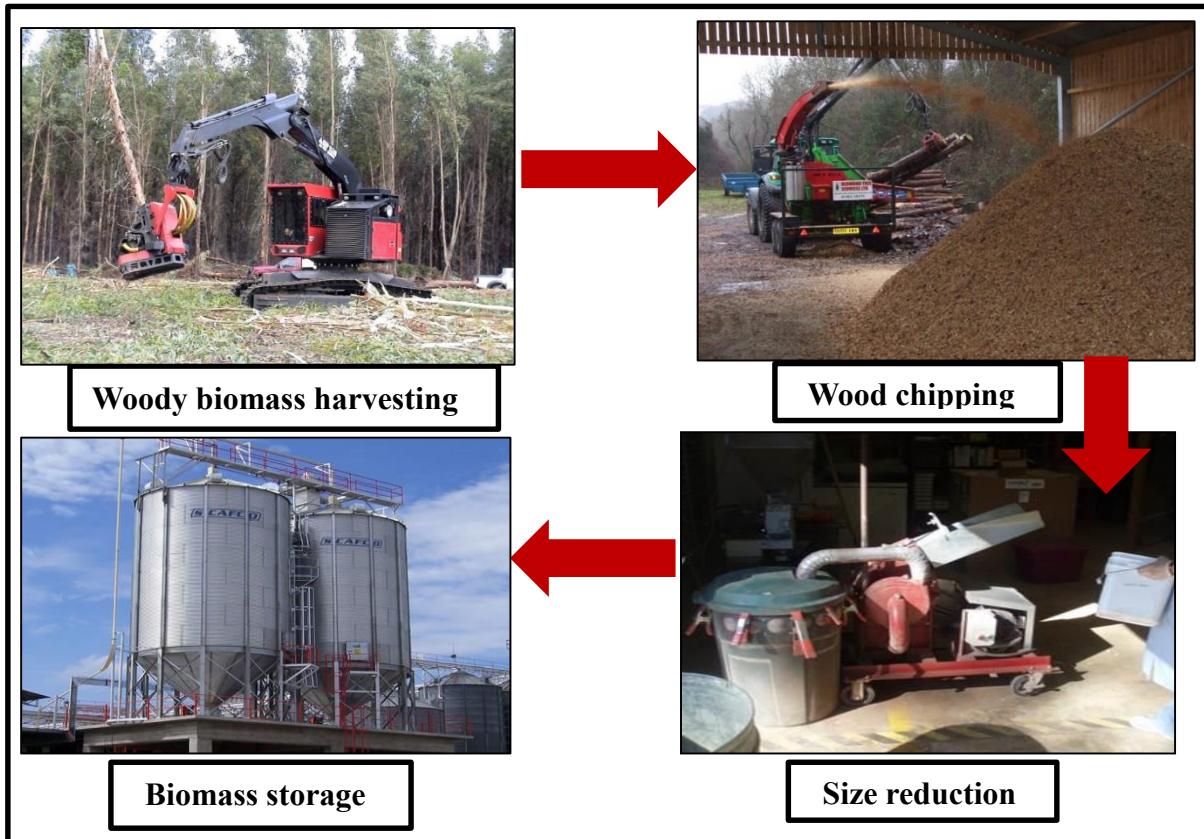


**Figure 2.1: Flow chart of biomass supply logistics**

(Source: [www.fs.fed.us](http://www.fs.fed.us); [www.directindustry.com](http://www.directindustry.com); [www.glosco-wood.com](http://www.glosco-wood.com); [www.southeasttree.com](http://www.southeasttree.com)).

### 2.3 Size reduction and particle size

Size reduction of woody biomass is necessary because current conversion technologies require the use of small sized particles that are typically less than 1 mm (Wei et al, 2009; Kumar et al, 2009). Size reduction as a pretreatment process changes the particle size, shape, particle density and bulk density of biomass. It increases the total surface area of the material and the

number of contact points for inter-particle bonding (Drzymala, 1993). More importantly, size reduction of lingo-cellulosic biomass minimizes mass and heat transfer limitations during conversion processes (Schell and Harwood, 1994). Chundawat et al. (2006) found that size reduction of corn stover and separation to various size fractions affected pretreatment and hydrolysis processes. The author further found that glucan and xylan conversions were enhanced by 15–20% when corn stover was ground to particle size of <0.15 mm.

Size reduction of woody biomass usually involves two steps. The first step is wood chipping where a wood log is fed to the disk chipper and the wood chips produced usually have sizes ranging from 5 to 50 mm (Naimi et al., 2006). The second step is biomass milling, which further reduces the wood chips into smaller particles. Wood particles produced by biomass milling usually have sizes ranging from 0.1 to 10 mm (Zhang et al., 2010). Equipment such as hammer mills, knife mills, ball mills, needle mills, shredders, linear knife grids, and disk attrition mills are used for biomass milling (Igathinathane et al., 2009; Zhu et al., 2009). Hammer mill is the most commonly used size reduction equipment because it is relatively cheap, easy to operate, high throughput rate, versatility in grinding different materials and produce wide range of particles (Bitra et al., 2009; Lopo, 2002). Hammer mill utilizes impact load produced by a rotating shaft with attached fixed or swinging hammers to break down larger sized particles into smaller size particles (Austin, 2002).

Size reduction is an energy intensive operation accounting for up to one-third of the power requirements of the entire bioconversion to ethanol (US Department of Energy, 1993). Energy consumption for grinding depends on biomass initial and final particle size, moisture content, material properties, mass feed rate and machine variables such as screen size and type of grinding equipment (Mani et al., 2004). Specific energies between 46 kJ/kg and 107 kJ/kg were reported

for size reduction of corn stover (Dilts, 2007). Mani et al. (2004) observed an increase in energy requirement with decreasing final particle size and increased moisture content for corn stover and barley straw. Size reduction of corn stover from particle size of 12.5 mm to particle sizes of 3.2 - 0.8 mm respectively with increase in moisture content from 6.2 to 12% (wb) resulted in increased average energy requirement from 25.06 to 123.5 kJ/kg. Increase in average energy requirement from 49.6 to 358.2 kJ/kg was also reported for barley straw with size reduction from particle size of 20.52 mm to size range of 3.2-0.8 mm and moisture content increase from 6.2 to 12.0% (wb). Datta (1981) reported that coarse size reduction of hardwood chips (0.2–0.6 mm) required 72–144 kJ/kg of energy. The grinding energy requirement increased five times (360- 720 kJ/kg) when the chips were ground to smaller particle size of 0.15–0.3 mm.

Particles generated during size reduction are not uniformly sized. Therefore, particle size distribution is sometimes used as a measure of efficiency for the size reduction process (Bitra et al., 2009). Particle size distribution is a measure of the variation in size of particles after size reduction. The distribution for biomass materials are skewed (i.e., log-normal distribution). Examples of this can be found in studies published on alfalfa forage grinds (Yang et al., 1996), corn stover grind (Mani et al., 2004), barley, canola, oat and wheat straw (Adapa et al., 2009) and peanut hull (Fasina, 2008). This skewness is typically obtained for naturally occurring particle population (Rhodes, 1998).

An effective way of expressing and comparing particle size distribution of ground material on a statistical basis is the geometric mean diameter and the geometric standard deviation. The geometric mean diameter is the median size of particles by mass or median size of particles retained on a sieve during a sieve analysis. It is used to describe the particle size and distribution of ground materials. The geometric standard deviation is the deviation of particle diameters by

mass in a log-normal size distribution curve (ASABE Standards, 2008). These two parameters are often used in characterizing the particle size of ground materials measured either by a sieving analysis or an image analysis.

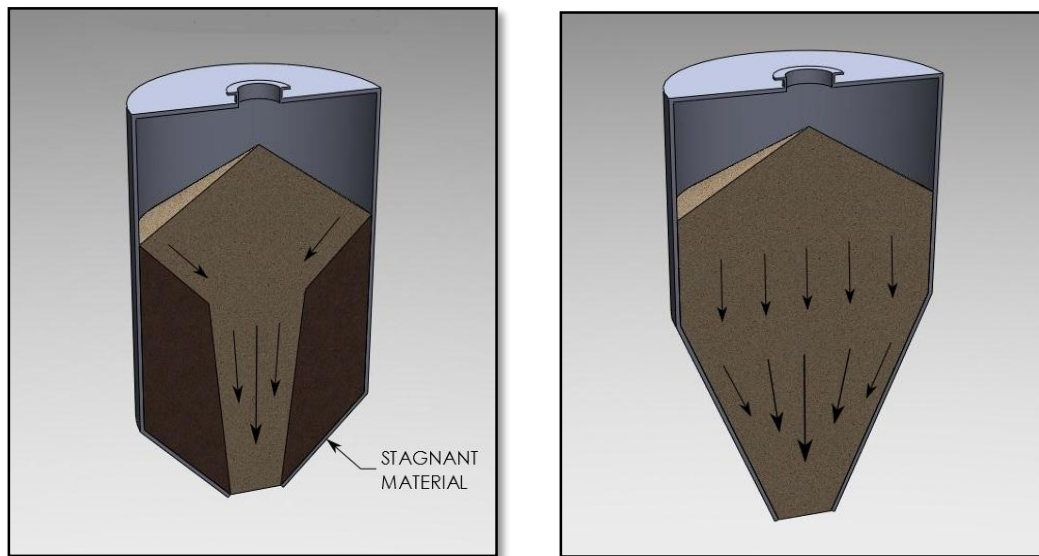
Particle size is dependent on the screen size of the milling equipment and the biomass material. Mani et al. (2004) reported geometric mean diameters for corn stover and switchgrass using a hammer mill screen size of 0.8, 1.6 and 3.2 mm to be 0.19 and 0.25 mm; 0.26 and 0.28 mm; 0.41 and 0.44 mm respectively. It can be observed from the results that increase in the screen size resulted in increase in the geometric mean diameter. Also, although the same screen sizes were used for the two feedstock materials, there was a difference in the geometric mean diameters with switch grass having a higher geometric mean diameter as compared to corn stover. The variation in the particle sizes of ground biomass is an underlying factor which influences physical and flow behavior of ground biomass.

#### **2.4 Flow patterns and flow problems**

Flow is defined as the relative movement of bulk particles in comparison to neighboring particles or along the wall of a storage container. Flowability therefore is a measure of the cohesiveness and adhesiveness of bulk material (Peleg, 1977; Woodcock and Mason, 1987). Particles that do not flow well tend to have strong tendency to stick to one another (high cohesion) due to attractive forces between particles. Adhesion occurs when particles in storage silos or bins ‘stick’ to the walls or exterior surface of the storage container. The two main types of flow patterns that exist when bulk materials are discharged from storage equipment are funnel flow and mass flow.

Funnel flow (Figure 2.2a) occurs when the particles move out through a central ‘funnel’ that forms within the material, followed by collapse of particles against the walls and moving of

these collapsed particles through the funnel (Johanson, 2002; Purutyan, et al., 1998; Shamlou, 1988). It is a first-in last-out flow pattern which is unsatisfactory for bulk solids that degrade with time. It is also unsatisfactory for fine bulk solids of low permeability. Such materials may aerate during discharge through flow channel and this can lead to flooding problem or uncontrolled discharge (Roberts, 1994). In mass flow (Figure 2.2b), the bulk solid is in motion at every point within the bin and is moving downwards towards the opening. Mass flow is a ‘first-in first-out’ flow pattern and it guarantees complete discharge of the bin contents at predictable flow rates (Roberts, 1994).



(a) Funnel flow

(b) Mass flow

**Figure 2.2: Types of flow patterns in a storage vessel: (a) Funnel flow; (b) Mass flow.**  
(Source: *jenike.com*)

The two problems that are usually associated with these two flow patterns are shown in Figure 2.3 (cohesive arching for mass flow and ratholing for funnel flow). An arch (Figure 2.3a) is a stable obstruction that forms within the hopper section (i.e., the converging portion of the bin) usually near the bin outlet. Such an arch supports the rest of the bin’s contents preventing discharge of the remaining powder. A rathole (Figure 2.3b) is a stable pipe or vertical cavity that empties

above the bin outlet. Material is left stranded in stagnant zones that usually remain in place until an external force is applied to dislodge it. Flow problems such as ratholing and arching can result in structural failure and damaging of silos, process inefficiencies, and frequent equipment downtime (Prescott and Barnum, 2000; Johanson, 2002; Merrow, 1988).

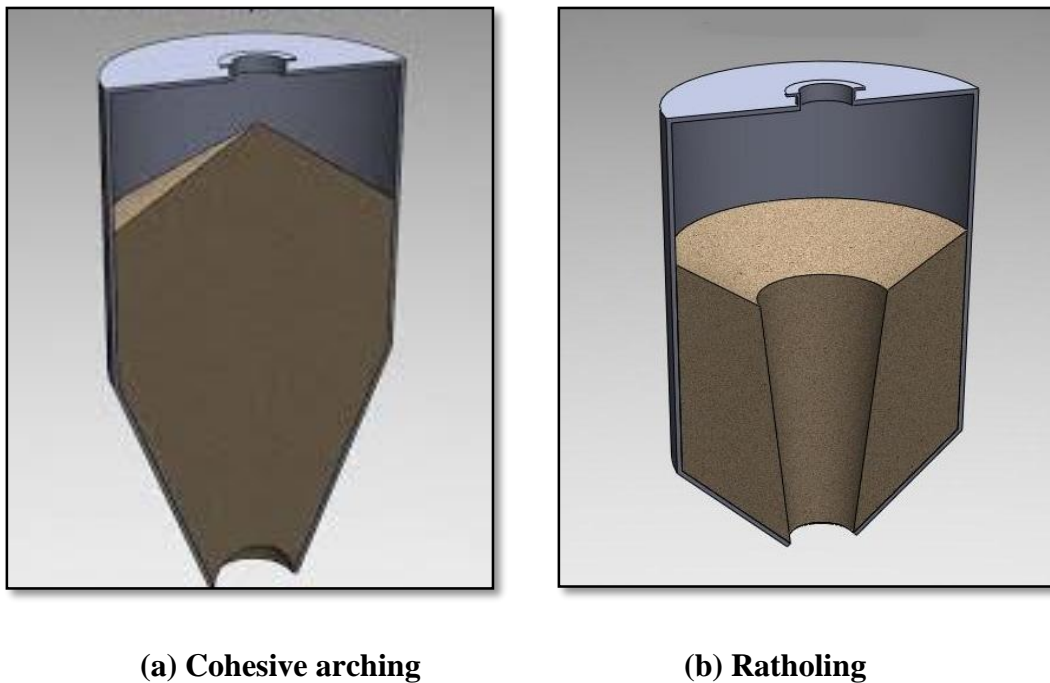


**Figure 2.3: Typical flow problems associated with bulk solids (Source: *jenike.com*)**

These flow problems have been documented to exist during the storage and handling of ground biomass feedstock. This is due to the non-uniform particle sizes obtained after size reduction and change in moisture content of biomass feedstock. Liu (2008) stated that ground corn and DDGS are a mix of particulate materials in which the relative amounts of particles present, sorted according to size affects the handling characteristics of the materials. The ground material possesses a distribution of particle sizes which contributes differently to its flow behavior during discharge from storage vessels. For example, Gil et al. (2012) carried out an experiment on the handling characteristics of Cardoon (*Cynara cardunculus L.*), a herbaceous perennial plant used

as a biomass feedstock. Frequent and continuous bridging was observed during the discharge of the ground whole cardoon (comprising of the capitula, stems and leaves) with particle size range of 0.5 – 1.0 mm. This problem was attributed to the interlocking elongated particles of the stem and the capitula hairs which possess a small diameter and a great length, hence having a tendency to entangle, build up structures that trap other small sized particles which ultimately impeded the flow. A better understanding of the contribution of the varying particle fractions to the overall flowability of the whole ground feedstock can be achieved through fractionation.

Fractionation is the separation of a material into multiple component parts (Adapa et al., 2004). Size sensitive fractionating or screening is a unit operation in which a mixture of various sizes of solid particles can be separated into two or more fractions by passing over a screen. Screens usually made from metal bars, perforated plates, perforated cylinders, woven cloth or fabrics are employed for this operation. Screening (known as sieving) is also used for particle size analysis to determine the size distribution of granular and powder materials (Brennan et al., 1969). Rosentrater et al. (2006) however stated that size sensitive fractionation has the potential to achieve the following: (i) more controlled particle size range manipulation to achieve desired specifications for certain applications. For example; a decrease in particle size of a given mass of material leads to an increase in the exposed surface area of the solid. This increase in area is of great importance in many rate-dependent processes; (ii) separation of desired constituents from a composite stream. Fractionation of ground woody biomass into size classes therefore will help in quantifying the contribution of particle size to the physical and flow properties of the whole ground material, which is the main focus of this research.



## **2.5 Physical Properties**

Physical properties that are relevant to the handling, storage, and processing of biological materials include bulk density, particle density, tap density, porosity and compressibility (Ortega-Rivas, 2003). Ground loblolly pine is a bulk solid and therefore will possess typical flow issues associated with bulk material. Physical properties are used to design new and retrofit existing bins, hoppers and feeders; determine the basis of flow problems and understand differences between various bulk materials or grades of the same material (Fitzpatrick *et al.*, 2004). Particle size and moisture content are two intrinsic factors that influence these physical properties; hence the need to study the effect of particle size and moisture on physical properties of ground loblolly pine.

### **2.5.1 Bulk density**

Bulk density is the ratio of the mass of a bulk material to its bulk volume. Bulk density significantly impacts supply logistics, engineering design and operation of transportation equipment, material handling systems and processing in the bio-refinery (Sokhansanj and Fenton, 2006; Woodcock and Mason, 1987). This is because bulk density is used in estimating storage capacity and the amount of space needed during biomass logistics. Bulk density of granular and biological materials, which is affected by particle size and moisture content, is also used in describing the flowability of the materials. Flow indicators such as compressibility index and Hausner ratio (HR) are calculated from the density values of the material (Abdullah and Geldart, 1999; Probst *et al.*, 2013).

Bulk density generally decreases with increase in particle size. The larger particles occupies more pore volume than the smaller particles, hence the higher bulk density of the smaller particles up to a certain diameter. Mani *et al.* (2004) found an inverse relationship between bulk density and particle sizes of corn stover and switchgrass. The bulk density of corn stover decreased

from 158 to 131 kg/m<sup>3</sup> with an increase in the particle size from 0.19 to 0.41 mm. A similar trend was reported for switchgrass with a decrease in the bulk density from 182 to 115 kg/m<sup>3</sup> as particle size increased from 0.25 to 0.46 mm. Manickam and Suresh (2011) reported a decrease in the bulk density of coir pith from 200 to 100 kg/m<sup>3</sup> with increased particle size from 0.655 to 0.925 mm. Similar trend was reported for the bulk densities of ground canola (203 to 144 kg/m<sup>3</sup>), barley (155 to 99 kg/m<sup>3</sup>), oat (196 to 111 kg/m<sup>3</sup>) and wheat (154 to 107 kg/m<sup>3</sup>) with increase in particle size from 0.37 to 0.89 mm, 0.46 to 0.88mm, 0.40 to 0.94 mm and 0.45 to 0.99 mm respectively (Adapa et al., 2011).

However, when switchgrass was fractionated into size classes from 0.25 to 0.71mm, Lam et al. (2008) reported that the bulk density was found to increase from 149 to 194 kg/m<sup>3</sup> with increased particle size. This change is attributed to the fact that biomass grinds collected after fractionation exhibit different packing as compared to the unfractionated biomass grinds. A similar observation was reported for the bulk density of fractionated ibuprofen powder (a pharmaceutical powder). The bulk density increased from 350 kg/m<sup>3</sup> to 440 kg/m<sup>3</sup> with increase in particle size from 46 to 215  $\mu$ m. The bulk density of the larger fractions was also reported to be higher than the bulk density (401 kg/m<sup>3</sup>) of the bulk mixture (Liu et al., 2008). This is an indication that the larger particles have a strong effect on the bulk density of a bulk material.

Moisture content is the amount of water present in the biomass feedstock. Several published studies have shown that moisture content significantly influences the bulk density of biomass. As moisture content increases, there is a corresponding decrease in bulk density. This is a result of the increase in mass due to moisture gain being lower than the accompanying volumetric expansion of the bulk. The amount of storage space required for a given material will therefore increase with moisture content increase (Colley et al., 2006). Peleg *et al.* (1973) and Peleg and

Moreyra (1979) studied the effect of moisture content on food powders' bulk density. They observed reduced bulk density of water-soluble powders upon increasing moisture content. The reduction in powder bulk density was attributed to the presence of inter-particle liquid bridges which kept them further apart and produced a more-open structure than if the particles were non-cohesive. This effect also produced greater compressibility for moist powders than for dry powders.

Bahram et al. (2013) reported a reduction in the bulk density of wormy compost from 854 to 658 kg/m<sup>3</sup> as moisture content increased from 25 to 35 % (wb). Probst et al. (2013) also reported that the bulk density of ground corn was found to decrease from 627.4 to 607.8 kg/m<sup>3</sup> as moisture content increased from 10.4 to 19.6% (wb). Similar trends were documented for granular biological materials such as rice (Kibar et al., 2010), soybean (Deshpande et al., 1993) and green gram (Nimkar and Chattopadhyay, 2001). This shows that the volume necessary to store or transport biological materials (with identical mass) will increase as moisture content increases (Littlefield et al., 2011).

### **2.5.2 Particle density**

Particle density is the ratio of the average mass to average volume of particle that form the bulk solid. Particle density measures the density of the particle matter excluding the air pores, hence it is called true density (Ileleji and Rosentrater, 2008). Although, particle density is not required in the design of storage silo, however it is an important parameter that is needed in the design of systems for ventilation and cooling of biomass during storage (Fasina and Sokhansanj, 1995; Pabis et al., 1998). Particle density is also used as an indicator of the pelletability of a material. Higher values result in good quality pellets and easier pelletability since less energy is needed to achieve densification of the material (MacBain, 1966; Leaver, 1985). The relationship

between particle size and particle density of biological materials have been reported by several authors. Gil et al. (2013) reported an increase in particle densities of poplar and cornstover from 1293 to 1457 kg/m<sup>3</sup> and 1450 to 1472 kg/m<sup>3</sup> respectively with a reduction in particle size from 0.70 to 0.26 mm. Mani et al. (2004) also reported an increase in the particle density of switchgrass from 950 to 1170 kg/m<sup>3</sup> as the particle size decreases from 0.46 to 0.25 mm at a moisture content of 8% (wb). The increased particle density due to particle size reduction is because the smaller the particle size, the lesser the air pores in the particle. This phenomenon has been confirmed for DDGS particles (Ileleji et al., 2007).

Due to the exclusion of air pores during the measurement of particle density, the values reported for most biological materials are relatively higher than bulk density. For example, Adapa et al (2011) reported the particle density of barley at particle size of 0.46 mm to be 1149 kg/m<sup>3</sup> while bulk density was reported to be 155 kg/m<sup>3</sup>. This shows that reduction of pore spaces among particles will lead to higher density therefore enhancing effective logistics of biomass. However, this will result in reduced flowability as the material will become compacted.

Similarly, particle density of biological material has been reported to generally decrease linearly with increase in moisture content. For example, at a geometric mean diameter of 0.68 mm, corn stover was reported to decrease in particle density from 1120 to 1112 kg/m<sup>3</sup> with an increase in moisture content from 7 to 15% (wb) (Mani et al., 2004). Bahram et al. (2013) reported a particle density reduction from 1652 to 1443 kg/m<sup>3</sup> of wormy compost with an increase in moisture content from 25 to 35% (wb). This implies that the volume of biological materials increases at a higher rate than the increase in mass as moisture content increases (McMullen et al., 2005).

### 2.5.3 Porosity

Porosity is a measure of the void spaces in a material, and is a fraction of the volume of voids over the total volume with values that range between 0 and 100%. Porosity of a material can be classified based on the bulk density and particle density of the material. For example, food powders have bulk densities in the range of 300 to 800 kg/m<sup>3</sup> while the particle density of most food powders is about 1,400 kg/m<sup>3</sup>, so these values are an indication that food powders have high porosity, which can be internal, external or both (Ortega- Rivas, 2009). Porosity can be a good prediction of the sphericity or irregularity of the particles in a bulk solid. An average porosity calculation of 0.4 is normal for spheroid particles, whereas irregular shaped or very small particulates have higher porosity values (Woodcock and Mason, 1987). High porosity values are a sign of logistical and economic problems that can be encountered during the storage and transportation of biomass, unless some form of densification is utilized (Fasina, 2007).

Particle size and moisture content have a significant effect on porosity of biological materials. Lam et al., (2008) reported an increase in porosity of ground corn stover from 0.91 to 0.94 with an increase in particle size from 0.25 to 0.71 mm. Littlefield (2010) also found the porosity of pecan shell to significantly increased ( $p < 0.05$ ) from 0.67 to 0.71 as particle size increased from the 0.21 to 2.19 mm. However, Lam et al. (2008) reported that the porosity of switchgrass decreased from 0.87 to 0.82 with increase in particle size from 0.25 to 0.71 mm. The change in the trend may be due to the particle shape and type of the biomass. Although there was a reduction in the porosity of switchgrass and increase in the porosities of pecan shell and corn stover with increase in particle size, the values obtained for these three materials are typical of extremely irregular-shaped particles that have cohesive tendencies (Woodcock and Mason, 1987).

Bahram et al. (2013) reported the particle and bulk densities of wormy compost at a moisture content range of 25 to 35% (wb) and hammer mill screen size of 0.6mm to be 1554 – 1531 kg/m<sup>3</sup> and 814 - 685 kg/m<sup>3</sup>. Based on these data, the porosity of wormy compost varies between 0.52 – 0.45, which indicates a reduction in porosity with increase in moisture content. Manickam and Suresh (2011) also reported a reduction in the porosity of coir pith from 0.86 to 0.62 with an increase in moisture content from 10.1% to 60.2% (wb). Increase in moisture content of biological material causes volumetric expansion which is faster than increase in the mass of the material, therefore this results to less air space among particles thereby leading to reduction in porosity.

#### **2.5.4 Compressibility**

Compressibility is a measure of the increase in strength (or density) of powder-like materials with increase in consolidating (normal) pressure and it is sometimes used to assess the flowability of bulk material (Table 2.1, Fayed and Skocir, 1997). It is a direct function of the elasticity of the material under applied pressure (Schulze, 1996). The two types of compressibility in relation to biological materials are vibrational and mechanical compressibility.

Mechanical compressibility occurs due to applied weight above the material while vibrational compressibility occurs when a bulk solid material is subjected to tapping/vibration (e.g during transportation). Both mechanical and vibrational compressibility can occur at the same time. For example, during transportation of a deep bed sample, the portion of the sample at the bottom of the bed will experience both mechanical and vibrational compression (Fasina, 2008). Mechanical compressibility is used as a measure of flowability. Table 2.1 shows that materials with high compressibility are deemed to have low flowability (Fayed and Skocir, 1997).

The compressibility of biomass feedstock is dependent on its particle size as there is a direct relationship between the two properties. Littlefield et al. (2011) showed that the compressibility of pecan shell significantly decreased with an increase in particle size and applied pressure. Bernhart and Fasina (2009) reported the effect of particle fractions on compressibility of poultry litter. The result showed that the fine fraction of poultry litter was the most compressible while the coarse fraction was the least compressible. When compared to the compressibility of the raw sample, it was reported that the fine fraction was the dominant contributor to the compressibility of poultry litter. A similar trend was reported by Zhou et al. (2008) on the compressibility of corn stover. An increase in compressibility from 20.9 to 28.4 % as the particle size decreased from 6.4 to 1.6 mm at < 10 % moisture content was reported. There was also an increase in the compressibility of corn stover from 26.4 to 30.5 % with a particle size reduction from 6.4 to 1.6 mm at moisture content level greater than 20 %.

**Table 2.1: Flowability classification of bulk solids based on mechanical compressibility (Fayed and Skocir, 1997).**

<b>Compressibility (%)</b>	<b>Bulk Solid Description</b>	<b>Flow</b>
5 - 15	free-flowing granules	excellent flow
12 - 16	free-flowing powdered granules	good flow
18 - 21	flowable powdered granules	fair to passable flow
23 - 28	very fluid powders	poor flow
28 - 35	fluid cohesive powders	poor flow
33 - 38	fluid cohesive powders	very poor flow
> 40	cohesive powders	extremely poor flow

Increase in moisture content causes an increase in the compressibility of bulk materials because of increased formation of liquid bridges between particles that increases its cohesiveness (Teunou and Fitzpatrick, 1999; Barbosa–Canovas et al., 2005). Biological materials also become

softer and therefore deform more when they absorb moisture. The compressibility of ground corn stover with particle size of 1.6mm was reported to increase from 28.4 to 30.5 % as the moisture content increased from 10 to 20 % (wb). Littlefield et al. (2011) and Bernhart and Fasina (2009) also reported the effect of moisture content on compressibility of pecan shells and poultry litter respectively and found that the compressibility of pecan shells and poultry litter increased with moisture content.

### **2.5.5 Hausner ratio**

The ratio between tapped (defined as a certain number of taps) and aerated bulk density is known as the Hausner ratio (Geldart *et al.*, 1984). Hausner ratio (HR) is an empirical constant that is sometimes used to assess the flowability of a bulk material (Table 2.2) (Fitzpatrick, 2003). Abdullah et al. (2010) observed a reduction in the Hausner ratio of silica gel with increase in particle size. Two distinctive sizes were observed as bordering criteria; silica gel of less than 28  $\mu\text{m}$  particle size had a Hausner ratio  $< 1.25$ , hence classified as cohesive, silica gel with particle size greater than 36  $\mu\text{m}$  had a Hausner ratio  $> 1.4$ , hence classified as free-flowing powder and silica gel with particle size in between 28 and 36  $\mu\text{m}$  were said to be in transition group (i.e. exhibiting mixed cohesive and free flowing powder behavior). Liu et al. (2008) also reported a reduction in the Hausner ratio of fractionated ibuprofen powder 1.39 to  $\sim 1.25$  with increased particle size from 46 to 215  $\mu\text{m}$ . This is an indication of improved flowability with increase in particle size. Liu et al. (2008) further observed that the fractionated powder had a lower Hausner ratio as compared to the bulk powder in which even the smallest size fraction has a Hausner ratio smaller than that of the bulk powder. Similar trend of reduction in Hausner ratio with increased particle size were also reported for biological materials (wheat straw, switchgrass and corn stover) by Lam et al. (2008).



**Table 2.2: Flowability classification using Hausner ratio (Source: Carr, 1965).**

<b>Hausner ratio</b>	<b>Flow character</b>
1.00-1.11	Excellent
1.12-1.18	Good
1.19-1.25	Fair
1.26-1.34	Passable
1.35-1.45	Poor
1.46-1.59	Very poor
>1.60	Very, very poor

On the other hand, moisture content has been reported not to have significant effect on Hausner ratio. This is because the reduction rate of bulk density is similar to the rate of decrease of tap density as moisture content decreases (Bernhart and Fasina, 2009). Zhou et al. (2008) observed that there was no significant difference between the Hausner ratio values obtained for wet (> 20% MC) and dry (< 10% MC) corn stover samples within the particle size range of 6.4-1.6 mm. The values were in the range of 1.3-1.5 which was indicative of poor flow characteristic. This was also in accordance to the result obtained by Emery et al. (2009) for Hydroxypropyl Methylcellulose (HPMC, a pharmaceutical powder). Moisture content (0% – 10 % wb) was observed not to have any significant effect on the Hausner ratio of HPMC. Also, a similar trend was observed by Emery et al. (2009) for Aspartame powder with moisture content range of 2 to 10% (wb). However the values reported for both powders (1.3–1.7) were above the threshold value of 1.25, which is an indication of poor flow characteristics. Probst et al. (2013) also reported that moisture content (10.39 – 19.64% wb) had no significant effect on Hausner ratio (1.5- 1.6) of ground corn.

## 2.6 Flow Properties

Bulk material properties that influence flow or flowability are termed flow properties. Flow properties are used in designing and sizing equipment for storage, transportation, or general handling of bulk solids that will lead to reliable and consistent flow of bulk solids out of hoppers and feeders. Flow properties are also used in investigating the cause of flow problems of bulk solids (Prescott and Barnum, 2000; Schwedes, 2003). Flow properties of bulk solid materials includes: flow function, cohesion, angle of internal friction and angle of wall friction.

Particle size and moisture content are one of the most important intrinsic bulk material characteristics which affect the flowability (or flow properties) of bulk materials. In general, materials with narrow particle size distribution have a better flow than materials with wider particle size distribution (Benkovic and Bauman, 2009). Also, it is generally considered that materials with particle sizes larger than 200  $\mu\text{m}$  are free flowing, while fine powders with particle sizes less than 200  $\mu\text{m}$  are subject to cohesion and flowability problem. The reduced flowability at smaller particle sizes is because of the increased surface area per unit mass of the material. There is more surface area or surface contacts available for frictional forces to resist flow (Fitzpatrick, 2005; Teunou et al., 1999; Fitzpatrick, 2007).

Flowability of bulk solids is commonly determined using procedures developed by Jenike (1964). The procedure employs the principle of plastic failure with the Mohr Coulomb failure criteria. The Jenike shear cell unit (Figure 2.4) is used in quantifying properties such as unconfined yield strength, major consolidation stress, angle of internal friction and flow function (Bhadra et al., 2009; Thomson, 1997).

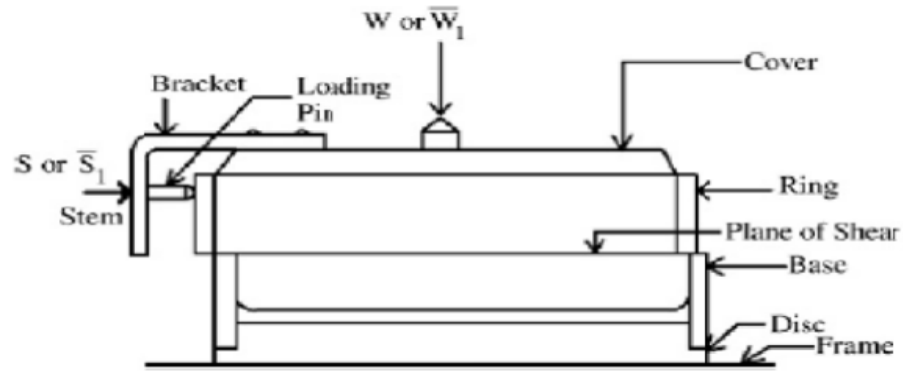


**Figure 2.4 Jenike shear cell (Zulfiqar et al., 2006).**

Jenike's method involves pre-consolidating the samples to be tested under different normal stresses until a steady state is reached. Upon reaching a steady state, a consolidating pressure and a horizontal shear force are applied to the sample. The shear stress required to cause the sample to fail under the applied consolidation stress will be measured. A yield locus (Figure 2.5), which is a plot of the failure shear stress versus normal stress for a given consolidation stress is then plotted. The test can be replicated to obtain different yield loci (Chen et al., 2012; Bhadra et al., 2009; Fitzpatrick et al., 2004).

Measurement of wall friction properties with Jenike shear tester involves replacing the base of the shear cell with a sample of the wall material to be examined (such as stainless steel, mild steel or galvanized steel) as shown in Figure 2.4 (Chen et al., 2012). This test is used in determining the wall material needed for consistent and reliable flow out of a storage silo or bin.

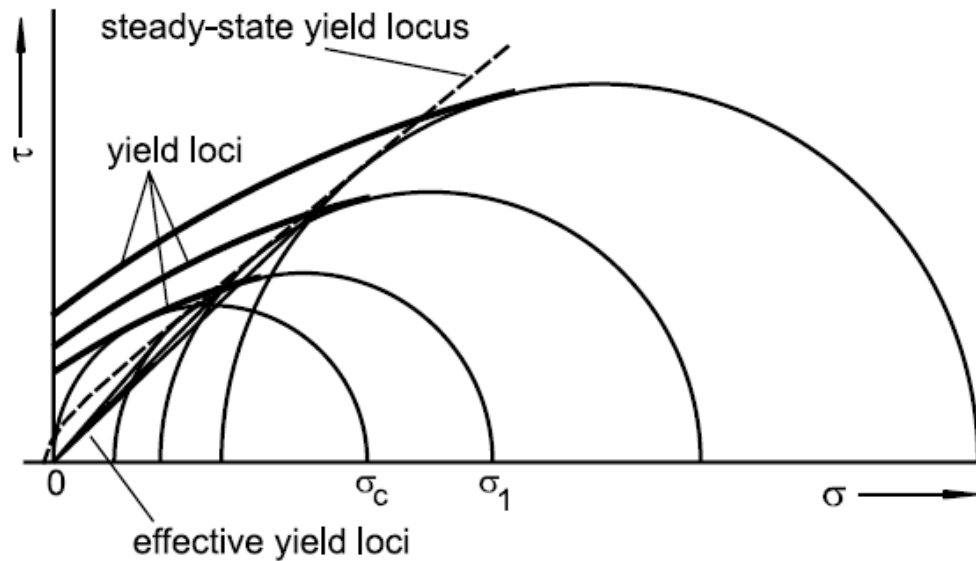


**Figure 2.5: Typical plot of yield loci of a bulk solid (Schulze, 2008).**

### 2.6.1 Cohesion

Cohesion is the mutual attraction and resistance to separation of contacting particles of identical material (Nokhodchi, 2005). Cohesion in bulk solid materials is commonly caused by liquid bridges and Van der Waals forces (Weber et al., 2004). Liquid bridges are formed by small regions of liquid in the contact area of particles, in which due to surface tension effects, a low capillary pressure prevails. Van der Waals' force is a weak intermolecular force that exists between particles (Schulze, 2006). High moisture content and small particle size enhances high cohesive strength in biological materials which can lead to flow problems such as caking, arching and ratholing.

Krantz et al. (2009) measured the flow properties of two coating powder samples (Polyester-Epoxy and Polyurethane) with particle sizes ranging between 22 and 31  $\mu\text{m}$ . The authors found that the cohesion increased with decreasing particle size for both powder formulations. This resulted because the finer the particle size, the more contact area between particles, which leads to greater cohesive forces among the particles (Marinelli and Carson, 1992).

Gil et al. (2013) reported the particle size effect on cohesion of ground poplar and corn stover. The authors also observed an increase in cohesion from 0.14 to 0.64 kPa for ground poplar with reduction in particle size from 0.61 to 0.30 mm. The cohesion of ground corn stover was also reported to increase from 0.16 to 0.68 kPa with reduction in particle size from 0.70 to 0.26 mm. A similar trend was documented for wormy compost where cohesion increased from 0.23 to 0.81 kPa as particle size reduced from 1.18 to 0.30 mm (Bahram et al., 2013).

Moisture content is an important variable that also affects cohesive strength of bulk solids (Johanson, 1978) during storage with cohesion generally increasing with moisture content (Fitzpatrick et al., 2004). The cohesion of pecan shells was found to increase from 0.36 to 1.69 kPa as moisture content increased from 4.2 to 24.6% wb (Littlefield et al., 2011). Increased cohesion due to increase in moisture content was reported for flour powder, tea powder and whey permeate powder by Teunou and Fitzpatrick (1999). The authors observed that the strength of liquid bridges formed between particles depends on the amount of moisture adsorbed by the particles. This trend was also in accordance with Rennie et al. (1999) work on whole milk powder and skimmed milk powder. Buma (1971) hence concluded that increase in cohesion at higher moisture content was due to increased plasticity of powder particles. The increased moisture content could have softened the water soluble constituents of the bulk material, resulting in deformation of the particles hence leading to higher contact surface and cohesiveness. In another research, Hargreaves et al. (2010) reported the cohesion of superheated steam dried distiller's spent grain of 0% soluble content to increase between 0.078 to 0.324 kPa within moisture content range of 5 to 15% (wb). Unloading of bulk material using gravity discharge alone requires that cohesive strength do not exceed a critical value of 2 kPa (Puri, 2002).

### 2.6.2 Angle of wall friction

Angle of wall friction is the resistance to flow of bulk solids along the hopper/silo wall material. Wall friction also represents the adhesion of bulk solid to the wall material of the storage equipment. Increase in angle of wall friction during storage can lead to difficulties in unloading bulk material from storage equipment. This flow property is a function of the bulk material and the wall surface in contact with it (Prescott et al., 1999; Iqbal and Fitzpatrick, 2006).

Wall friction is a critical parameter in the design and selection of storage equipment. A low wall friction value results in higher normal loads being transferred onto the wall surfaces of the silo (Iqbal and Fitzpatrick, 2006). Wall friction value is also required in determining the minimum hopper angle of hopper and selection of the type of surface finish to be used in lining wall of the storage equipment. Wall friction characteristics are influenced by factors such as wall surface characteristics (e.g surface roughness, wear and corrosion), properties of the bulk solids (e.g. particle size and moisture content) and storage/handling conditions (Iqbal and Fitzpatrick, 2006).

Smaller particle sizes tend to increase wall friction angle, as there is greater contact surface area between smaller particles and the wall surface. This is in accordance with Fitzpatrick et al. (2004). The wall friction angle ( $18.2^{\circ}$ ) of soy flour with particle size of  $20.2\ \mu\text{m}$  was found to be higher than wall friction angle ( $13^{\circ}$ ) of corn flour with particle size of  $49\ \mu\text{m}$ .

Moisture content plays a fundamental role in combination with the kind of wall surface. The effect of moisture content on angle of wall friction varies with the type of wall surface used. Increased moisture content will cause the particles to become stickier resulting in increased adhesion of the particles to the wall of storage containers (Iqbal and Fitzpatrick, 2006). Duffy and Puri (1996) observed that the angle of wall friction of confectionery sugar on stainless and aluminum surface decreased from  $31.0^{\circ}$  to  $24.2^{\circ}$  and  $32.2^{\circ}$  to  $29.2^{\circ}$  respectively with increase in

moisture content from 0.3 to 3.2% (wb). However, increase in angle of wall friction was observed for detergent powder on stainless steel (14.6<sup>0</sup> to 20.8<sup>0</sup>), galvanized steel (16.4<sup>0</sup> to 29.0<sup>0</sup>) and aluminum surface (25.6<sup>0</sup> to 33.4<sup>0</sup>) with increase in moisture content from 1.38 to 4.22 % (wb). Increased wall friction angle with increase in moisture content have been documented for ground poplar and corn stover (Gil et al., 2013) and flour, tea and whey permeate flour (Iqbal and Fitzpatrick, 2006).

### 2.6.3 Flow function and index

Flowability of a bulk solid is characterized mainly by its unconfined yield strength as a function of the consolidating normal stress. The unconfined yield strength of a material is the force or stress required to deform or break a material when it is not confined by a container (free unstressed surface. It can also be expressed as the stress required to fail or fracture a consolidated mass of material to initialize flow. Major consolidation stress is the force required to consolidate/compress a mass of material. The slope of the plot of the unconfined yield strength of the powder versus major consolidating stress is the flow function (Figure 2.6). A flow function lying towards the bottom of the graph represents easy flow, and more difficult flow is represented as the flow function move upwards in an anticlockwise direction. The flow index (ffc) is defined as the inverse of the flow function. Jenike (1964) used the flow index to classify powder flowability (Table 2.3).

**Table 2.3: Jenike classification of powder flowability by flow index (ffc).**

Flowability	Hardened	Very cohesive	Cohesive	Easy flow	Free flowing
Flow index (ffc)	<1	<2	<4	<10	>10

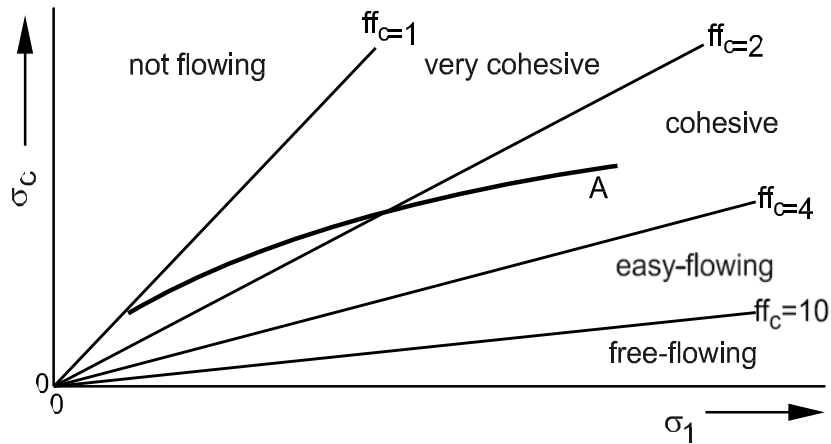


**Figure 2.6: Flow function: easy versus difficult flow (Schulze, 2008).**

Fitzpatrick et al. (2004) measured the flow indices for 13 food powders. Six of the samples (tomato, salt 200, cocoa, corn flour, sugar 140 and wheat flour) were classified as very cohesive, four (soy flour, corn starch, tea and NFM) were cohesive and the remaining three (maltodextrin, cellulose and salt 140) were easy flow. The powders that were classified as very cohesive have a particle size range between 320 - 51  $\mu\text{m}$  and moisture content of 17.8- 10% (w/w) while the easy flow have a particle size range of 12 - 55  $\mu\text{m}$  and moisture content of 0.04 - 4.3% (w/w). The difficult flow nature of the powders with higher particle was attributed to high moisture contents of the powders. Littlefield et al. (2011) further found that as the moisture content of pecan shells increased from 4.2 to 24.6%, the flow index values reduced from 15.77 to 3.14, indicating that flowability reduced from free flowing to cohesive flowing. Emery et al (2009) also reported a similar trend for a pharmaceutical powder named Hydroxypropyl Methylcellulose (HPMC). The author also classified four pharmaceutical powders (HPMC, Aspartame, API and Respitose) as cohesive powder within a moisture content range of 0 to 10 % (wb).

Cagli et al. (2007) studied the effect of particle size on flow index of 3 different sand samples (Yalikoy, Safaalani and yellow), soda, limestone, dolomite and clay. The authors reported an increase in the flow index from 2.8 to 13.8 with increase in particle size from 43 to 413  $\mu\text{m}$ .



Clay which has a particle size of 43  $\mu\text{m}$  was found to have the lowest flow index of 2.8, which is an indication of cohesive flow while the soda with flow index of 13.8, is classified as free flowing material. The other materials were classified as easy flowing. The high flow indices observed for these materials is in accordance with Woodcock and Mason (1993) conclusion, that free flowing materials such as dry sand, have zero unconfined yield stress, and hence a cohesive arch cannot occur. Similarly, Liu et al. (2008) observed an increase in the flow index of fractionated magnesium stearate lubricated ibuprofen powder from 5.1 to 11.1 with increase in particle size from 53 to 250  $\mu\text{m}$ . It was also noted that the smallest fraction with particle size 53  $\mu\text{m}$  has a flow index slightly lower than the bulk mixture. However, based on Jenike classification, the fractionated magnesium stearate lubricated ibuprofen powder is classified as east flowing.

#### **2.6.4 Design of hopper for mass flow**

A hopper is the conical or converging section of a powder storage vessel through which the stored materials flows out (Holdich, 2002). The storage equipment is very crucial in any bulk solids handling installation. This is because occurrence of flow problems adversely affects the downstream production line because of the erratic supply of material. For a system to operate satisfactorily, bulk solid must flow from the hopper when required and in a predictable manner. Thus, as with any other part of the handling system, gravity-flow storage hoppers should be designed or selected to handle the actual product under consideration (Woodcock and Mason, 1987).

One of the important applications of flow properties is the design of discharge hoppers. Design of a discharge hopper to ensure consistent and reliable discharge involves determining the minimum hopper half angle (to the vertical) and discharge opening size. The minimum hopper half angle is designed to ensure a mass flow (Figure 2.2b), which is the preferred flow pattern for a

consistent and reliable flow. If the hopper half angle is less than this angle, then it is likely that a funnel flow pattern (Figure 2.2a) will exist (Holdich, 2002; Teunou et al., 1999; Fitzpatrick, 2007; Iqbal and Fitzpatrick, 2006). The flow properties required for designing a discharge hopper are flow function (FF), the effective angle of internal friction, angle of wall friction and bulk density.

Jenike's mathematical methodology is the engineering standard practice for designing a hopper i.e for calculating the minimum hopper angle and opening size for mass flow. Jenike's design approach is based on calculation of stresses inside the hopper and postulates that the major consolidating stress ( $\sigma_1$ ) in the lower part of hopper is proportional to the distance from the vertical hopper apex. Jenike (1964) solved the stress equations and determined the borderlines between funnel flow and mass flow in conical or wedge shaped hoppers as a function of angle of wall friction, hopper half angle and the effective angle of internal friction, as shown in design chart (Figure 2.7). The steps employed in using the flow properties are (Fitzpatrick et al., 2004):

- Values of effective angle of internal friction and angle of wall friction are used in calculating the hopper half angle ( $\theta$ ) and the flow factor (ff).
- The critical applied stress (CAS) is determined from the intersection of the flow function and the flow factor line (Figure 2.8)
- The hopper opening size is then calculated using the values of CAS, hopper half angle and bulk density. For example, the opening diameter for a conical hopper is given below

$$D = \frac{H(\theta).CAS}{\rho_B.g}$$

where  $H$  is a function of the hopper half angle,  $\rho_B$  is the bulk density and  $g$  is the gravitational acceleration constant.

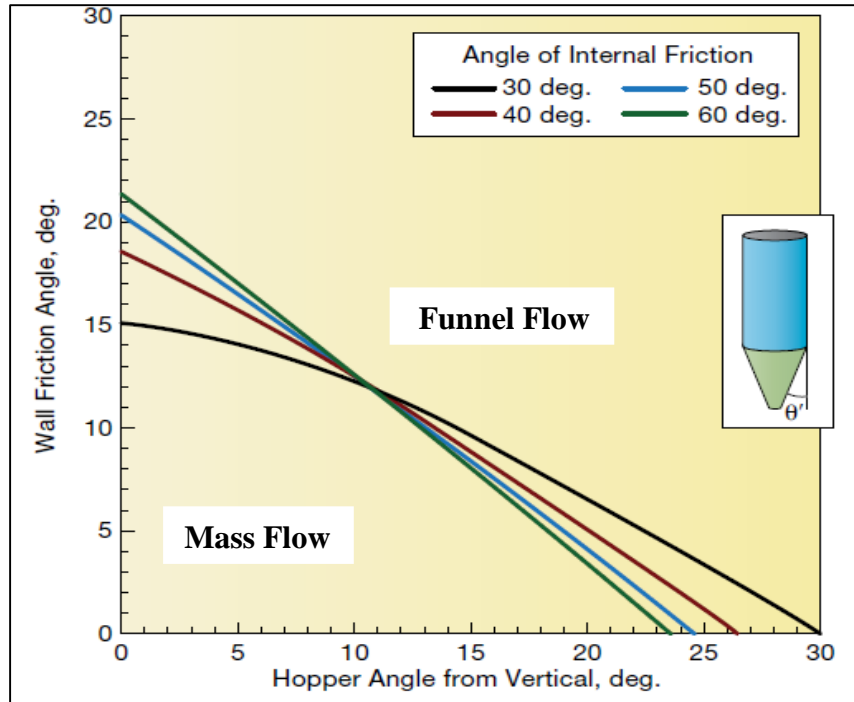


Figure 2.7 Hopper design chart for a conical hopper based on the Jenike's theory. (Source: Maynard, 2013)

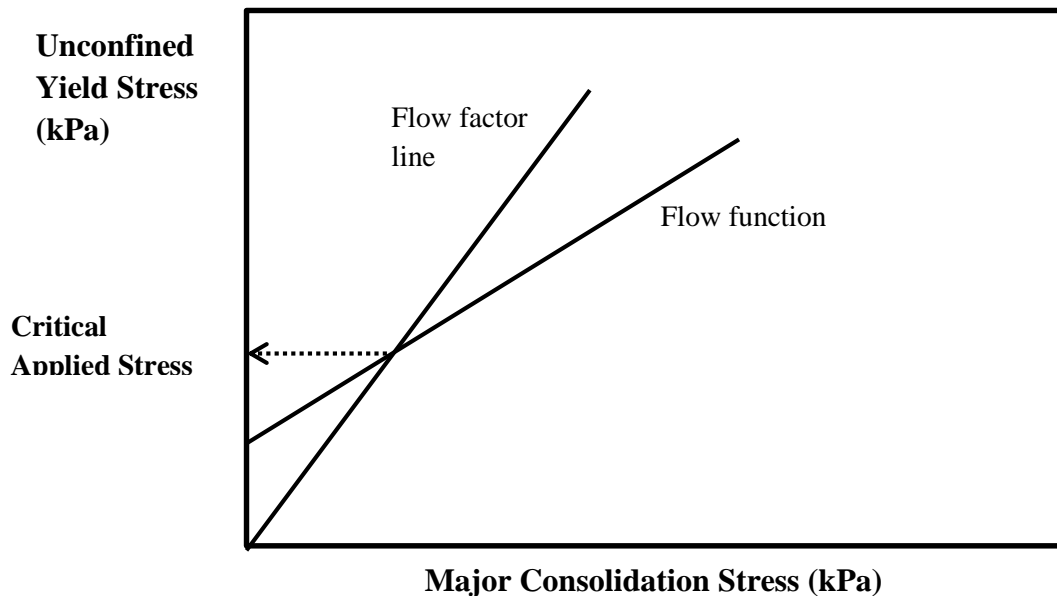


Figure 2.8: Evaluation of critical applied stress (CAS). (UYS is the unconfined yield strength and MCS is the major consolidation stress).

## Summary

The necessity for an effective and efficient storage and handling vessels for lignocellulosic biomass is due to the large amount estimated to be produced annually from the abundant biomass resources in the United States. Therefore, improper design and selection of storage vessels can result in biomass degradation, material loss, flow blockage and/or safety problems.

The use of biomass requires feedstock in particulate form. However, ground biomass obtained after size reduction have non- uniform particle size and also as a biological material, it has a tendency to exchange moisture with the environment. Therefore, ground biomass will have the typical flow problems associated with bulk materials during storage.

Characterization of particle size and moisture effect on physical and flow properties of biomass will enhance a better prediction of biomass flow behavior and design of an appropriate storage vessel. Obtaining a reliable and consistent flow out of storage equipment is critical to successful biofuel production. Hence, the design of storage equipment requires the understanding of the physical and flow properties of the biomass. The physical and flow properties include density (bulk, tap and particle), compressibility, Hausner ratio, porosity, flow index and frictional properties (cohesion, angles of wall friction and internal friction).

Loblolly pine, an energy feedstock which has been identified as a potentially significant source of fuel, is the most commercially important species in the southeast United States due to its rapid growth and ease of establishment. Hence, the focus of this research is to investigate the contribution of particle size and moisture content to flowability of fractionated ground loblolly pine in order to ensure a proper design of silo which will allow easy flow of biomass without obstruction or dust generation.

## **Chapter 3: Particle Size and Moisture Effect on Physical Properties of Fractionated Ground Loblolly Pine**

### **3.1 Abstract**

Particle size and moisture content are two intrinsic biomass characteristics that influence its physical properties. This study focused on the contribution of particle size and moisture content to the physical properties of fractionated ground loblolly pine. Loblolly pine chips were ground through a hammer mill fitted with a 3.18 mm screen and the moisture content of the ground biomass was adjusted between 4.78 and 25.53% (wb). The moisture adjusted ground biomass was fractionated into six size classes with 250  $\mu\text{m}$  to 1.40 mm screen aperture and the physical properties of the fractions were quantified. The particle size distribution of the unfractionated sample was unimodal and skewed to the left. An increase in moisture content resulted in a wider spread of the particles in the particle size distribution of the fractionated samples. The geometric mean diameters for the fractions ranged from 0.10 mm to 2.38 mm. Bulk and tap densities of the fractions increased with fraction size while particle density generally decreased with increase in fraction size. The densities (bulk, particle and tap) and porosity decreased with increased moisture content. Moisture content had no significant effect on compressibility and Hausner ratio. The heating values (18-19 MJ/kg) and volatile matter (84.91 - 87.48% d.b) were not affected by the fraction size while ash content (0.22 - 2.64% d.b) increased with reduction in the fraction size.

### 3.2 Introduction

Loblolly pine grows naturally in the southern region of the United States because of its adaptability to variety of soil, its rapid growth rate and ease of establishment. It grows on about 11.7 million ha (29 million acres) in the south, which is about one-half of the standing pine volume in this region. Therefore, it has been identified as the most commercially important species in the southeast United States (Baker and Langdon, 2013; Cunningham et al., 2008) and also as a potentially significant renewable and sustainable source of biomass feedstock that can be converted to useful energy forms.

In the southern United States, woody biomass for energy is typically harvested, pre-processed, transported and used, all within several days. Due to supply and demand imbalances that relate to inclement weather and energy prices (Rupar and Sanati, 2004), there is a need for adequate storage capabilities. Proper storage of woody biomass during excess production when demand exceeds supply is an important step in ensuring a reliable, continuous supply of feedstock. Selection and design of biomass handling and storage equipment strongly depends on the physical properties of biomass feedstock, therefore, the physical properties of biomass need to be determined (Wu et al., 2011).

Physical properties of biomass are used in designing handling and logistic systems, estimating capacity of storage vessels, determining quality of feedstock supplied to the refinery and final conversion process (Tumuluru et al., 2014). Physical properties required in the selection and design of an appropriate storage vessel includes densities (bulk, tap and particle), porosity, compressibility and Hausner ratio.

Bulk density is the ratio of the mass of a bulk material to the bulk volume. Knowledge of bulk density is essential in designing and estimating the capacity of storage bins, hoppers, conveying and conversion equipment. Particle density is the ratio of the average mass to the average volume of the particles. Higher particle density signifies higher compression and energy density (Mani et al., 2006). Tap density is an increased bulk density attained after mechanically tapping a vessel containing the material (US Pharmacopeiai, 2011). Porosity is a measure of the void spaces in a material (Rahman, 2005). Compressibility is a measure of the increase in strength of powder-like material with increase in consolidating normal pressure (Schulze, 1996). Hausner ratio is an empirical constant which indicates the ratio of tapped density and bulk density. It is used to assess flowability of bulk solid (Fitzpatrick, 2003).

The use of loblolly pine will require the feedstock to be ground into particulate form. However, ground biomass obtained after the size reduction process possesses non-uniform particle sizes. Particle size and moisture content have been documented to significantly affect the physical properties of biological materials (Manickam and Suresh, 2011; Adapa et al., 2011; Bahram et al., 2013; Probst et al., 2013). Also, fractionation of biomass into size classes has been documented to enable the fundamental understanding of contribution of fractions to the properties of bulk biological materials (Ndegawa et al., 1991; Bernhart and Fasina, 2009). Therefore, the objectives of this study were (1) to quantify the effect of particle size on the physical and compositional properties, and (2) quantify the effect of moisture content on the physical properties of fractionated ground loblolly pine.

### 3.3 Materials and Methods

#### 3.3.1 Sample preparation

Clean loblolly pine wood chips used in this study were collected from West Fraser Inc. Sawmill, Opelika, Alabama. Before use, the samples were ground through 3.18 mm screen using a hammer mill (Model 358, New Holland grinder, New Holland, PA).

Experiments were carried out on the ground samples that were adjusted to five moisture content levels between 4.78% and 25.56% (wb). The initial moisture content of the samples after grinding was 8.69% (w.b). To adjust the moisture content of the samples to the desired level, the samples were either dried using a humidity chamber (ESL-2CA, Espec North America, Inc.) set at a temperature of 50 °C and relative humidity of 20% (for moisture content reduction) or the samples were sprayed with a known volume of water (to increase the moisture content of samples). After moisture adjustment, the samples were stored in an air tight container for 24 hours to allow moisture equilibration to take place. The moisture contents of samples were then verified with a moisture analyzer (model MB 45, Ohaus Corporation, Pine Brook, NJ).

A sieve shaker (RO-TAP Model RX- 29, WS Tyler, OH) was used in fractionating the moisture adjusted ground samples into six fractions by fitting the sieve shaker with a #12 (1.4 mm aperture), #18 (1.0 mm aperture), #25 (710 µm aperture), #35 (500 µm aperture), #60 (250 µm aperture) screens and pan. The choice of sieve sizes was based on preliminary study on the particle size distribution of the raw ground samples. The particle size distributions of the raw and fractionated samples were determined according to ASABE Standard S319.3 (ASABE Standards, 2008). The physical properties of the fractions were carried out at each moisture level while the compositional properties were carried out on a dry basis.



### 3.3.2 Particle size distribution

A digital image analysis system (Model Camsizer, Retsch Technology, Haan, Germany) equipped with two digital cameras was used to measure the particle size of the sample fractions. Approximately, 50 g mass of the sample was loaded onto the hopper of the instrument. The sample was then conveyed and dropped via a vibratory feeder onto the measurement field of the cameras. The particle size distribution on volume basis of the sample was recorded and analyzed by the software provided by the equipment manufacturer. The procedure was carried out in triplicate after which the geometric mean diameter and geometric mean standard deviation were calculated from the data obtained from the equipment software according to ASABE Standard S319.3 (2008) as follows:

$$d_{gw} = \log^{-1} \left[ \frac{\sum_{i=1}^n (W_i \log \bar{d}_i)}{\sum_{i=1}^n W_i} \right] \quad 3.1$$

$$S_{\log} = \left[ \frac{\sum_{i=1}^n (\log \bar{d}_i - \log d_{gw})^2}{\sum_{i=1}^n W_i} \right]^{1/2} \quad 3.2$$

$$S_{gw} = \frac{1}{2} d_{gw} \left[ \log^{-1} S_{\log} - (\log^{-1} S_{\log})^{-1} \right] \quad 3.3$$

where;  $d_{gw}$  = geometric mean diameter or median size of particles by mass (mm);

$S_{\log}$  = geometric standard deviation of log normal distribution by mass in 10-based logarithm (dimensionless);

$S_{gw}$  = geometric standard deviation of particle diameter by mass (mm);

$W_i$  = mass on  $i$ th sieve (g);

$n$  = number of sieves plus one pan;

$$\bar{d}_i = (d_i \times d_{i+1})^{1/2}$$

$d_i$  = nominal sieve aperture size of the  $i^{\text{th}}$  sieve (mm);

$d_{i+1}$  = nominal sieve aperture size of the  $i^{\text{th}+1}$  sieve (mm)

### 3.3.3 Bulk density

Bulk density was determined by a bulk density measuring apparatus (Burrows Co., Evanston, Illinois, US) and according to ASABE Standard S269.4 (ASABE, 2007). This method involves pouring the sample fraction into a container (volume of 1137 mm<sup>3</sup>) from a funnel. The material was leveled across the top of the surface of the container and weighed. The bulk density ( $\rho_b$ ) of the fraction was taken as the mass of sample in the container ( $m_c$ ) divided by the volume ( $V_c$ ) of the container (Equation 3.4) (Littlefield et al., 2011). This procedure was performed in triplicate.

$$\rho_b = \frac{m_c}{V_c} \quad 3.4$$

### 3.3.4 Particle density

A gas comparison pycnometer (Model AccuPyc 1340, Micromeritics Instrument Corp., Norcross, GA) was used to determine the particle density of the sample. In the pycnometer, helium under pressure was allowed to flow from a previously known reference volume into a cell containing a sample of the material. By applying the ideal gas law to the pressure change from the reference cell to the sample cell, the pycnometer calculates the volume of the material in the sample cell. Particle density was taken as the ratio of the mass of material in the sample cell to the volume measured by the pycnometer. A digital balance accurate to 0.001 g (Model AR3130, Ohaus Corp, Pinebrook, NJ) was used to measure the sample mass. The particle density measurements were conducted in triplicate and the average values were used (Bernhart and Fasina, 2009).

Porosity ( $\emptyset$ ) was calculated from the values of bulk density and particle density using the equation below:

$$\emptyset = 1 - \frac{\rho_{\text{bulk}}}{\rho_{\text{particle}}} \quad 3.5$$

### 3.3.5 Tap density, compressibility and hausner ratio

Tap bulk density of the sample was measured using an automated tap density meter (Model TD-12, Pharma-Alliance Group Inc., Valencia, CA) and according to ASTM Standard B527 (ASTM, 2005). A 250 mL graduated cylinder was filled with the sample and weighed. The cylinder was then placed in the tap density tester. Tapping of the cylinder (500 times) at a rate of 300 taps/min was then carried out by the tester. Each tap consisted of the cylinder being raised 14 mm and then dropped under its own weight. After the first 500 taps, the new volume of the sample was recorded. The cylinder was then tapped 750 times and a second new volume recorded. If the difference in volume after the 500 taps and the 750 taps was >2%, the process was repeated; otherwise the experiment was completed. After the completion of tapping, the tap density ( $\rho_t$ ) of the sample was taken as the mass of sample in the container ( $m_c$ ) divided by the volume ( $V_t$ ) of the sample after the completion of the tapping (Equation 3.6) (Bernhart and Fasina, 2009). This procedure was performed in triplicate.

$$\rho_t = \frac{m_c}{V_t} \quad 3.6$$

Compressibility is a measure of the relative volume change of a fluid or solid as a response to a pressure change. The compressibility values for the sample fractions at each moisture level were obtained from the same equipment used for tap density.

Hausner ratio is the ratio of average tap density to average bulk density of the sample (Equation 3.7). The Hausner ratio for each fraction was also provided by the software of the tap density equipment.

$$H_r = \frac{\rho_t}{\rho_b} \quad 3.7$$

### **3.3.6 Composition and energy determination**

#### ***3.3.6.1 Sample preparation***

According to ASTM standards E 872, the fractionated samples with geometric mean diameter above 1 mm were ground through a Wiley mill with screen size of 1mm for further size reduction to ensure thorough intermix and homogeneity of the samples. The size-adjusted samples were analyzed for energy, ash and volatile content.

#### ***3.3.6.2 Energy content***

The heating value of the sample fractions was measured using a bomb calorimeter (Model No. C200, IKA Works Inc., Wilmington, NC). Approximately 0.5 g of a sample was compressed with a press (Model No.-C21, IKA Works Inc., Wilmington, NC) to form a pellet and then placed in a steel container. Cotton thread connected to an ignition wire was used to ignite the sample after the sample was placed in the container and pressurized to 30 bars. The bomb calorimeter was filled with water and the pressurized steel container placed in the bomb calorimeter where combustion occurred. The heating value after the combustion process was displayed on the software screen provided by the manufacturer.

#### ***3.3.6.3 Ash content***

Ash content of the sample fractions was determined according to the NREL Laboratory Analytical Procedure (LAP, 2005). About  $1\text{g} \pm 0.1$  of the sample was placed in a crucible and then transferred into a muffle furnace (Model No.-F6020C, Thermoscientific, Dubue, IO). The furnace was programmed to heat up to  $105^{\circ}\text{C}$ , ramped to  $250^{\circ}\text{C}$  at  $10^{\circ}\text{C}/\text{minute}$  and held at this temperature for 30 minutes. After this, the temperature was ramped to  $575^{\circ}\text{C}$  at  $20^{\circ}\text{C}/\text{min}$  and held for 180 minutes and then finally lowered to  $105^{\circ}\text{C}$ . Crucibles and contents were then placed in the desiccator for 1 hour and allowed to cool to room temperature. The mass of the samples was

measured to 0.1 mg using a weighing balance. Ash content on dry basis was calculated according to equation 3.8.

$$\text{Ash (\% d.b)} = \left[ \frac{100(M_{cs} - M_{ca})}{M_{cs} - M_c} \right] - \left( \frac{100 M_{wb}}{100 - M_{wb}} \right) \quad 3.8$$

$M_{ca}$  is the mass of crucible and ash (g)

$M_c$  is the mass of the crucible (g)

$M_{cs}$  is the mass of crucible and sample before heating (g)

$M_{wb}$  is the moisture content on wet basis (% w.b)

#### **3.3.6.4 Volatile matter**

Volatile matter of the sample fractions was measured according to ISO 562 (ISO 562, 2010). About  $1\text{g} \pm 0.1$  of sample was placed in crucibles. The crucibles were placed in a volatile matter furnace (Model No.-VMF 10/6/3216P, Carbolite, Hope Valley, England) at  $900^\circ\text{C}$  for 7 mins. Crucibles and contents were then removed from the furnace and placed in a desiccator to cool down to room temperature. The final mass of the crucibles with sample was measured and the volatile matter ( $V_d$ ) on dry basis was calculated as follows;

$$V_d = \left[ \frac{100(M_2 - M_3)}{M_2 - M_1} \right] - \left( \frac{100 M_{wb}}{100 - M_{wb}} \right) \quad 3.9$$

$M_1$  is the mass of the empty crucibles with lid (g);

$M_2$  is the mass of the crucibles and sample with lid before heating (g);

$M_3$  is the final mass of the crucibles and sample with lid after heating (g);

$M_{wb}$  is the moisture content on wet basis (% w.b)

### **3.3.7 Experimental design and statistical analysis**

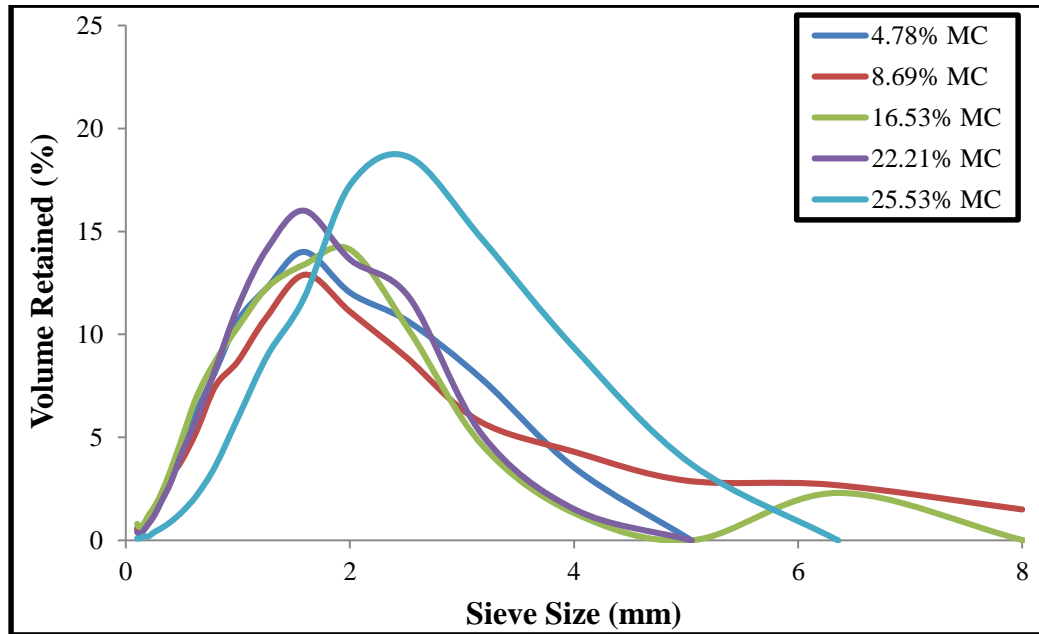
Particle size and moisture content of fractionated ground loblolly pine were the predictors while the response variable was the physical properties. Aside from the particle size distribution, all the experiments were carried out in triplicate.

Microsoft Excel 2010 was used in summarizing and generating graphs. A significant test ( $\alpha < 0.05$ ) using the Proc GLM procedure in the statistical software SAS 9.3 (SAS Institute Inc., Cary, NC) was conducted to show the effect of particle size and moisture content on the physical properties. The Tukey test was also used to compare the means of values of these properties at the different moisture contents and particle sizes. The results were presented in mean and standard deviation.

## **3.4 Results and Discussion**

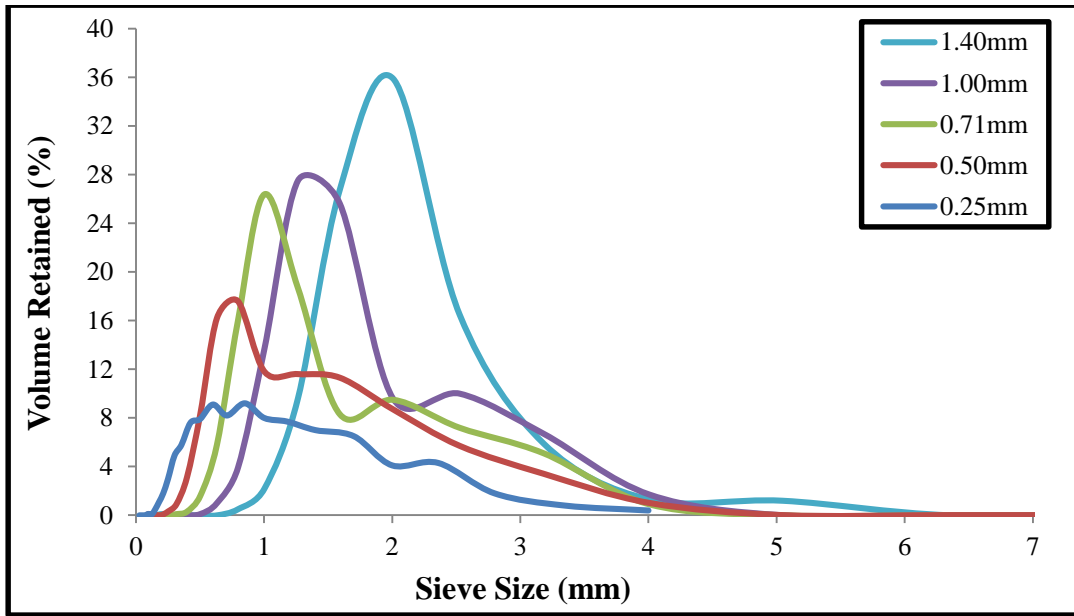
### **3.4.1 Particle size distribution**

Figure 3.1 shows the particle size distribution of the unfractionated ground loblolly pine. The curves are left skewed which represent naturally occurring particle population (Rhodes, 1998). A similar trend has been reported for biological materials (Probst et al., 2013; Yang et al., 1996; Mani et al., 2004). The particle size distributions of the unfractionated ground samples are unimodal. Also, at the 25.53% moisture levels, a wider distribution existed with most of the particles falling uniformly between 0 and 6 mm as compared to the other curves. This result is an indication of wider spread of particles at higher moisture level. Probst et al. (2013) also reported a similar result for ground corn at 10.39% moisture content having a narrower distribution and a wider distribution at higher moisture content of 16.02 and 19.64% (wb).



**Figure 3.1: Particle size distribution of unfractionated ground loblolly pine.**

Figure 3.2(a-f) shows the particle size distributions of the fractionated ground loblolly pine at the five moisture levels. As the size of the fraction increases, the particle size distribution move from been left skewed to a symmetric distribution. This change was more vivid with the particle distribution of fraction size 1.40 mm. The change in particle size distribution with increase in fraction size, shows that the log-normal distribution of biological materials is as a result of fine particles in the material. Benkovic and Bauman (2009) observed that powders with narrow particle size distributions have a better flow than powders with wider particle size distributions. Therefore, an increase in moisture content may cause a reduction in flowability. In Figure 3.2f, the particle size distributions of fractions retained on the pan (hereafter referred to as size 0.05mm based on ASABE Standards S319.3, 2008) are similar for all moisture levels except for 8.69% which had a narrow distribution. The narrow distribution is an indication of better flow. The distributions have multi-peaks which indicate that the samples can still be further separated into different fractions based on these peaks (Bernhart and Fasina, 2008).



**Figure 3.2a: Particle size distribution of fractionated ground loblolly pine at 4.78% moisture level.**

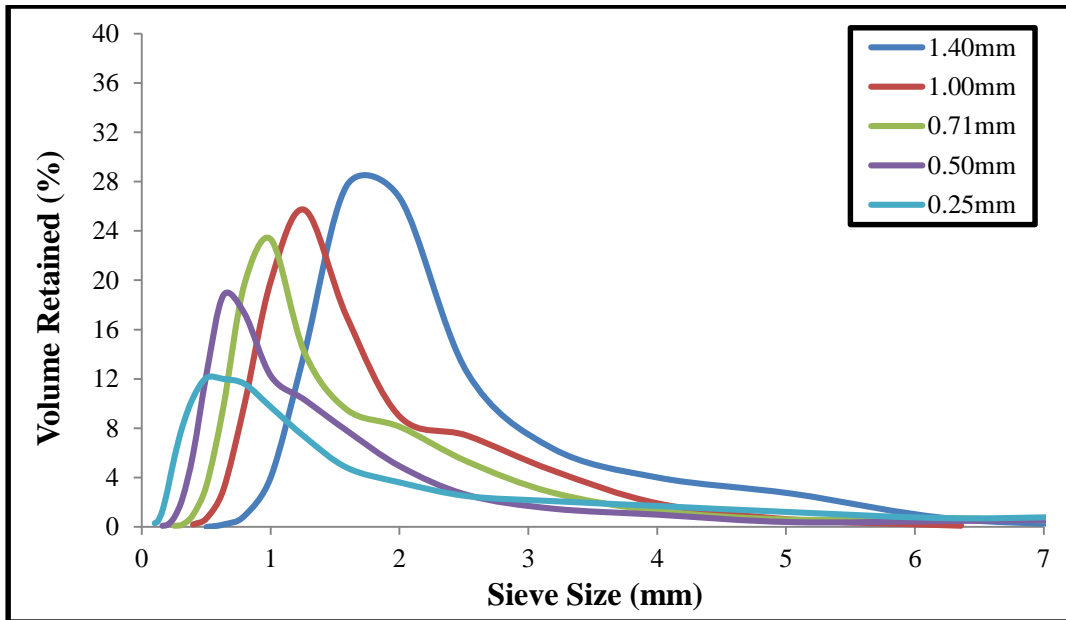


**Figure 3.2b: Particle size distribution of fractionated ground loblolly pine at moisture content of 8.69% (wb).**



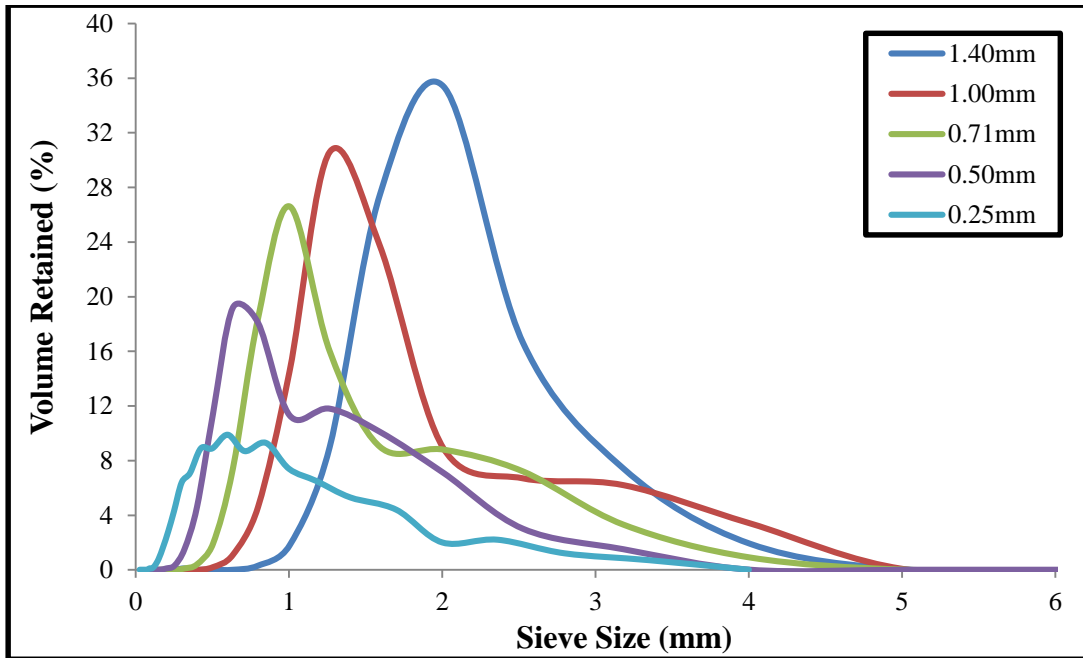


**Figure 3.2c: Particle size distribution of fractionated ground loblolly pine at moisture content of 16.53% (wb).**

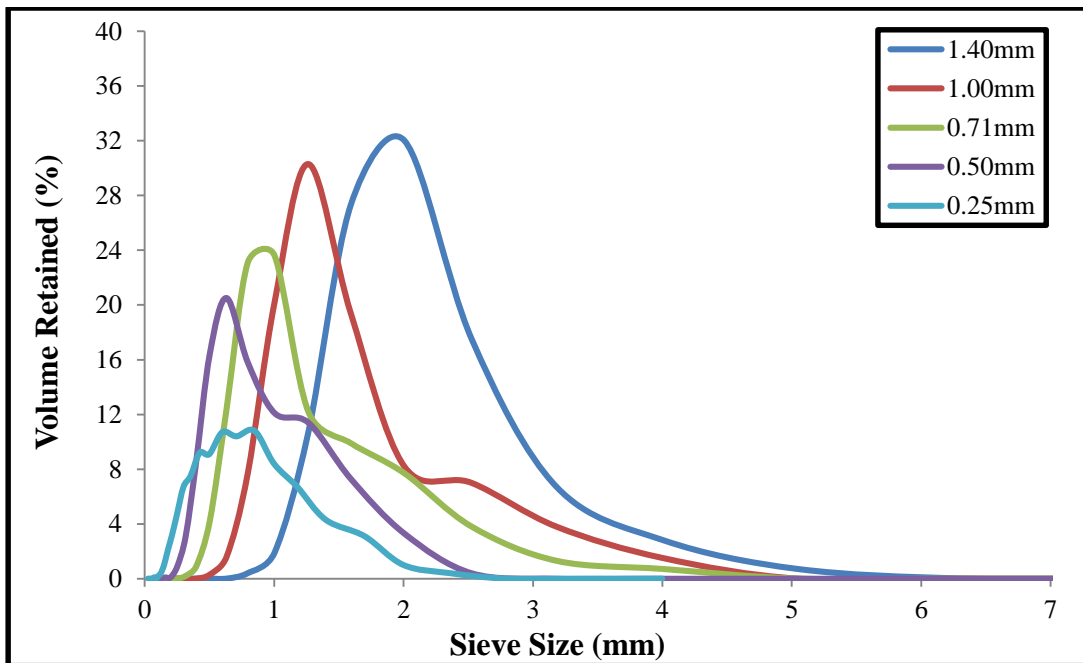


**Figure 3.2d: Particle size distribution of fractionated ground loblolly pine at moisture content of 22.21% (wb).**

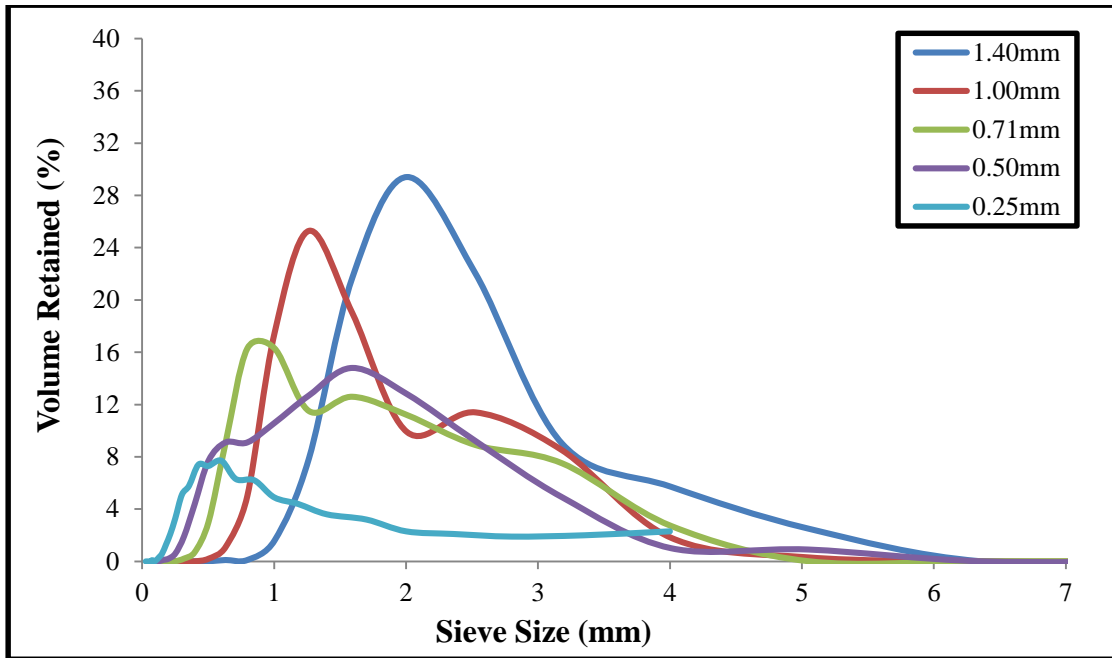


Figure 3.2e: Particle size distribution of fractionated ground loblolly pine at moisture content of 25.53% (wb).

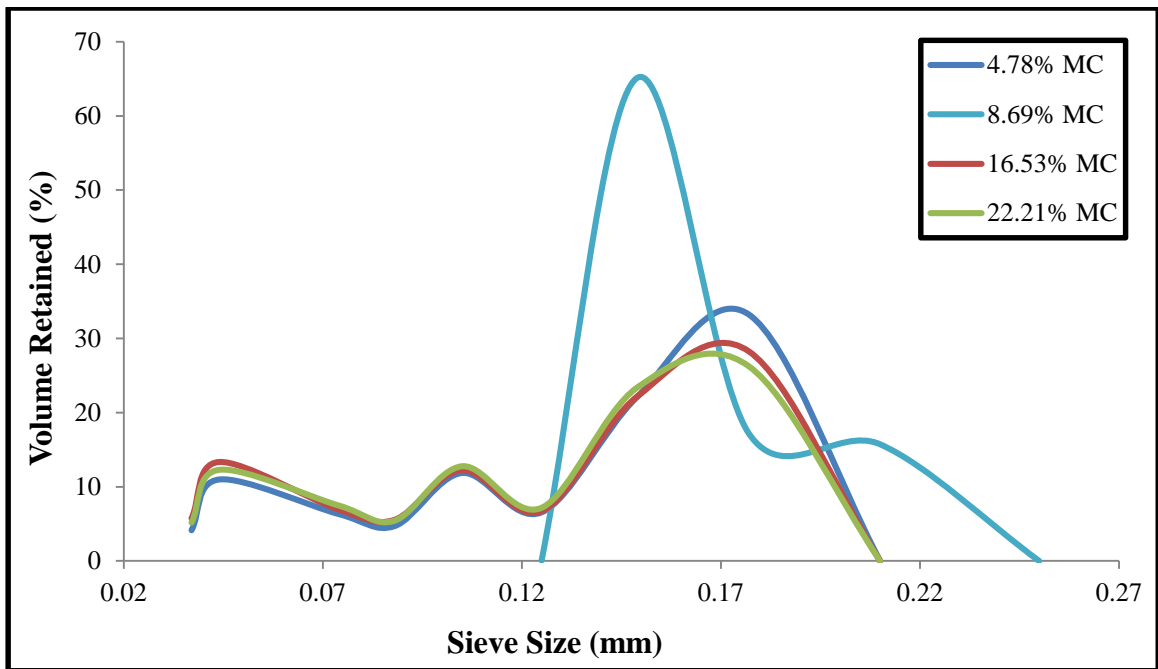


Figure 3.2f: Particle size distribution of fractions retained on the pan (size 0.05mm).

Table 3.1 shows the geometric mean diameters and geometric standard deviations of the fractionated and unfractionated ground samples. There was no fraction of size 0.05mm at 25.53% moisture level. Due to the high moisture content leading to increase particle size and stickiness between particles, particles did not pass through a screen size of 0.25mm, hence there was no fraction retained on screen size 0.05mm. The geometric mean diameters of the fractionated samples varied between 0.10 and 2.38 mm with fractions at the 25.53% moisture level having the highest geometric mean diameters. This shows that increased moisture content will lead to particle swelling hence increase in the particle size. However, it is generally considered that particles with sizes larger than 200  $\mu\text{m}$  are free flowing, while particle with sizes less than 200  $\mu\text{m}$  are subject to cohesion and flowability problem. The reduced flowability at smaller particle sizes is because of the increased surface area per unit mass of the powder. There is more surface area or surface contacts available for frictional forces to resist flow (Fitzpatrick, 2005; Teunou et al., 1999; Molenda et al., 2002). Therefore, ground loblolly pine fraction of size 0.05 mm and having geometric mean diameters between 0.10 and 0.15 mm is expected to be a source of flowability problem. An increase in the quantity of this fraction within the unfractionated ground sample will result in reduced flowability as well. Furthermore, the geometric mean diameter of the unfractionated ground sample which varies between 1.31 and 2.19 mm falls within the range of acceptable particle sizes needed for most biomass conversion processes.

**Table 3.1: Geometric mean diameters (mm) and geometric standard deviations of fractionated ground loblolly pine.**

Screen size (mm)	Moisture content (% wb)				
	4.78	8.69	16.53	22.21	25.53
<b>0.05</b>	0.11 ± 0.06	0.15 ± 0.03	0.10 ± 0.06	0.10 ± 0.05	NC*
<b>0.25</b>	0.85 ± 0.68	0.81 ± 0.72	0.70 ± 0.51	0.64 ± 0.41	0.86 ± 0.92
<b>0.50</b>	1.16 ± 0.69	0.97 ± 0.59	1.01 ± 0.55	0.84 ± 0.42	1.33 ± 0.90
<b>0.71</b>	1.38 ± 0.67	1.28 ± 0.68	1.33 ± 0.62	1.17 ± 0.53	1.46 ± 0.84
<b>1.00</b>	1.72 ± 0.70	1.54 ± 0.69	1.69 ± 0.69	1.55 ± 0.6	1.73 ± 0.75
<b>1.40</b>	2.16 ± 0.66	2.14 ± 0.83	2.17 ± 0.63	2.18 ± 0.67	2.38 ± 0.82
<b>Raw</b>	1.31 ± 1.00	1.36 ± 1.27	1.33 ± 1.12	1.39 ± 0.99	2.19 ± 1.39

NC\*: Experiment was not conducted at this moisture level

### 3.4.2 Bulk Density

Statistical analysis indicated that particle size and moisture content had a significant effect ( $p < 0.05$ ) on the bulk density (Table 3.2). Bulk density of the loblolly pine fractions significantly increased with increase in fraction size and with decrease in moisture content. The bulk densities ranged from 136.7 to 277.7 kg/m<sup>3</sup>. Lam et al. (2008) reported a similar result with an increase in the bulk density of fractionated switchgrass from 149 to 194 kg/m<sup>3</sup> as the particle size increased from 0.25 to 0.71 mm. The increased bulk density is attributed to the fact that biomass grinds collected after fractionation exhibit different packing as a result of particles having the same size as compared to the unfractionated biomass grinds which comprises of different particle size range. Liu et al. (2008) also reported an increase in the bulk density of fractionated ibuprofen powder from 350 to 440 kg/m<sup>3</sup> as particle size increased from 46 to 215  $\mu$ m.

**Table 3.2: Bulk density (kg/m<sup>3</sup>) of fractionated ground loblolly pine.**

Screen size (mm)	Moisture content level (% w.b)				
	4.78	8.69	16.53	22.21	25.53
0.05	162.53 <sup>[f,w]</sup> ±0.81	159.40 <sup>[f,w]</sup> ±3.27	141.69 <sup>[g,x]</sup> ± 0.47	136.67 <sup>[f,y]</sup> ±0.62	NC*
0.25	184.60 <sup>[e,w]</sup> ±2.25	179.28 <sup>[e,w]</sup> ±1.85	157.99 <sup>[f,x]</sup> ±1.81	146.64 <sup>[e,y]</sup> ±1.57	140.84 <sup>[f,z]</sup> ±2.88
0.50	205.02 <sup>[d,w]</sup> ±2.21	210.38 <sup>[d,w]</sup> ±2.98	176.02 <sup>[e,x]</sup> ±1.58	165.94 <sup>[d,y]</sup> ±5.46	159.46 <sup>[e,y]</sup> ±0.62
0.71	247.11 <sup>[c,w]</sup> ±2.47	247.58 <sup>[c,w]</sup> ±3.80	204.05 <sup>[d,x]</sup> ±1.76	186.65 <sup>[c,y]</sup> ±1.46	185.96 <sup>[d,y]</sup> ±1.86
1.00	265.30 <sup>[b,w]</sup> ±0.57	255.98 <sup>[b,x]</sup> ±1.69	227.09 <sup>[c,y]</sup> ±2.89	217.86 <sup>[b,z]</sup> ±2.75	220.52 <sup>[c,z]</sup> ±1.86
1.40	277.66 <sup>[a,w]</sup> ±1.31	272.37 <sup>[a,w]</sup> ±2.24	238.46 <sup>[b,y]</sup> ±2.29	234.22 <sup>[a,y]</sup> ±3.53	244.68 <sup>[a,x]</sup> ±0.35
Raw	266.83 <sup>[b,x]</sup> ±0.81	275.53 <sup>[a,w]</sup> ±1.93	232.51 <sup>[a,y]</sup> ±1.52	227.36 <sup>[a,z]</sup> ±0.46	234.04 <sup>[b,y]</sup> ± 1.84

Particle size effect: values in each column with same letter (a-f) are not significantly different (p<0.05).

Moisture effect: values in each row with same letter (w-z) are not significantly different (p<0.05).

NC\* experiment was not conducted because there was no fraction at 25.53% moisture level.

Effect of moisture content on bulk density of fractionated ground loblolly pine is similar to other published works on biological materials such as wormy compost (Bahram et al., 2013), switchgrass (Lam et al., 2007), soybean (Kashaninejad et al., 2008). The reduction in bulk density with increased moisture content is because of the increase in mass due to moisture gain being lower than the accompanying volumetric expansion of the bulk (Colley et al., 2006). The amount of storage space required for a ground loblolly pine will therefore increase with moisture content which will lead to increased cost of logistics. However, there was no significant difference in the bulk density at a moisture level of 4.78% and 8.69 % (wb) while there was a sharp drop in the bulk density from moisture content level of 8.69% to 16.53% (wb). The difference indicated that at lower moisture content, there was no significant change in bulk density hence, there may be no need to expend energy in drying the material to a moisture level of 4.78% (wb).

Abdullah and Geldart (1999) stated that a bulk solid with a strong structural strength will resist collapse when dispersed in a container and will have a low bulk density, while a structurally weak bulk solid will collapse easily and have a high bulk density. High friction between the particles results in a low bulk density. As fraction size decreases, the bulk density decreases, this implies that 0.05 mm and 0.25 mm fractions will have higher friction between their particles hence resulting in low bulk density values. High friction between particles is an indication of possible flowability problem. It is more pronounced as the moisture content increase. Fractions of sizes 1.40 mm and 1.00 mm had the highest bulk density values. Therefore, increased quantity of 1.40 mm and 1.00 mm fractions in the unfractionated ground sample may improve flowability of ground loblolly pine.

### **3.4.3 Tap Density**

Tap density represents an increased bulk density attained after mechanically tapping a bulk material and allowing it to fall under its own mass. Result of the statistical analysis of particle size and moisture effect on tap density of fractionated ground loblolly pine is presented in Table 3.3. The result showed that particle size and moisture content had a significant ( $p < 0.05$ ) on tap density of the fractionated samples. The tap density significantly increased with increase in fraction size and reduction in moisture content. The tap density ranged from 218.3 to 330.0 kg/m<sup>3</sup>. The tap density of the unfractionated sample was significantly higher than the fractionated sample. Tap density value is observed to have a higher value as compared to bulk density. This depicts that a reduction in volume of bulk material due to efficient packing of particles when subjected to vibration (e.g. during transportation) will result in increased density.

**Table 3.3: Tap density (kg/m<sup>3</sup>) of fractionated ground loblolly pine.**

Screen size (mm)	Moisture content level (w.b)				
	4.78 %	8.69%	16.53%	22.21%	25.53%
<b>0.05</b>	262.67 <sup>[d,w]</sup> ± 4.04	267.00 <sup>[de,w]</sup> ±1.00	232.00 <sup>[e,x]</sup> ±2.65	230.00 <sup>[d,x]</sup> ±1.00	NC*
<b>0.25</b>	247.00 <sup>[e,x]</sup> ± 2.00	258.33 <sup>[e,w]</sup> ±1.16	218.33 <sup>[d,z]</sup> ±2.08	223.00 <sup>[d,z]</sup> ±6.08	235.67 <sup>[e,y]</sup> ±1.53
<b>0.50</b>	264.67 <sup>[d,x]</sup> ± 0.58	276.67 <sup>[d,w]</sup> ±2.52	226.67 <sup>[e,y]</sup> ±0.58	222.00 <sup>[d,z]</sup> ±1.73	230.00 <sup>[e,y]</sup> ±1.00
<b>0.71</b>	309.67 <sup>[c,x]</sup> ± 1.53	318.00 <sup>[bc,w]</sup> ±1.73	252.00 <sup>[d,y]</sup> ±1.00	249.33 <sup>[c,y]</sup> ±2.31	251.00 <sup>[d,y]</sup> ±1.00
<b>1.00</b>	323.67 <sup>[b,w]</sup> ± 2.08	314.67 <sup>[c,x]</sup> ±1.53	275.33 <sup>[c,y]</sup> ±4.04	270.67 <sup>[b,y]</sup> ±0.58	277.33 <sup>[c,y]</sup> ±3.06
<b>1.40</b>	327.67 <sup>[b,w]</sup> ± 2.31	330.00 <sup>[b,w]</sup> ±3.46	287.00 <sup>[b,x]</sup> ±2.00	279.00 <sup>[b,y]</sup> ±2.65	286.67 <sup>[b,x]</sup> ±3.22
<b>Raw</b>	354.33 <sup>[a,w]</sup> ± 5.86	359.67 <sup>[a,w]</sup> ± 11.02	303.67 <sup>[a,x]</sup> ±0.58	303.67 <sup>[a,x]</sup> ±3.06	311.67 <sup>[a,x]</sup> ±1.53

Particle size effect: values in each column with same letter (a-f) are not significantly different (p<0.05).  
 Moisture effect: values in each row with same letter (w-z) are not significantly different (p<0.05).  
 NC\* experiment was not conducted because there was no fraction at 25.53% moisture level.

Volume reduction due to re-arrangement of particles after tapping may lead to difficulty in unloading the material from storage vessels (Bernhart and Fasina, 2009). The reduction in tap density with moisture increase further confirms the moisture content – density relationship previously discussed indicating that bulk volume increased at a rate faster than the mass of the bulk. This result signifies that a flow problem will exist due to vibration during the transport, loading and unloading of ground loblolly pine from storage vessels. The material will compact as a result of vibrations hence resulting in difficulties in unloading ground loblolly pine from transport vehicles. Similar trends have been reported for other biological materials (Lam et al., 2008; Bernhart and Fasina, 2009).

Because the inter-particulate interactions influencing the properties of a bulk material are also the interactions that interfere with its flow, a comparison of the bulk and tapped densities can

provide a measure of the relative importance of these interactions in a given material. Such a comparison is often used as an index representing the ability of the powder to flow (WHO, 2012). Such index include compressibility value and Hausner ratio.

#### **3.4.4 Hausner ratio**

Hausner ratio (ratio of tap density to bulk density) is used at times to characterize the flowability of bulk material (Table 2.2). The Hausner ratio of fractionated loblolly pine significantly decrease ( $p < 0.05$ ) from 1.6 to 1.2 with increase in fraction size from 0.05 to 1.40 mm (Table 3.4). Moisture content had no significant effect ( $p < 0.05$ ) on the Hausner ratio of unfractionated loblolly pine: 0.05, 1.00 and 1.40 mm fractions. However, there was a significant increase in the Hausner ratio with moisture content for 0.25, 0.50 and 0.71 mm fractions.

Size fractions of 0.05, 0.25, 0.50 and 0.71mm had a poor flow behavior while 1.00 and 1.40 mm fractions had a fair/good flow behavior. The results obtained for the Hausner ratio confirms that the reduction in volume after tapping of the 0.05 mm fractions was higher than the 1.40 mm fractions. Therefore, 0.05 mm fractions have higher tendency of becoming compacted or compressed due to vibration hence, resulting in flow problems.



**Table 3.4: Hausner ratio of fractionated ground loblolly pine.**

Screen size (mm)	Moisture Content Level (w.b)				
	4.78 %	8.69%	16.53%	22.21%	25.53%
<b>0.05</b>	1.50 <sup>[a,w]</sup> ± 0.06	1.59 <sup>[a,w]</sup> ±0.09	1.52 <sup>[a,w]</sup> ±0.01	1.59 <sup>[a,w]</sup> ±0.01	NC*
<b>0.25</b>	1.27 <sup>[bc,z]</sup> ± 0.01	1.39 <sup>[b,xy]</sup> ±0.02	1.35 <sup>[b,y]</sup> ±0.02	1.44 <sup>[b,x]</sup> ±0.01	1.62 <sup>[a,w]</sup> ±0.05
<b>0.50</b>	1.27 <sup>[bc,y]</sup> ± 0.05	1.30 <sup>[bc,xy]</sup> ±0.03	1.28 <sup>[c,y]</sup> ±0.03	1.38 <sup>[c,wx]</sup> ±0.01	1.43 <sup>[b,w]</sup> ±0.01
<b>0.71</b>	1.24 <sup>[bc,y]</sup> ± 0.03	1.27 <sup>[bc,xy]</sup> ±0.03	1.26 <sup>[cd,xy]</sup> ±0.03	1.31 <sup>[d,wx]</sup> ±0.01	1.34 <sup>[c,w]</sup> ±0.03
<b>1.00</b>	1.22 <sup>[c,w]</sup> ± 0.00	1.25 <sup>[c,w]</sup> ±0.01	1.22 <sup>[de,w]</sup> ±0.01	1.25 <sup>[e,w]</sup> ±0.00	1.25 <sup>[d,w]</sup> ±0.03
<b>1.40</b>	1.21 <sup>[c,w]</sup> ± 0.04	1.23 <sup>[c,w]</sup> ±0.07	1.17 <sup>[e,w]</sup> ±0.01	1.21 <sup>[f,w]</sup> ±0.01	1.21 <sup>[d,w]</sup> ±0.01
<b>Raw</b>	1.34 <sup>[b,w]</sup> ± 0.06	1.31 <sup>[bc,w]</sup> ±0.02	1.31 <sup>[bc,w]</sup> ±0.02	1.33 <sup>[d,w]</sup> ± 0.01	1.34 <sup>[c,w]</sup> ± 0.04

Particle size effect: values in each column with same letter (a-f) are not significantly different (p<0.05).  
 Moisture effect: values in each row with same letter (w-z) are not significantly different (p<0.05).  
 NC\* experiment was not conducted because there was no fraction at 25.53% moisture level.

### 3.4.5 Compressibility

Compressibility is a measure of the increase in strength of powder-like materials with increase in consolidating pressure. Statistical analysis showed that there was a significant reduction (p<0.05) in compressibility with increase in particle size. As reported earlier for moisture effect on the Hausner ratio, moisture content had no significant effect on compressibility of unfractionated samples and size fraction of 0.05, 1.00 and 1.40mm while there was a significant increase (p<0.05) in compressibility of size fractions 0.25, 0.50 and 0.71mm with increase in moisture content (Table 3.5). This is because Hausner ratio and compressibility values are obtained from the same values of bulk and tap density. The compressibility value ranged from 17.3% to 38.3%.

**Table 3.5: Compressibility (%) of fractionated ground loblolly pine.**

Screen size (mm)	Moisture content level (w.b)				
	4.78 %	8.69%	16.53%	22.21%	25.53%
<b>0.05</b>	33.07 <sup>[a,w]</sup> ±2.81	36.93 <sup>[a,w]</sup> ±3.45	34.27 <sup>[a,w]</sup> ±0.61	37.20 <sup>[a,w]</sup> ±0.40	NC*
<b>0.25</b>	21.47 <sup>[bc,z]</sup> ±0.61	28.00 <sup>[b,xy]</sup> ±0.80	25.73 <sup>[b,y]</sup> ±1.29	30.53 <sup>[b,x]</sup> ±0.61	38.27 <sup>[a,w]</sup> ±1.80
<b>0.50</b>	21.33 <sup>[bc,y]</sup> ±3.23	23.20 <sup>[bc,xy]</sup> ±1.60	21.60 <sup>[c,y]</sup> ±1.83	27.33 <sup>[c,wx]</sup> ±0.61	30.27 <sup>[b,w]</sup> ±0.23
<b>0.71</b>	19.33 <sup>[bc,y]</sup> ±1.80	21.20 <sup>[c,xy]</sup> ±1.83	20.27 <sup>[cd,y]</sup> ±1.89	23.73 <sup>[d,wx]</sup> ±0.46	25.20 <sup>[c,w]</sup> ±1.44
<b>1.00</b>	18.13 <sup>[c,w]</sup> ±0.23	19.73 <sup>[c,w]</sup> ±0.46	17.73 <sup>[de,w]</sup> ±0.92	20.13 <sup>[e,w]</sup> ±0.23	19.87 <sup>[d,w]</sup> ±1.97
<b>1.40</b>	17.33 <sup>[c,w]</sup> ±2.44	18.67 <sup>[c,w]</sup> ±4.62	14.80 <sup>[e,w]</sup> ±0.40	17.33 <sup>[f,w]</sup> ±0.46	17.60 <sup>[d,w]</sup> ±0.69
<b>Raw</b>	25.33 <sup>[b,w]</sup> ±3.63	23.73 <sup>[bc,w]</sup> ± 0.92	23.73 <sup>[bc,w]</sup> ± 0.92	24.93 <sup>[d,w]</sup> ± 0.61	25.07 <sup>[c,w]</sup> ±2.05

Particle size effect: values in each column with same letter (a-f) are not significantly different (p<0.05).  
 Moisture effect: values in each row with same letter (w-z) are not significantly different (p<0.05).  
 NC\* experiment was not conducted because there was no fraction at 25.53% moisture level.

Compressibility is a measure of flowability - the greater the compressibility of a bulk solid, the less flowable it is (Ganesan et al., 2008). This shows that 0.05 mm fraction is more compressible and would be less flowable during unloading from storage vessels. This is also in accordance with the results obtained for the other physical properties showing that at increased moisture content and reduced particle size; the material becomes more compressible hence resulting in flowability problem. The difficult flow behavior that characterizes ground loblolly pine at high moisture content is attributable to the formed liquid bridges between particles thereby making them more cohesive (Teunou and Fitzpatrick, 1999). Also as moisture content increases, biological materials become softer thus deformation of the material is greater at higher moisture contents (Bernhart and Fasina, 2009) which might result in unloading difficulty of materials from storage or transport vessels.

### 3.4.6 Particle density

Table 3.6 shows the effect of particle size and moisture content on the particle density of ground loblolly pine fractions. Significant test ( $p < 0.05$ ) showed that particle size and moisture had a significant effect on particle density. The particle density of the fractionated ground loblolly pine varied from 1382.8 to 1497.1 kg/m<sup>3</sup>. The particle density was observed to generally decrease with increase in fraction size however at a moisture content level of 4.78 % (wb), there was no significant difference ( $p < 0.05$ ) in the particle densities of the loblolly pine fractions. This may be due to shrinkage of the particles hence nullifying particle size effect on particle density at lower moisture content. Mani et al. (2004) reported a reduction in the particle density of corn stover from 1210 to 1085 kg/m<sup>3</sup> with increase in particle size from 0.41 to 0.68 mm. The authors asserted that the decrease in particle density may be due to reduction in porosity of the ground corn stover when the particles are reduced to a smaller size.

Particle density was highest at 16.53% moisture level giving a distinction between the particle densities at 4.78% and 8.69% moisture levels and the particle densities at 22.21% and 25.53% moisture levels. The particle densities at 4.78% and 8.69% moisture levels were higher than that of 22.21% and 25.53% moisture levels. The decline in particle density with increased moisture content is due to the volumetric expansion of the particles, occurring at a faster rate than the increase in mass of particles due to addition of moisture (McMullen et al., 2005). Bahram et al., (2013) reported a particle density reduction from 1652 to 1443 kg/m<sup>3</sup> of wormy compost with an increase in moisture content from 25 to 35% (wb).

**Table 3.6: Particle density (kg/m<sup>3</sup>) of fractionated ground loblolly pine.**

Screen size (mm)	Moisture content level (% w.b)				
	4.78	8.69	16.53	22.21	25.53
0.05	1464.10 <sup>[a,x]</sup> ± 2.63	1460.23 <sup>[b,x]</sup> ± 5.95	1485.60 <sup>[a,w]</sup> ± 6.18	1440.47 <sup>[a,y]</sup> ± 2.74	NC*
0.25	1464.23 <sup>[a,wx]</sup> ± 0.15	1459.77 <sup>[b,wx]</sup> ± 5.53	1486.50 <sup>[a,w]</sup> ± 2.71	1437.47 <sup>[a,xy]</sup> ± 2.71	1411.53 <sup>[ab,y]</sup> ± 2.82
0.50	1464.53 <sup>[a,x]</sup> ± 0.99	1454.27 <sup>[bc,x]</sup> ± 3.35	1493.83 <sup>[a,w]</sup> ± 7.41	1423.33 <sup>[b,y]</sup> ± 0.25	1421.97 <sup>[a,y]</sup> ± 9.58
0.71	1462.93 <sup>[a,w]</sup> ± 2.19	1448.80 <sup>[bc,x]</sup> ± 4.46	1455.83 <sup>[bc,wx]</sup> ± 5.07	1412.50 <sup>[c,y]</sup> ± 2.85	1411.27 <sup>[ab,y]</sup> ± 6.44
1.00	1462.43 <sup>[a,w]</sup> ± 1.08	1443.93 <sup>[c,x]</sup> ± 4.80	1462.03 <sup>[b,w]</sup> ± 7.49	1413.20 <sup>[c,y]</sup> ± 3.92	1401.10 <sup>[ab,y]</sup> ± 8.67
1.40	1459.43 <sup>[a,x]</sup> ± 4.22	1497.13 <sup>[a,w]</sup> ± 6.25	1459.20 <sup>[bc,x]</sup> ± 1.31	1415.60 <sup>[c,y]</sup> ± 2.46	1382.77 <sup>[b,z]</sup> ± 3.42
Raw	1459.30 <sup>[a,w]</sup> ± 2.85	1445.13 <sup>[c,x]</sup> ± 3.89	1444.10 <sup>[c,x]</sup> ± 5.37	1417.80 <sup>[bc,y]</sup> ± 0.40	1387.50 <sup>[ab,z]</sup> ± 0.40

Particle size effect: values in each column with same letter (a-f) are not significantly different (p<0.05).

Moisture effect: values in each row with same letter (w-z) are not significantly different (p<0.05).

NC\* experiment was not conducted because there was no fraction at 25.53% moisture level.

Particle density measures the density of the particle matter excluding the air pores, hence it is called true density (Ileleji and Rosentrater, 2008). This shows that reduction of pore spaces within particles will lead to higher density hence resulting in flowability problem as the material will have higher compressibility. Therefore, the higher particle density of the fine fraction at screen size of 0.05 mm and 0.25 mm is an indication of reduced flowability. Also, their particle densities are significantly higher than the particle density of the unfractionated sample. This shows that a large quantity of these fine fractions in unfractionated ground loblolly pine will lead to difficulty in effective discharge of ground loblolly pine from storage vessels.

### 3.4.7 Porosity

Porosity measures the pore spaces between particles. It was found to significantly increased (p< 0.05) from 0.81 to 0.91 with decrease in fraction size from 1.40mm to 0.05mm and increase in moisture content from 4.78% to 25.53% (wb) (Table 3.7). An average porosity calculation of

0.4 is normal for spheroid particles, whereas irregular shaped or very small particulates have higher porosity values (Woodcock and Mason, 1987). The porosities of the loblolly pine fractions are higher than 0.4 which is an indication of highly irregular shaped particles. The shape irregularities of the particles can be attributed to the size reduction process of using hammer mill for loblolly pine wood chips. Lam et al., (2008) reported that the porosity of switchgrass decreased from 0.87 to 0.82 with increase in particle size from 0.25 to 0.71 mm. Based on the data of Bahram et al. (2013), the porosity of wormy compost varied between 0.52 – 0.45, and reduced with increase in moisture content. Manickam and Suresh (2011) also reported a reduction in the porosity of coir pith from 0.86 to 0.62 with an increase in moisture content from 10.1% to 60.2% (wb). The values obtained for these biological materials are also typical of extremely irregular-shaped particles that have cohesive tendencies (Woodcock and Mason, 1987).

High porosity value is an indication of highly compressible material. Therefore, the reduced particle size and increase in moisture content resulting in increased porosity leads to ground loblolly pine becoming more compressible and compactable. This will therefore lead to flow problem as the particles sticks tightly together after compression and compaction.

**Table 3.7: Porosity of fractionated ground loblolly pine.**

Screen Size (mm)	Moisture Content Level (w.b)				
	4.78 %	8.69%	16.53%	22.21%	25.53%
<b>0.05</b>	0.889 <sup>[a,x]</sup>	0.891 <sup>[a,x]</sup>	0.905 <sup>[a,w]</sup>	0.905 <sup>[a,w]</sup>	NC*
<b>0.25</b>	0.874 <sup>[b,y]</sup>	0.877 <sup>[b,y]</sup>	0.893 <sup>[b,x]</sup>	0.898 <sup>[b,wx]</sup>	0.900 <sup>[a,w]</sup>
<b>0.50</b>	0.860 <sup>[c,y]</sup>	0.855 <sup>[c,y]</sup>	0.882 <sup>[c,x]</sup>	0.883 <sup>[c,wx]</sup>	0.887 <sup>[b,w]</sup>
<b>0.71</b>	0.831 <sup>[d,y]</sup>	0.829 <sup>[d,y]</sup>	0.859 <sup>[d,x]</sup>	0.867 <sup>[d,w]</sup>	0.868 <sup>[c,w]</sup>
<b>1.00</b>	0.818 <sup>[e,x]</sup>	0.823 <sup>[e,x]</sup>	0.845 <sup>[e,w]</sup>	0.846 <sup>[e,w]</sup>	0.843 <sup>[d,w]</sup>
<b>1.40</b>	0.810 <sup>[f,z]</sup>	0.818 <sup>[f,y]</sup>	0.839 <sup>[f,w]</sup>	0.835 <sup>[f,w]</sup>	0.823 <sup>[f,x]</sup>
<b>Raw</b>	0.817 <sup>[e,y]</sup>	0.809 <sup>[g,z]</sup>	0.837 <sup>[f,w]</sup>	0.840 <sup>[f,w]</sup>	0.831 <sup>[e,x]</sup>

Particle size effect: values in each column with same letter (a-f) are not significantly different ( $p < 0.05$ ).  
 Moisture effect: values in each row with same letter (w-z) are not significantly different ( $p < 0.05$ ).  
 NC\* experiment was not conducted because there was no fraction at 25.53% moisture level.

### 3.4.8 Compositional analysis

#### 3.4.8.1 Energy content

Figure 3.3 shows the effect of particle size on energy content of fractionated ground loblolly pine. Statistical analysis showed that particle size had no significant effect ( $p < 0.05$ ) on energy content of ground loblolly pine. The energy content was between 18-19 MJ/kg. Similar results were reported by Garcia et al. (2012) for miscanthus (18.1 MJ/kg), coffee husk (18.3 MJ/kg) and walnut shell (18.4 MJ/kg) but higher than other biological materials such as sorghum (11.9 MJ/kg), barley (16.5 MJ/kg) and wheat bran (17.4 MJ/kg). The high energy content value recorded for loblolly pine as compared to other biological materials is confirmed by its low ash content (see Figure 3.5), which is an indication of large amount of combustible material which are primarily carbon and hydrogen (Fasina, 2006).

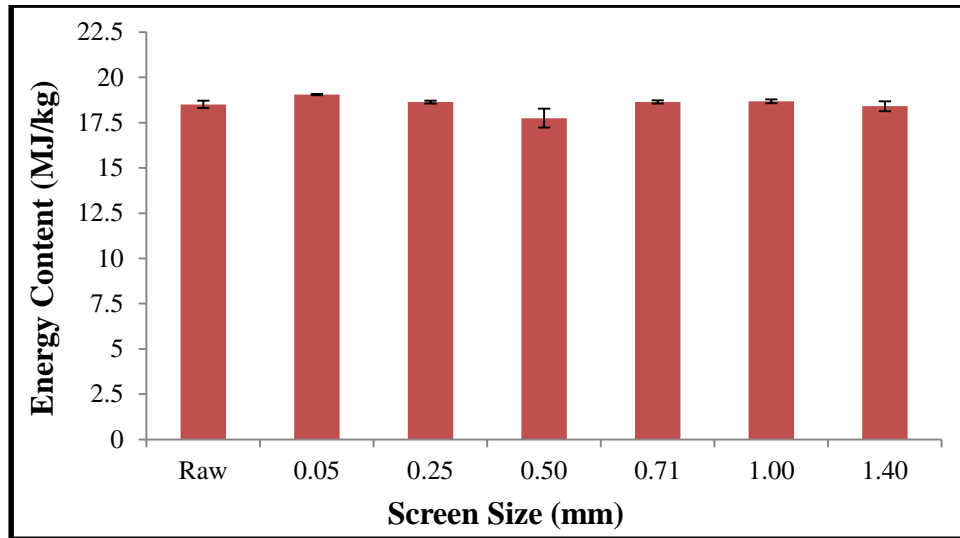


**Figure 3.3: Particle size effect on energy content of fractionated loblolly pine.**

#### **3.4.8.2 Ash content**

Ash content is a measure of amount of inorganic components in material. It represents the bulk mineral materials left over after combustible elements of a material are given off during combustion. The ash content of the fractionated ground loblolly pine is presented in Figure 3.4. Statistical analysis showed that particle size had a significant effect ( $p < 0.05$ ) on the ash content of ground loblolly pine. The ash content values (db) were between 0.22% and 2.64%. The ash content increased with reduction in the particle size. The low ash content of ground loblolly pine corroborate the results obtained for energy content showing that loblolly pine contains large amount of combustible material which are primarily carbon and hydrogen. The ash content obtained for the loblolly pine is low as compared to other biological materials such as rice straw (18.67% db), switchgrass (8.97% db), wheat straw (7.02% db) and rice hulls (20.26% db) (Jenkins et al., 1998). Information on ash content of ground loblolly pine is essential for the choice of an appropriate combustion and gas cleaning technologies. Also, ash deposit formation, fly ash emissions and ash handling as well as ash utilization/disposal options are dependent on this parameter (Oberberger, 1997; CEN/TC, 2003). The low ash content value of ground loblolly pine

shows that there will be a low deposit of bulk inorganic material after its combustion. Published works had shown that woody biomass has a relatively low amount of ash. For example, coniferous and deciduous wood without bark have 0.30% (db) of ash content and short rotation coppice willow has a 2.0% (db) ash content (CEN/TC, 2003).

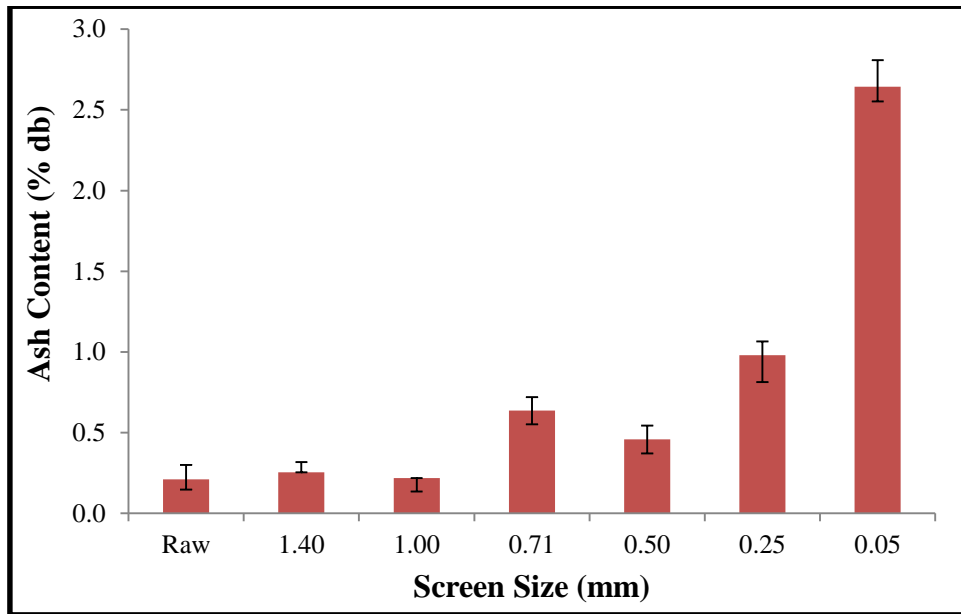


**Figure 3.4: Particle size effect on ash content of fractionated loblolly pine.**

### 3.4.8.3 Volatile matter

Volatile matter refers to the components of a material except for moisture, which are liberated at a high temperature in the absence of air. It is an indication of the burning characteristics of a material. Statistical analysis showed that particle size had no significant effect ( $p < 0.05$ ) on the volatile matter of the fractionated ground loblolly pine (Figure 3.5). The volatile matter ranged from 84.55% to 85.38% (db). The high volatile matter value is an indication that ground loblolly pine possesses low fixed carbon and can therefore be easily ignited. Jenkins et al (1998) reported similar results for sugarcane bagasse (85.61% db) and hybrid poplar (84.81% db) while lower values were reported for biological materials such as wheat straw (75.27% db), switchgrass (76.69% db) and rice hulls (63.52% db).



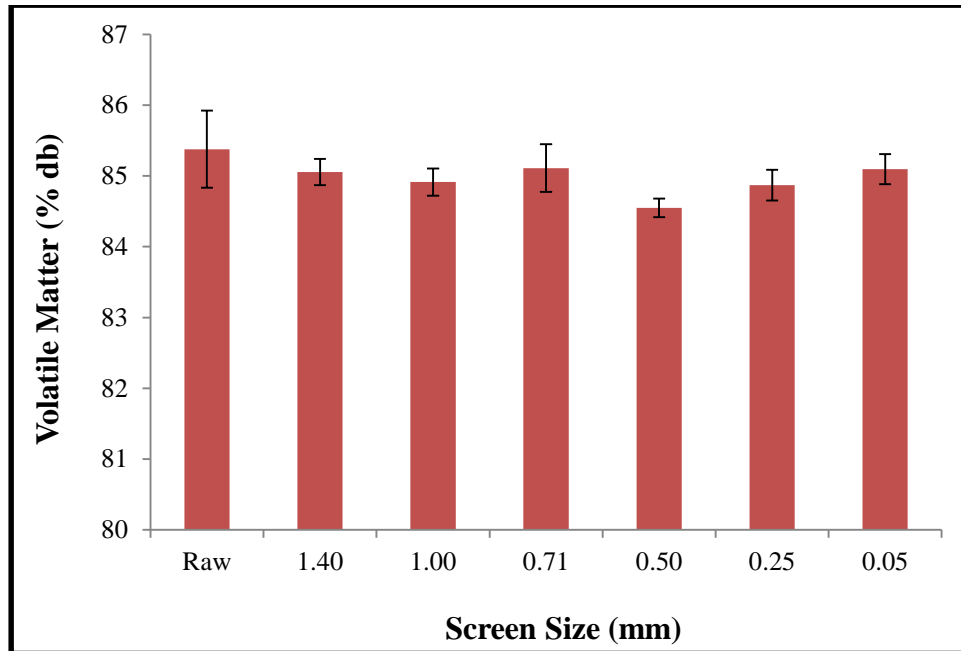


**Figure 3.5: Particle size effect on volatile matter of fractionated loblolly pine.**

### 3.5 Conclusion

In this study, ground loblolly pine was fractionated into six sizes. The physical and compositional properties of the fractionated samples were quantified at five moisture levels. It was found that:

- Reduction in particle size and increased moisture content were found to influence the physical properties of the ground loblolly pine and resulting into possible flow problem. This is further characterized in chapter 4. The bulk and tap densities were found to increase with increase in fraction size while particle density generally decreased with increase in fraction size. The porosity, Hausner ratio and compressibility of the fractions were also found to decrease with increase in the size of the fraction. Furthermore, increased moisture content was found to significantly cause a reduction in the densities (bulk, tap and particle) and porosity however, it had no significant effect on hausner ratio and compressibility.

- The heating value of the fractions which was found to be 18-19 MJ/kg and volatile matter (84.91 - 87.48% d.b) were not significant affected by particle size but the ash content was found to increase with reduction in the size of the fraction.

The results of this work can be used in conjunction with the flow properties of the ground loblolly pine in designing and selecting the appropriate storage and handling vessels. Also, information on the compositional properties influences the choice of an appropriate conversion system and gas cleaning technologies for ground loblolly pine.

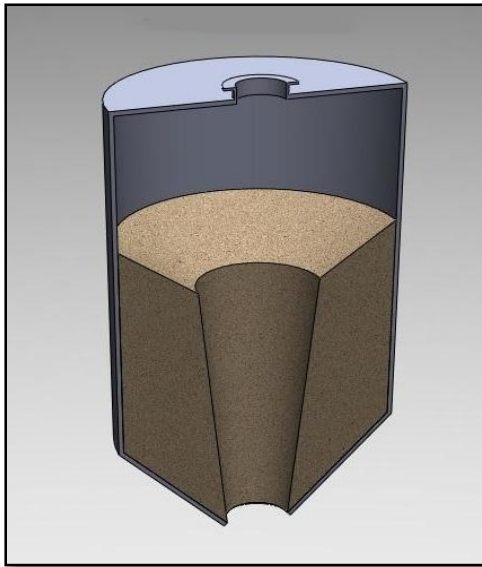
## **CHAPTER 4: Particle size and moisture effect on flow properties of fractionated ground loblolly pine and sensitivity of silo design parameters to flow properties**

### **4.1 Abstract**

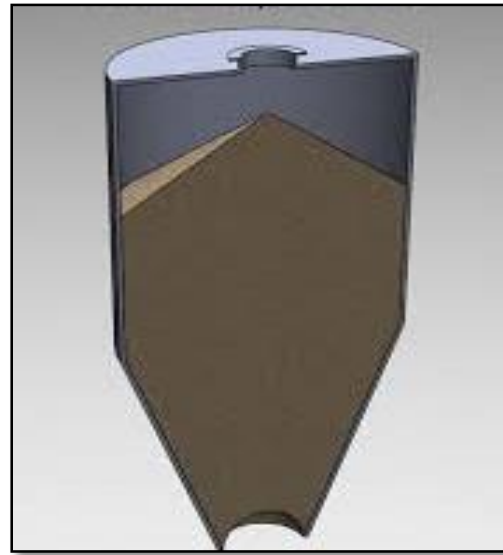
The flow properties of fractionated ground loblolly pine were quantified with analysis conducted on the sensitivity of silo design parameters to change in flow and physical properties. Flow index values of 4.11, 4.17 and 4.29 were recorded for fractions of size 1.40 mm at moisture content levels of 4.78%, 8.69% and 16.53% respectively. However, a reduction in flowability was observed when the 1.40 mm fraction was dosed with 0.50 mm fractions. Lower angles of wall friction were obtained at lower moisture contents when stainless steel and mild steel surfaces were used. Tivar 88 wall surface had low angles of wall friction ranging from 10.88 to 15.54° at all the moisture levels. Sensitivity analysis indicated that there was a reduction in the hopper half angle with increased moisture content and reduction in the fraction size. The hopper half angle also decreased with increase in angle of wall friction. The adjusted hopper outlet sizes varied between 1.20 and 28.56 mm. The wall normal and vertical pressure acting on the cylindrical section of the silo increased from 9.35 to 45.42 kPa and 15.34 to 48.91 kPa respectively with increase in fraction size and decrease in moisture content. The initial fill and flow induced pressures acting on the hopper section of the silo increased from 15.34 to 48.91 kPa and 24.71 to 78.79 kPa respectively with increase in fraction size and decrease in moisture content.

## 4.2 Introduction

Bulk material handling operations are key operations in process industries such as food, chemicals and pharmaceuticals industries (Opalinski et al., 2012). In order to ensure a successful production operation, a consistent and reliable flow of bulk materials from storage vessels without dust generation and flow obstruction are required. However, two major flow problems are associated with bulk solid handling, namely ratholing and arching. An arch (Figure 4.1a) is a stable obstruction that forms with the hopper section usually near the bin outlet. The arch has enough strength to support the rest of the bin's content hence preventing the discharge of the remaining content. A rathole (Figure 4.1b) is a stable pipe or vertical cavity that empties above the bin outlet. The silo content in the stagnant zones remains stationary until an external force is applied to dislodge it. Ratholing and arching can result in structural failure of silos, process inefficiencies and frequent equipment downtime (Prescott and Barnum, 2000; Johanson, 2002; Merrow, 1988).



(a) Cohesive arching



(b) Ratholing

**Figure 4.1: Typical flow problems associated with bulk solids (Source: *jenike.com*).**

Silo design requires information about the flow properties of the bulk material. These include unconfined yield strength, major consolidation stress, flow index, angle of internal friction, angle of wall friction, cohesion and bulk density. Flow properties are used in the design of discharge hoppers, hopper opening size, hopper half angle (to the vertical) and estimation of silo wall pressures. The hopper opening size is selected in order to ensure that arching (the flow problem related with mass flow pattern) does not occur and the required flow rate is achieved (Roberts, 1994). The minimum hopper half angle is needed for mass flow, the preferred flow pattern for a consistent and reliable flow. If the hopper half angle is less than the minimum, then it is likely that a funnel flow pattern will exist (Holdich, 2002; Teunou et al., 1999; Fitzpatrick, 2007; Iqbal and Fitzpatrick, 2006). A detailed description of Jenike's methodology for hopper design is found in the chapter 2 (subsection 2.6.4) of this thesis work.

Several studies have been documented on the contribution of particle size and moisture content to flow properties of biological materials (Kashaninejad et al., 2008; Bahram et al., 2013; Iqbal and Fitzpatrick, 2006; Teunou et al., 1999). The design and selection of an efficient storage vessel for ground loblolly pine requires a fundamental understanding of the impact of particle size and moisture content on the flow properties of the ground material. Therefore the objectives of this work are to:

1. quantify the effect of particle size and moisture content on the flow properties of fractionated ground loblolly pine;
2. investigate the sensitivity of silo design parameters to the physical and flow properties.

## **4.3 Materials and Methods**

### **4.3.1 Sample preparation**

Clean loblolly pine wood chips used in this study were collected from West Fraser Inc. Sawmill, Opelika, Alabama. Before use, the samples were ground through a 3.18 mm screen using a hammer mill (Model 358, New Holland grinder, New Holland, PA).

Experiments were carried out on the ground samples at five moisture content levels between 4.78% and 25.56% (wb). The initial moisture content of the samples after grinding was 8.69% (wb). To adjust the moisture content of the samples to the desired level, the samples were either dried using a humidity chamber (ESL-2CA, Espec North America, Inc.) set at a temperature of 50°C and relative humidity of 20% (for moisture content reduction) or the samples were sprayed with a known quantity of water (to increase the moisture content of samples). After moisture adjustment, the samples were stored in an air tight container for 24 hours to allow moisture equilibration to take place. The moisture contents of the samples were then verified with a moisture analyzer (Model MB 45, Ohaus Corporation, Pine Brook, NJ).

A sieve shaker (RO-TAP Model RX- 29, WS Tyler, OH) was thereafter used in fractionating the moisture adjusted ground samples into six fractions by fitting the sieve shaker with #12 (1.4 mm aperture), #18 (1.0 mm aperture), #25 (710 µm aperture), #35 (500 µm aperture), #60 (250 µm aperture) screens and pan. The choice of sieve sizes was based on preliminary study on the particle size distribution of the unfractionated ground samples. At each moisture level, the flow properties of the fractions were carried out and recorded.

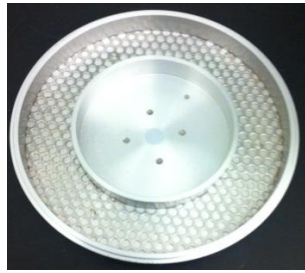
### **4.3.2 Flow properties**

A powder flow tester (Powder Flow 230VAC, Brookfield Engineering Laboratories, Inc., Middleboro, MA) was used to quantify the flow behavior of the samples. The tester (Figure 4.2a)

is equipped with a 152.4 mm diameter annular split cell (Figure 4.2c) and a vane lid (with 18 small compartments). The vane lid (Figure 4.2b) is used to trap the sample particles and cause them to shear against the sample particles in the trough.



**b) Vane Lid**



**c) Sample Trough**



**a) Powder Flow Tester**

**Figure 4.2: Powder flow tester and accessories.**

To run a flow test, the mass of a test sample that filled the space between the inner and outer rings of the sample trough was recorded. The software provided by the equipment manufacturer was activated. This caused the lid to descend to a position slightly above the sample in the trough. The axial load and the torsional load test data were automatically recorded by the software. These load data are then used to calculate the cohesion, angle of internal friction, flow function, major consolidating stress, and unconfined yield strength. This procedure was carried out in triplicate for each test sample.

### 4.3.3 Wall friction properties

Wall friction properties were determined by the flow tester using the procedure similar to that used for the flow properties determination. Instead of the annular vane lid, the flow tester was fitted with a smooth bottom surface lid that was manufactured with the wall material of interest. The three wall surfaces that were tested in this study are stainless steel, mild steel or Tivar 88. The angles of wall friction of the sample on these surfaces were obtained from this test.

### 4.3.4 Hopper design calculation

Silo design involves the bulk material properties, geometric design (to prevent arching, ratholing and to ensure proper flow pattern) and structural design (distribution of pressure and shear stresses on walls caused by stored materials). Conical hopper geometry was designed using the works of Enstad (1981) and Jenike (1964). Details of the symbols and nomenclatures used in the equations are presented in Appendix A.

#### 4.3.4.1 Hopper half angle

Hopper half angle was determined using the following equations:

$$\alpha = \frac{\pi}{2} - \frac{1}{2} \cos^{-1} \left[ \frac{1 - \sin \delta}{2 \sin \delta} \right] - \beta \quad 4.1$$

where:

$$\beta = \frac{\phi_w + \sin^{-1} \left[ \frac{\sin \phi_w}{\sin \delta} \right]}{2} \quad 4.2$$

As a margin of safety in silo design, the hopper half angle is reduced by 3°.

#### 4.3.4.2 Minimum hopper outlet size

Hopper outlet size was determined by evaluating for cohesive arching tendency. The procedure involves calculation of flow function (FF) and flow factor (ff) from equations 4.3 and 4.4 respectively.

$$\text{Flow Function: } FF = \frac{\text{Unconfined yield stress}}{\text{Major consolidating stress}} = \frac{UYS}{MCS} \quad 4.3$$



$$\text{Flow factor: } ff = \frac{Y(1+\sin\delta)H(\alpha)}{2(X-1)\sin\alpha} \quad 4.4$$

$$\text{where } \frac{1}{H(\alpha)} = \left[ \frac{65}{130+\alpha} \right]^m \left[ \frac{200}{200+\alpha} \right]^{1-m} \quad 4.5$$

(m =1 for conical hoppers)

$$X = \frac{2^m \sin\delta}{1-\sin\delta} \left\{ \frac{\sin(2\beta+\alpha)}{\sin\alpha} + 1 \right\} \quad 4.6$$

$$A = [2(1 - \cos(\beta+\alpha))]^m (\beta+\alpha)^{1-m} \sin\alpha \quad 4.7$$

$$B = \sin\beta \sin^{1+m}(\beta+\alpha) \quad 4.8$$

$$C = (1-\sin\delta) \sin^{2+m}(\beta+\alpha) \quad 4.9$$

$$Y = \frac{A+B}{C} \quad 4.10$$

The critical applied stress ( $\sigma_c$ ) represents the critical value of the unconfined yield strength at which a stable arch can be formed. This was obtained by the intersection of the flow function and flow factor (Figure 2.8). The value of the critical applied stress was used in equation 4.11 to calculate the minimum hopper outlet size.

$$D_{\min.} = \frac{H(\alpha)}{\rho g} \sigma_c \quad 4.11$$

The hopper outlet size was multiplied by 1.20 (0.20% greater) in order to achieve the desired flow rate.

#### **4.3.4.3 Silo wall loads**

The silo is divided in to two sections: cylindrical and hopper sections (Figure 4.3). The vertical and wall normal pressure exerted by the ground loblolly pine in a 100 feet (30.48 m) high and 50 feet (15.24 m) diameter silo was estimated using Janseen's equations (Janseen, 1985).

##### **4.3.4.3.1 Stresses in the cylindrical section**

Janseen's equations for estimating the vertical and wall normal pressure in the cylindrical section are given below:

Vertical pressure: 
$$P_v = \frac{\rho g A}{K \mu C} \left[ 1 - \exp\left(-\frac{\mu K C}{A} h\right) \right] \quad 4.12$$

Wall pressure: 
$$P_w = \frac{\rho g A}{\mu C} \left[ 1 - \exp\left(-\frac{\mu K C}{A} h\right) \right] \quad 4.13$$

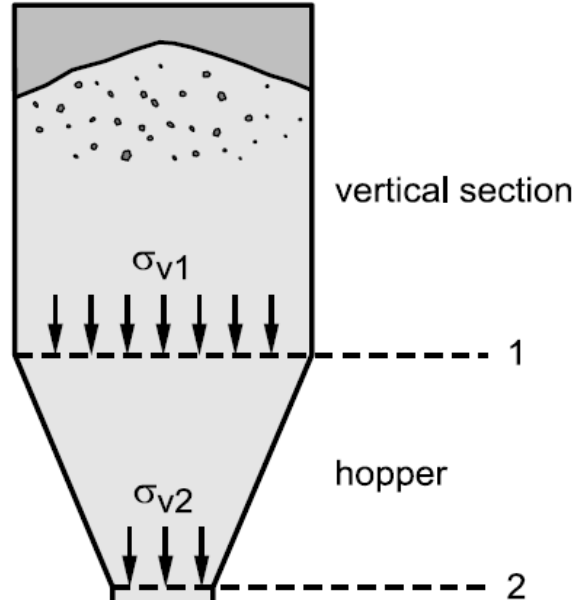


**Figure 4.3: Silo subdivision into vertical and hopper section (Schulze, 2008).**

#### 4.3.4.3.2 Stresses in the hopper section

The stresses exerted by ground loblolly pine during storage and flow (Figure 4.4) were estimated using the equations below (Rotter, 2001).

Initial fill load: 
$$P_{vf} = P_{vft} \left( \frac{x}{h_h} \right)^n + \frac{\gamma h_h}{n-1} \left[ \left( \frac{x}{h_h} \right) - \left( \frac{x}{h_h} \right)^n \right] \quad 4.14$$

$$n = 2a\mu_h \cot(\alpha) \quad 4.15$$

Flow induced load: 
$$P_{ve} = P_{vft} \left( \frac{x}{h_h} \right)^n + \frac{\gamma h_h}{n-1} \left[ \left( \frac{x}{h_h} \right) - \left( \frac{x}{h_h} \right)^n \right] \quad 4.16$$

$$\varepsilon = \phi_w + \sin^{-1} \left( \frac{\sin \phi_w}{\sin \delta} \right) \quad 4.17$$

$$F_e = \frac{1 + \sin \delta \cos \varepsilon}{1 - \sin \delta \cos(2\alpha + \varepsilon)} \quad 4.18$$

$$n = 2(F_e \mu_h \cot(\alpha) + F_e - 1) \quad 4.19$$

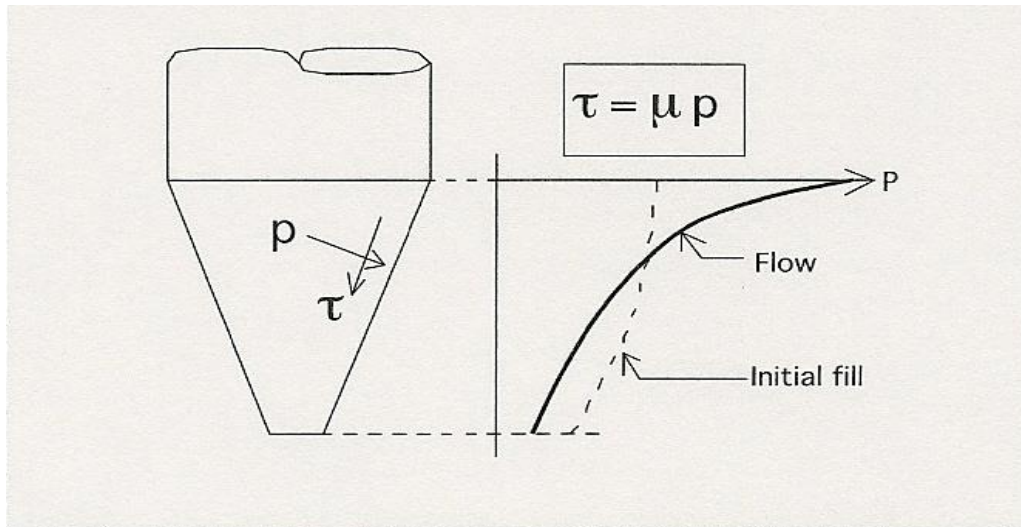


**Figure 4.4: Initial fill and flow induced pressure on the hopper section of a silo.**

#### **4.3.5 Experimental design and statistical analysis**

Particle size and moisture content of fractionated ground loblolly pine were the predictors while the response variables was the flow properties. The type of wall material was also used as a predictor during the angle of wall friction experiment. All the experiments were carried out in triplicate.

Microsoft Excel 2010 was used in summarizing and generating graphs. A significant test ( $\alpha < 0.05$ ) using the Proc GLM procedure in the statistical software SAS 9.3 (SAS Institute Inc., Cary, NC) was conducted to show the effect of particle size and moisture content on the flow properties. The Tukey test was used to compare the means of values of these properties at the different moisture contents and particle sizes. The results were presented in mean and standard deviation.

## 4.4 Results and Discussion

### 4.4.1 Flow classification of fractionated ground loblolly pine

The flow function curves (plot of unconfined yield strength and major consolidating stress) for the fractions at the five moisture levels are shown in Figure 4.5(a-e). The curves show that a linear increase of unconfined yield strength (UYS) occurred as major consolidating stress (MCS) increased. The flow index (inverse of the flow function) was used to compare the effects of particle size and moisture content on the UYS versus MCS relationship and to characterize the flow properties of the fractions.

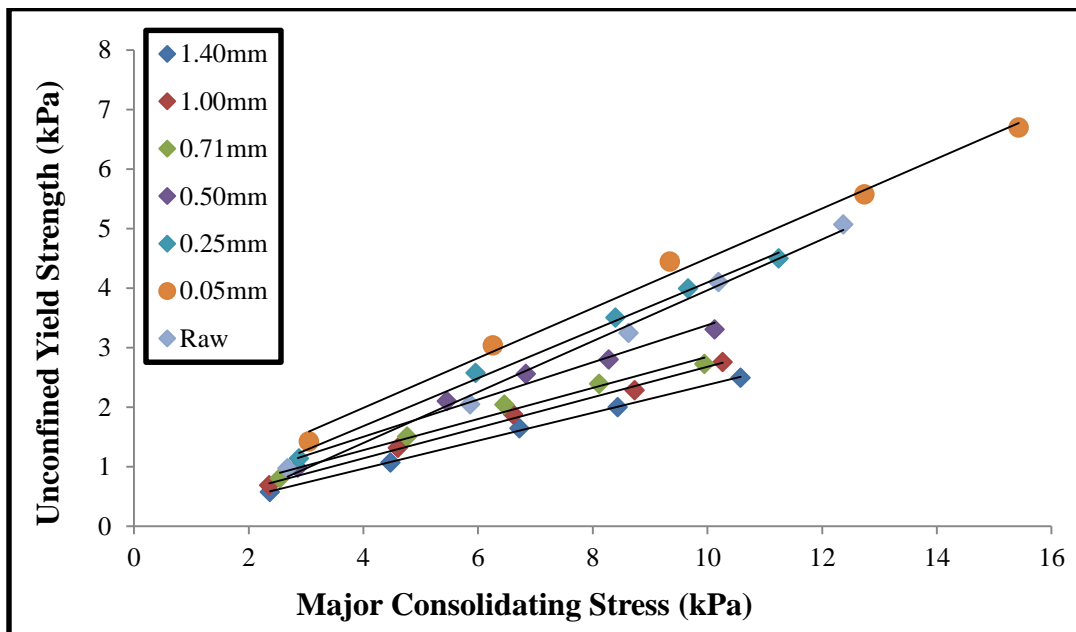


Figure 4.5a: Flow function of fractionated loblolly pine at 4.78% moisture content.

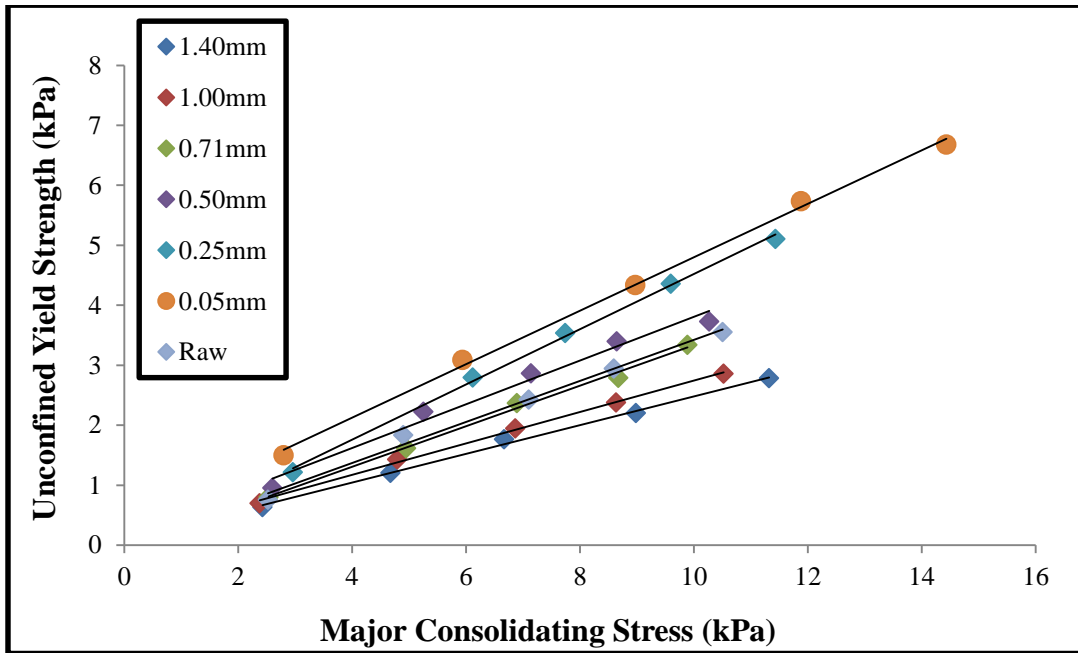


Figure 4.5b: Flow function of fractionated loblolly pine at 8.69% moisture content.

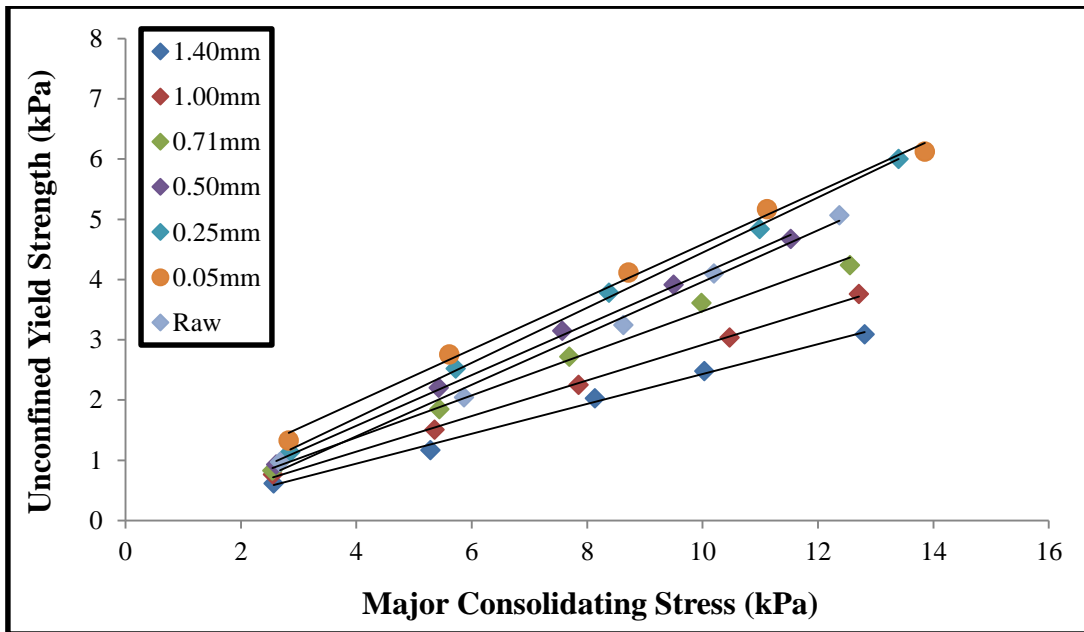


Figure 4.5c: Flow function of fractionated loblolly pine at 16.53% moisture content.

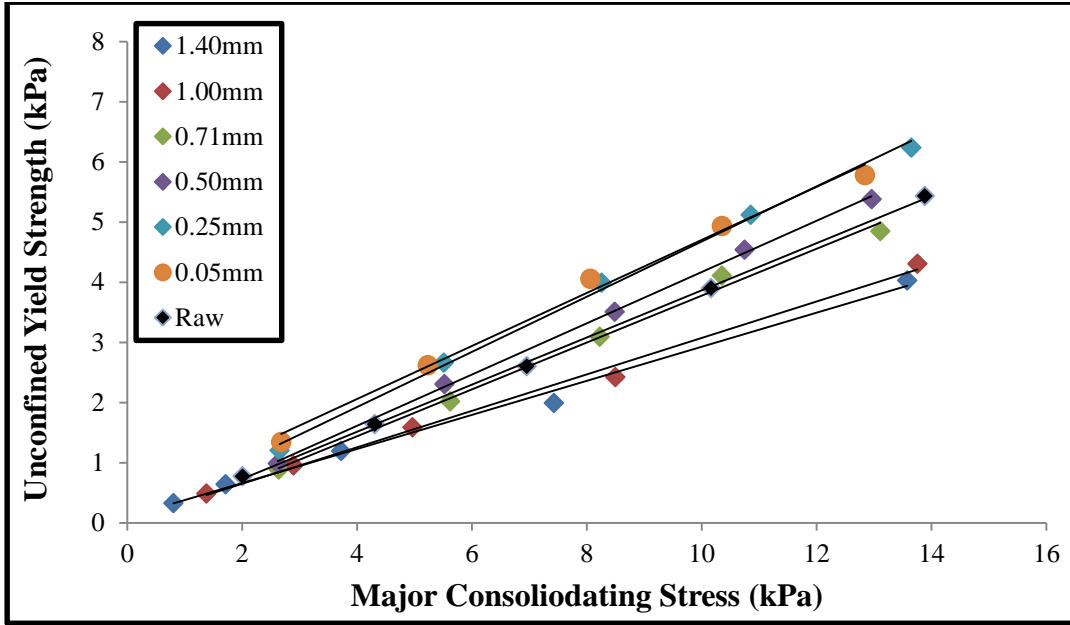


Figure 4.5d: Flow function of fractionated loblolly pine at 22.21% moisture content.

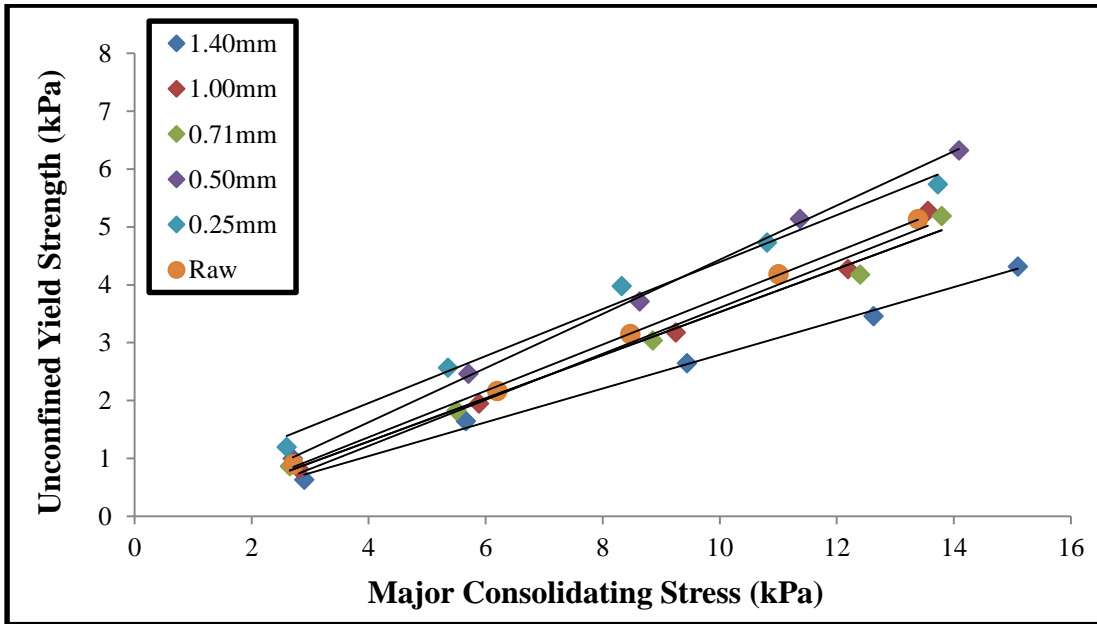


Figure 4.5e: Flow function of fractionated loblolly pine at 25.53% moisture content.

The flowability classification of the fractionated ground loblolly pine using flow index was based on Jenike's powder flow classification (Table 4.1). The flow index increased with increase

in particle size and decrease in moisture content. Except for 1.40 mm fraction at moisture levels of 4.78%, 8.69% and 16.53%, all of the samples were cohesive (Table 4.2). Based on Jenike’s classification, flow index value greater than 4 is classified as easy flowing material. Hence, the 1.40mm fraction at moisture levels of 4.78%, 8.69% and 16.53% were classified as easy flowing materials. However, at moisture levels of 22.21% and 25.53%, the flow indices of 1.40mm fractions were 3.37 and 3.41 respectively, which indicates cohesive flow. The flow indices obtained for the unfractionated ground loblolly pine was between 2.54 and 3.19, which also indicate a cohesive flow. This result is due to the fact that all the other fractions below size 1.40 mm were classified as cohesive therefore, making the whole ground material a cohesive material. The implication is that ground loblolly pine with large amount of fractions from size 0.05 to 1.00 mm will experience flowability problem during discharge out of storage bins and hopper.

**Table 4.1: Jenike classification of powder flowability by flow index (ffc).**

Flowability	Hardened	Very cohesive	Cohesive	Easy flow	Free flowing
Flow index (ffc)	<1	<2	<4	<10	>10

**Table 4.2: Flow classification of fractionated ground loblolly pine.**

Screen (mm)	Flow Index					Classification
	4.78%	8.69%	16.53%	22.21%	25.53%	
<b>1.40</b>	4.29	4.17	4.11	3.37*	3.41*	Easy flow
<b>1.00</b>	3.80	3.80	3.49	3.37	2.73	Cohesive
<b>0.71</b>	3.62	2.92	2.91	2.63	2.83	Cohesive
<b>0.50</b>	3.16	2.86	2.44	2.34	2.29	Cohesive
<b>0.25</b>	2.52	2.21	2.24	2.29	2.48	Cohesive
<b>0.05</b>	2.38	2.26	2.27	2.08	NC*	Cohesive
<b>Raw</b>	3.19	2.89	2.54	2.70	2.61	Cohesive

NC\* experiment was not conducted because there was no fraction at 25.53% moisture level.

\* Material have a cohesive flow

Grafton et al. (2009) characterize the flowability of 11 commercial agricultural limes with 5% moisture addition by weight. The authors observed the flowability of the materials altering from easy flow to cohesive flow with increase in moisture content. Teunou et al. (1999) also classified the flowability of four food powders (flour, skim milk, tea and whey permeate) and determined the flow index to be 2.71, 11.04, 4.22 and 5.85 respectively. The authors reported that skim milk powder was classified as free flowing due to its low moisture content (4.6% wb) and large particle size (197  $\mu\text{m}$ ). However, flour with a flow index of 2.71 was classified as cohesive. This was due to its high moisture content of 12.6% (wb) and low particle size of 73  $\mu\text{m}$ .

Further analysis was carried out to examine the change in flowability of fraction of size 1.40mm when mixed with different quantity of fractions with smaller particle size. The flow analysis was based on the assumption that reduction in the void spaces among the large particles will result in reduced flowability. Table 4.3 presents the flowability results of mixture of fractions retained on screen sizes 1.40 mm and 0.50mm at three mixing ratios of 10:1, 10:2 and 10:3 (Table 3.4). As expected, increase in the amount of 0.50 mm fraction and moisture content resulted in flowability reduction from easy flow to cohesive flow. This implies that the presence of fine fraction in unfractionated ground loblolly pine is responsible for ratholing and cohesive arching flow problems.

**Table 4.3: Flow indices of mixture of 1.40mm and 0.50mm fractions.**

Moisture content (% wb)	Ratio		
	10:1	10:2	10:3
4.78	3.92	3.75	3.45
8.69	4.00	3.90	3.41
16.53	3.70	3.23	-

\*Ratio 10:1 represent mixture mass ratio of 1.40mm: 0.50mm fractions



#### 4.4.2 Angle of internal friction

The angle of internal friction represents friction between particles during movement of bulk materials. Table 4.4 shows the angle of internal friction obtained for the fractionated and unfractionated ground loblolly pine. The angle of internal friction for the fractionated sample varied between 40.40<sup>0</sup> and 52.66<sup>0</sup>. The angle of internal friction significantly increased (p<0.05) with decrease in fraction size and increase in moisture content. The angles of internal friction of the unfractionated samples were also found to increase with moisture content from 43.29 and 48.93<sup>0</sup>. Gil et al. (2013) reported a similar result for corn stover and poplar. The angle of internal friction for poplar (30<sup>0</sup> - 32<sup>0</sup>) and corn stover (26<sup>0</sup> - 29<sup>0</sup>) increased with moisture content increase from 7 to 33% (wb) and decrease in particle size from 0.61 to 0.30mm for poplar and 0.70 to 0.26 mm. Kibar et al. (2010) also reported increase in angle of internal friction from 29.70<sup>0</sup> to 32.53<sup>0</sup> as the moisture content increased from 10% to 14% (db) for rice grains.

**Table 4.4: Angle of internal friction of fractionated ground loblolly pine.**

Screen size (mm)	Moisture content levels (% wb)				
	4.78	8.69	16.53	22.21	25.53
<b>0.05</b>	49.88 <sup>[a,x]</sup> ± 0.89	52.66 <sup>[a,v]</sup> ± 0.91	51.74 <sup>[a,vw]</sup> ± 1.12	51.55 <sup>[a,w]</sup> ± 1.12	NC*
<b>0.25</b>	46.57 <sup>[b,y]</sup> ± 0.99	48.15 <sup>[b,x]</sup> ± 0.99	49.43 <sup>[b,w]</sup> ± 1.09	50.89 <sup>[ab,v]</sup> ± 1.17	50.69 <sup>[a,v]</sup> ± 1.36
<b>0.50</b>	43.88 <sup>[c,x]</sup> ± 2.23	45.29 <sup>[c,x]</sup> ± 2.18	47.37 <sup>[c,w]</sup> ± 1.28	49.52 <sup>[bc,v]</sup> ± 1.43	49.49 <sup>[b,v]</sup> ± 1.12
<b>0.71</b>	42.12 <sup>[cd,x]</sup> ± 2.46	43.85 <sup>[cd,w]</sup> ± 1.86	46.67 <sup>[cd,v]</sup> ± 1.04	47.95 <sup>[c,v]</sup> ± 0.91	48.09 <sup>[c,v]</sup> ± 0.55
<b>1.00</b>	41.63 <sup>[e,x]</sup> ± 1.82	42.78 <sup>[d,x]</sup> ± 1.88	46.13 <sup>[d,w]</sup> ± 0.88	48.23 <sup>[c,v]</sup> ± 1.75	48.36 <sup>[c,v]</sup> ± 0.90
<b>1.40</b>	40.40 <sup>[e,z]</sup> ± 1.55	42.09 <sup>[d,y]</sup> ± 1.50	44.70 <sup>[e,x]</sup> ± 0.61	48.15 <sup>[c,v]</sup> ± 1.86	46.41 <sup>[d,w]</sup> ± 0.88
<b>Raw</b>	43.29 <sup>[cd,x]</sup> ± 2.60	45.51 <sup>[c,w]</sup> ± 1.89	47.40 <sup>[c,v]</sup> ± 0.99	48.93 <sup>[c,v]</sup> ± 1.88	48.08 <sup>[c,v]</sup> ± 0.80

Particle size effect: values in each column with same letter (a-f) are not significantly different (p<0.05).

Moisture effect: values in each row with same letter (v-z) are not significantly different (p<0.05).

NC\* experiment was not conducted because there was no fraction at 25.53% moisture level.

The increased angle of internal friction with moisture content and reduction in fraction size of fractionated ground loblolly pine was an indication of increased frictional resistance between particles of smaller sizes. This implies that increasing amount of the smaller particles at higher moisture content in the unfractionated ground loblolly pine will cause the typical flow problems associated with bulk solids therefore leading to difficulty in unloading the ground material from storage vessels.

Also, the measured angles of internal friction for the fractionated and raw samples were greater than the critical values of less than  $30^{\circ}$  required for gravity discharge of bulk materials from storage bins and silos (Puri, 2002). Therefore, it shows that unloading ground loblolly pine will be impossible with gravity discharge alone; there would be a need for a flow aid. Zulfiqar et al. (2006) reported the angle of internal friction for different blends of coal and sawdust/coal mixture to be in the range of  $54.36^{\circ}$  to  $62.08^{\circ}$ . The angle of internal friction documented for other biological materials such as switchgrass ( $39.4^{\circ} - 46.7^{\circ}$ ), wheat straw ( $41.6^{\circ} - 46.7^{\circ}$ ), corn stover ( $46.7^{\circ} - 49.5^{\circ}$ ) and  $41.25^{\circ}$  for pecan shell are above the critical values making them not amendable to gravity discharge also (Chevanan et al., 2009; Littlefield et al., 2011).

#### **4.4.3 Cohesive strength**

Statistical analysis showed that particle size had a significant effect ( $p < 0.05$ ) on cohesive strength (Table 4.5). However, moisture content was found to have no significant effect ( $p < 0.05$ ) on the cohesive strength of the fractions. The cohesive strength of the fractionated and unfractionated ground loblolly pine ranged between 0.42 and 1.05 kPa. Cohesive strength decreased with increase in particle size i.e. fractions of size 0.05 mm had the highest cohesive strength while fractions of size 1.40 mm had the lowest cohesive strength. The increased cohesive

strength in finer fraction is attributable to the increased total surface area and number of contact points for inter-particle bonding (Drzymala, 1993) that exists in fraction with smaller particles.

#### 4.4.4 Wall friction properties

Particle size and moisture effect on wall friction properties of the fractions were measured on three wall surfaces (stainless steel, mild steel and Tivar 88). Statistical analysis showed that particle size and moisture content had a significant effect on angle of wall friction of fractionated ground loblolly pine with an increase in the angle of wall friction as fraction size decrease and moisture content increased.

**Table 4.5: Cohesive strength (kPa) of fractionated ground loblolly pine.**

Screen size (mm)	Moisture content levels (% wb)				
	4.78	8.69	16.53	22.21	25.53
<b>0.05</b>	1.05 <sup>[a,v]</sup> ± 0.47	1.01 <sup>[a,v]</sup> ± 0.45	0.92 <sup>[a,v]</sup> ± 0.42	0.91 <sup>[a,v]</sup> ± 0.40	NC*
<b>0.25</b>	0.82 <sup>[ab,v]</sup> ± 0.33	0.88 <sup>[ab,v]</sup> ± 0.37	0.90 <sup>[ab,v]</sup> ± 0.44	0.93 <sup>[a,v]</sup> ± 0.45	0.91 <sup>[a,v]</sup> ± 0.44
<b>0.50</b>	0.63 <sup>[bc,v]</sup> ± 0.24	0.70 <sup>[bc,v]</sup> ± 0.29	0.76 <sup>[ab,v]</sup> ± 0.37	0.87 <sup>[ab,v]</sup> ± 0.44	0.88 <sup>[a,v]</sup> ± 0.45
<b>0.71</b>	0.52 <sup>[bc,v]</sup> ± 0.21	0.58 <sup>[c,v]</sup> ± 0.27	0.66 <sup>[ab,v]</sup> ± 0.33	0.73 <sup>[ab,v]</sup> ± 0.37	0.72 <sup>[a,v]</sup> ± 0.39
<b>1.00</b>	0.48 <sup>[c,v]</sup> ± 0.21	0.49 <sup>[c,v]</sup> ± 0.22	0.55 <sup>[ab,v]</sup> ± 0.28	0.46 <sup>[c,v]</sup> ± 0.35	0.74 <sup>[a,v]</sup> ± 0.41
<b>1.40</b>	0.43 <sup>[c,v]</sup> ± 0.20	0.45 <sup>[c,v]</sup> ± 0.22	0.45 <sup>[b,v]</sup> ± 0.22	0.39 <sup>[c,v]</sup> ± 0.33	0.60 <sup>[a,v]</sup> ± 0.32
<b>Raw</b>	0.65 <sup>[bc,v]</sup> ± 0.26	0.69 <sup>[bc,v]</sup> ± 0.31	0.78 <sup>[ab,v]</sup> ± 0.40	0.70 <sup>[ab,v]</sup> ± 0.45	0.75 <sup>[a,v]</sup> ± 0.38

Particle size effect: values in each column with same letter (a-f) are not significantly different (p<0.05).

Moisture effect: values in each row with same letter (v-z) are not significantly different (p<0.05).

NC\* experiment was not conducted because there was no fraction at 25.53% moisture level.

The angle of wall friction on stainless steel surface (Table 4.6) varied between 8.96 and 24.80°. The implication is that a high value of wall friction caused by reduction in particle and increase in moisture content leads to greater adhesion of the particles to the surface of storage wall

hence resulting in flow problem during material discharge. Fitzpatrick et al. (2004) stated that angle of wall friction represents the adhesion of powder to the silo wall (the higher the angle, the more difficult it is to move the powder along the surface). This implies that a strong adhesion will be developed by fractionated ground loblolly pine at low fraction size or increased moisture content, hence making it difficult for the ground biomass to flow along the wall surface of the storage vessel.

**Table 4.6: Angle of wall friction of fractionated loblolly pine using stainless steel wall.**

Screen size (mm)	Moisture Content Level (% wb)				
	4.78	8.69	16.53	22.21	25.53
<b>0.05</b>	12.30 <sup>[a,y]</sup> ± 1.28	14.90 <sup>[a,x]</sup> ± 2.05	17.14 <sup>[a,w]</sup> ± 2.75	26.49 <sup>[a,v]</sup> ± 4.61	NC*
<b>0.25</b>	9.83 <sup>[b,z]</sup> ± 0.52	12.39 <sup>[b,y]</sup> ± 1.27	14.00 <sup>[c,x]</sup> ± 1.54	19.50 <sup>[b,w]</sup> ± 2.64	24.80 <sup>[a,v]</sup> ± 3.96
<b>0.50</b>	9.45 <sup>[c,z]</sup> ± 0.50	11.24 <sup>[c,y]</sup> ± 0.90	13.79 <sup>[c,x]</sup> ± 1.43	17.60 <sup>[cd,w]</sup> ± 1.96	21.62 <sup>[b,v]</sup> ± 2.80
<b>0.71</b>	9.39 <sup>[c,z]</sup> ± 0.49	12.72 <sup>[b,y]</sup> ± 1.48	14.22 <sup>[c,x]</sup> ± 1.47	16.72 <sup>[d,w]</sup> ± 1.73	20.98 <sup>[bc,v]</sup> ± 2.58
<b>1.00</b>	9.49 <sup>[c,z]</sup> ± 0.50	11.44 <sup>[c,y]</sup> ± 1.00	14.40 <sup>[c,x]</sup> ± 1.38	17.35 <sup>[cd,w]</sup> ± 1.83	20.06 <sup>[cd,v]</sup> ± 2.51
<b>1.40</b>	8.96 <sup>[d,z]</sup> ± 0.38	10.82 <sup>[c,y]</sup> ± 0.97	14.18 <sup>[c,x]</sup> ± 1.31	16.52 <sup>[d,w]</sup> ± 1.65	18.76 <sup>[d,v]</sup> ± 2.05
<b>Raw</b>	9.53 <sup>[bc,z]</sup> ± 0.53	10.92 <sup>[c,y]</sup> ± 1.27	16.23 <sup>[b,x]</sup> ± 2.21	18.13 <sup>[c,w]</sup> ± 1.85	20.56 <sup>[bc,v]</sup> ± 2.54

Particle size effect: values in each column with same letter (a-f) are not significantly different (p<0.05)

Moisture effect: values in each row with same letter (v-z) are not significantly different (p<0.05)

NC\* experiment was not conducted because there was no fraction at 25.53% moisture level

The angle of wall friction on mild steel surface ranged between 10.48<sup>0</sup> and 19.73<sup>0</sup> (Table 4.7) with the fractions of size 0.05 mm having the highest wall friction value while the fractions on sieve size 1.40 mm had the lowest wall friction angle. However, the angles of wall friction recorded on mild steel surface were in the range of the values obtained for stainless steel.

**Table 4.7: Angle of wall friction of fractionated loblolly pine using mild steel wall.**

Screen size (mm)	Moisture Content Level (% wb)				
	4.78	8.69	16.53	22.21	25.53
<b>0.05</b>	12.33 <sup>[a,x]</sup> ± 1.10	16.10 <sup>[a,w]</sup> ± 2.63	15.22 <sup>[a,w]</sup> ± 1.72	21.35 <sup>[a,v]</sup> ± 3.15	NC*
<b>0.25</b>	10.48 <sup>[d,z]</sup> ± 0.45	13.11 <sup>[b,y]</sup> ± 1.21	14.29 <sup>[c,x]</sup> ± 1.32	18.12 <sup>[bc,w]</sup> ± 2.08	22.56 <sup>[a,v]</sup> ± 3.42
<b>0.50</b>	10.50 <sup>[cd,z]</sup> ± 0.39	12.09 <sup>[c,y]</sup> ± 0.72	15.07 <sup>[a,x]</sup> ± 1.36	18.18 <sup>[bc,w]</sup> ± 1.70	19.52 <sup>[b,v]</sup> ± 2.55
<b>0.71</b>	10.54 <sup>[cd,z]</sup> ± 0.35	12.17 <sup>[c,y]</sup> ± 0.71	15.31 <sup>[a,x]</sup> ± 1.34	17.42 <sup>[c,w]</sup> ± 1.58	19.73 <sup>[b,v]</sup> ± 2.28
<b>1.00</b>	10.81 <sup>[b,z]</sup> ± 0.36	12.43 <sup>[c,y]</sup> ± 0.76	15.01 <sup>[ab,x]</sup> ± 1.34	17.99 <sup>[c,w]</sup> ± 1.53	18.87 <sup>[bc,v]</sup> ± 2.18
<b>1.40</b>	10.76 <sup>[bc,y]</sup> ± 0.31	12.38 <sup>[c,x]</sup> ± 0.59	14.22 <sup>[c,w]</sup> ± 1.13	18.00 <sup>[c,v]</sup> ± 1.42	18.30 <sup>[c,v]</sup> ± 1.90
<b>Raw</b>	10.55 <sup>[bc,y]</sup> ± 0.37	12.16 <sup>[c,x]</sup> ± 0.92	14.53 <sup>[bc,w]</sup> ± 1.30	19.04 <sup>[b,v]</sup> ± 1.77	19.39 <sup>[bc,v]</sup> ± 2.29

Particle size effect: values in each column with same letter (a-f) are not significantly different ( $p < 0.05$ ).

Moisture effect: values in each row with same letter (w-z) are not significantly different ( $p < 0.05$ ).

NC\* experiment was not conducted because there was no fraction at 25.53% moisture level.

The angle of wall friction recorded using the Tivar 88 surface (ultra-high weight molecular polyethylene) surface ranged between  $10.88^{\circ}$  and  $15.54^{\circ}$  (Table 4.8). There was a significant increase ( $p < 0.05$ ) in the angles of wall friction with reduction in fraction size for the three wall surfaces. This is because there is greater contact surface area between smaller particles and the wall surface (Iqbal and Fitzpatrick, 2006) which led to the high wall friction angle recorded for fractions of size 0.05 mm.

The increased wall friction angle due to increase in moisture content had also been reported for other biological materials using different wall surfaces. Mani et al. (2004) reported a significant increase in angle of wall friction of corn stover grinds from  $0.18^{\circ}$  to  $0.26^{\circ}$  as the moisture content increased from 7% to 15% (wb) using a steel surface. The authors asserted that the increased wall friction angle is due to increased adhesion between corn stover grinds and the steel surface at higher moisture content. Iqbal and Fitzpatrick (2006) observed an increase from  $9.5^{\circ}$  to  $14.6^{\circ}$  of

wall friction angle for flour as moisture content increased from 12.6% to 15.1% (wb). The authors reported similar trend for tea and whey permeate powder. Grafton et al. (2009) also reported an increase in wall friction angle of different commercial agricultural limes with increased moisture content.

**Table 4.8: Angle of wall friction of fractionated loblolly pine using Tivar 88 wall surface.**

Screen size (mm)	Moisture Content Level (% wb)				
	4.78	8.69	16.53	22.21	25.53
0.05	14.80 <sup>[a,vw]</sup> ±1.71	15.54 <sup>[a,v]</sup> ±2.25	14.52 <sup>[a,w]</sup> ± 1.79	15.50 <sup>[a,v]</sup> ± 2.64	NC*
0.25	13.61 <sup>[b,w]</sup> ±1.09	13.48 <sup>[bc,w]</sup> ± 1.31	13.14 <sup>[b,w]</sup> ± 1.28	13.33 <sup>[c,w]</sup> ±1.70	15.23 <sup>[a,v]</sup> ± 2.46
0.50	12.48 <sup>[c,w]</sup> ± 0.87	12.87 <sup>[cd,vw]</sup> ±1.07	12.83 <sup>[b,vw]</sup> ±1.12	12.36 <sup>[d,w]</sup> ± 1.35	13.06 <sup>[b,v]</sup> ± 1.64
0.71	12.10 <sup>[cd,v]</sup> ± 0.98	12.32 <sup>[de,v]</sup> ± 1.03	12.01 <sup>[c,v]</sup> ± 1.05	12.02 <sup>[d,v]</sup> ±1.58	11.76 <sup>[c,v]</sup> ± 1.47
1.00	11.59 <sup>[d,w]</sup> ± 0.87	11.72 <sup>[ef,w]</sup> ± 0.97	11.24 <sup>[d,w]</sup> ± 0.99	12.81 <sup>[cd,v]</sup> ± 1.89	11.46 <sup>[c,w]</sup> ± 1.40
1.40	10.88 <sup>[e,y]</sup> ± 0.96	11.47 <sup>[f,vw]</sup> ± 1.15	11.61 <sup>[cd,w]</sup> ± 1.02	12.44 <sup>[cd,v]</sup> ± 1.74	10.98 <sup>[c,xy]</sup> ± 1.32
Raw	11.75 <sup>[d,x]</sup> ±0.90	14.07 <sup>[b,v]</sup> ±1.35	12.17 <sup>[c,wx]</sup> ±1.30	14.45 <sup>[b,v]</sup> ±2.28	12.55 <sup>[b,w]</sup> ±1.58

Particle size effect: values in each column with same letter (a-f) are not significantly different ( $p < 0.05$ ).  
 Moisture effect: values in each row with same letter (v-z) are not significantly different ( $p < 0.05$ ).  
 NC\* experiment was not conducted because there was no fraction at 25.53% moisture level.

Statistical analysis showed that the wall surface had a significant effect ( $p < 0.05$ ) on the angle of wall friction of the fractionated ground loblolly pine (see appendix for tables). At lower moisture level, the stainless steel and mild steel had a lower wall friction angle compared to Tivar 88 surface but as the moisture content increased, the angle of wall friction for the stainless steel and mild steel surface increased significantly. The high angles of wall friction recorded by stainless steel and mild steel can be attributed to their roughness factors which are 45µm and 15 µm respectively while Tivar 88 (classified as plastic) has a roughness factor of 1.5 µm (Darby, 2001).

Also, a scanning electron microscope images (Figure 4.6) of the stainless steel, mild steel and ultra- high weight molecular polyethylene surfaces showed that Tivar 88 surface has the smoothest surface which enhanced its low wall friction angles. This indicates that Tivar 88 surfaces will be a good wall lining material in the design of storage and handling vessel for ground loblolly pine with high moisture content while stainless and mild steel will perform well at lower moisture content.

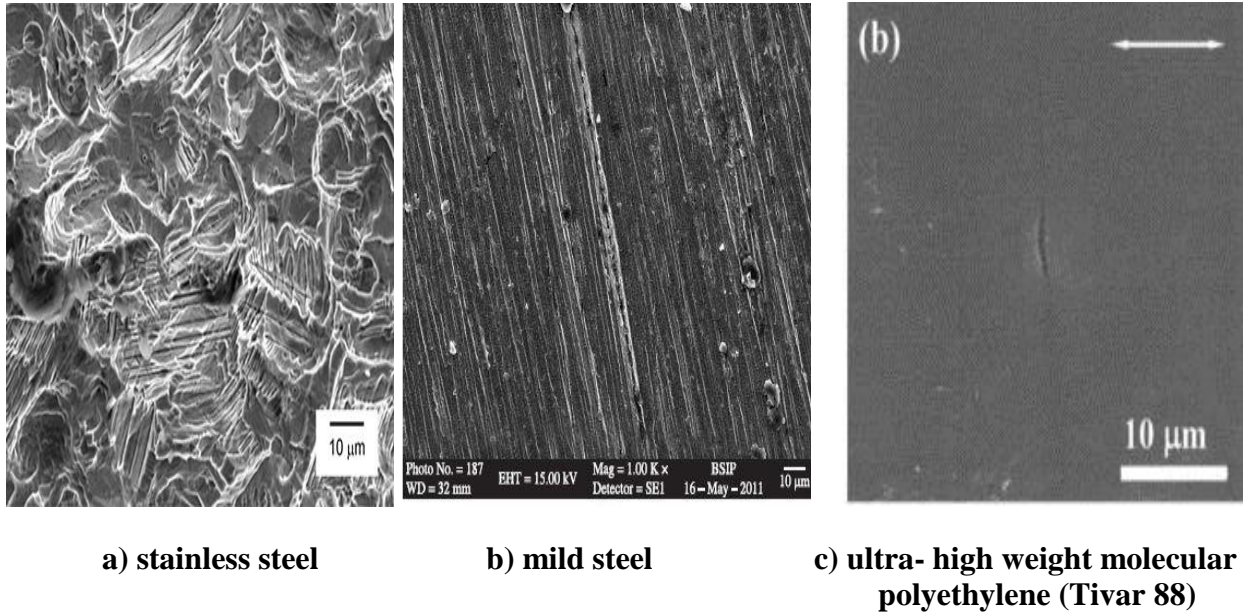


**Figure 4.6: SEM images of stainless steel, mild steel and Tivar 88 wall surfaces**  
*(Sources: Zhou and Komvopoulos, 2005; Günen et al., 2014; Farhat and Quraishi, 2010).*

Previous studies had shown the effect of wall material on angle of wall friction on biological materials. For example, Wu et al. (2011) compared the effect of four wall surfaces (Tivar 88, concrete, mild steel and stainless steel) on wall friction angles of wood pellets and wood chips. The authors observed that Tivar 88 surface had the lowest wall friction angles (11-17°) when compared with the other three surfaces with wall friction angle varying between 16 and 35°. This difference was attributed to the surface roughness of material with concrete having the coarsest surface, hence having the highest angle of wall friction and Tivar 88 having the smoothest surface hence it low wall friction angle. Fitzpatrick et al. (2004) reported the angle of wall friction for 13

different biological materials using a stainless steel surface. The wall friction angles ranged between  $11.8^{\circ}$  and  $27.3^{\circ}$ . Chen et al. (2012) found the angle of wall friction for brown coal, hard coal and saw dust to be  $26^{\circ}$ ,  $27.8^{\circ}$  and  $31.4^{\circ}$  respectively using a stainless steel as well. The wall friction between the hopper wall material and the bulk materials is very important in determining whether mass flow or funnel flow pattern will be obtained during discharge from a silo (Fitzpatrick, 2007). Therefore, in order to ensure reliable flow, the angle of wall friction of the storage vessel wall lining material must be low. This is an indication of a limited adhesion of the bulk material to the wall surface of the storage vessel.

#### **4.4.5 Hopper half angle and minimum hopper outlet size**

Jenike's methodology for estimating the conical hopper half angle was employed (Jenike, 1964). The measured angle of internal friction and wall frictions using the three surfaces were applied in the methodology. The hopper half angle varied between  $18.37^{\circ}$  and  $41.44^{\circ}$ . As a margin of safety during hopper design, the hopper half angle was reduced by  $3^{\circ}$  making the angle varied between  $15.37^{\circ}$  and  $38.44^{\circ}$  (Table 4.9). There was a reduction in the hopper half angle with increased moisture content and reduction in the fraction size (Figure 4.7 & 4.8). However, moisture content does not have an effect on hopper half angle using Tivar 88 surface when compared to stainless and mild steel surface (Figure 4.7). This is attributable to the low variation in angles of wall friction of Tivar 88 surface at all moisture levels.



**Table 4.9: Evaluation of hopper half angle, flow factor and minimum hopper opening size ( $D_{min}$ ) for a cylindrical hopper using Jenike's method.**

Screen Size (mm)	Moisture Content (%)	Particle diameter (mm)	Reduced Hopper Half Angle			Flow factor	Adjusted $D_{min}$ (mm)
			Stainless Steel	Mild Steel	Tivar 88		
<b>0.05</b>	<b>4.78</b>	<b>0.11</b>	32.19	32.15	29.27	1.06	1.32
	<b>8.69</b>	<b>0.15</b>	28.82	27.45	28.09	1.04	1.80
	<b>16.53</b>	<b>0.10</b>	26.34	28.55	29.36	1.05	1.20
	<b>22.21</b>	<b>0.10</b>	15.37	21.42	28.25	1.09	1.20
<b>0.25</b>	<b>4.78</b>	<b>0.85</b>	35.72	34.94	31.17	1.09	10.20
	<b>8.69</b>	<b>0.81</b>	32.36	31.51	31.07	1.08	9.72
	<b>16.53</b>	<b>0.70</b>	30.27	29.93	31.28	1.07	8.40
	<b>22.21</b>	<b>0.64</b>	23.66	25.28	30.84	1.07	7.68
	<b>25.53</b>	<b>0.86</b>	17.39	20.06	28.67	1.09	10.32
<b>0.50</b>	<b>4.78</b>	<b>1.16</b>	36.82	35.52	33.07	1.13	13.92
	<b>8.69</b>	<b>0.97</b>	34.29	33.26	32.30	1.12	11.64
	<b>16.53</b>	<b>1.01</b>	30.83	29.29	31.97	1.09	12.12
	<b>22.21</b>	<b>0.84</b>	26.01	25.33	32.17	1.08	10.08
	<b>25.53</b>	<b>1.33</b>	21.23	23.74	31.36	1.09	15.96
<b>0.71</b>	<b>4.78</b>	<b>1.38</b>	37.37	35.92	33.95	1.17	16.56
	<b>8.69</b>	<b>1.28</b>	32.78	33.46	33.28	1.14	15.36
	<b>16.53</b>	<b>1.33</b>	30.42	29.10	33.08	1.11	15.96
	<b>22.21</b>	<b>1.17</b>	27.20	26.36	32.79	1.09	14.04
	<b>25.53</b>	<b>1.46</b>	22.08	23.59	33.12	1.11	17.52
<b>1.00</b>	<b>4.78</b>	<b>1.72</b>	37.39	35.71	34.72	1.18	20.64
	<b>8.69</b>	<b>1.54</b>	34.62	33.38	34.27	1.16	18.48
	<b>16.53</b>	<b>1.69</b>	30.29	29.55	34.12	1.11	20.28
	<b>22.21</b>	<b>1.55</b>	26.46	25.69	31.87	1.09	18.60
	<b>25.53</b>	<b>1.73</b>	23.18	24.61	33.43	1.10	20.76
<b>1.40</b>	<b>4.78</b>	<b>2.16</b>	38.44	36.12	35.97	1.20	25.92
	<b>8.69</b>	<b>2.14</b>	35.58	33.60	34.75	1.17	25.68
	<b>16.53</b>	<b>2.17</b>	30.81	30.76	33.97	1.13	26.04
	<b>22.21</b>	<b>2.18</b>	27.47	25.70	32.34	1.09	26.16
	<b>25.53</b>	<b>2.38</b>	24.93	25.49	34.37	1.12	28.56
<b>Raw</b>	<b>4.78</b>	<b>1.31</b>	36.87	35.61	34.11	1.15	15.72
	<b>8.69</b>	<b>1.36</b>	34.63	33.13	30.80	1.12	16.32
	<b>16.53</b>	<b>1.33</b>	27.89	29.93	32.76	1.10	15.96
	<b>22.21</b>	<b>1.39</b>	25.44	24.36	29.81	1.09	16.68
	<b>25.53</b>	<b>2.19</b>	22.59	24.01	32.19	1.10	26.28

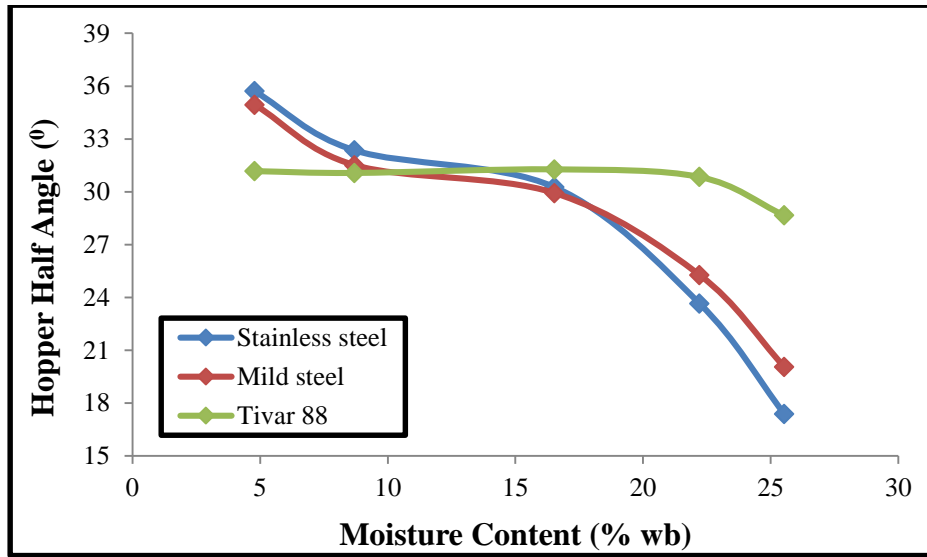


**Figure 4.7: Effect of moisture content on hopper half angle of 0.25 mm fraction.**

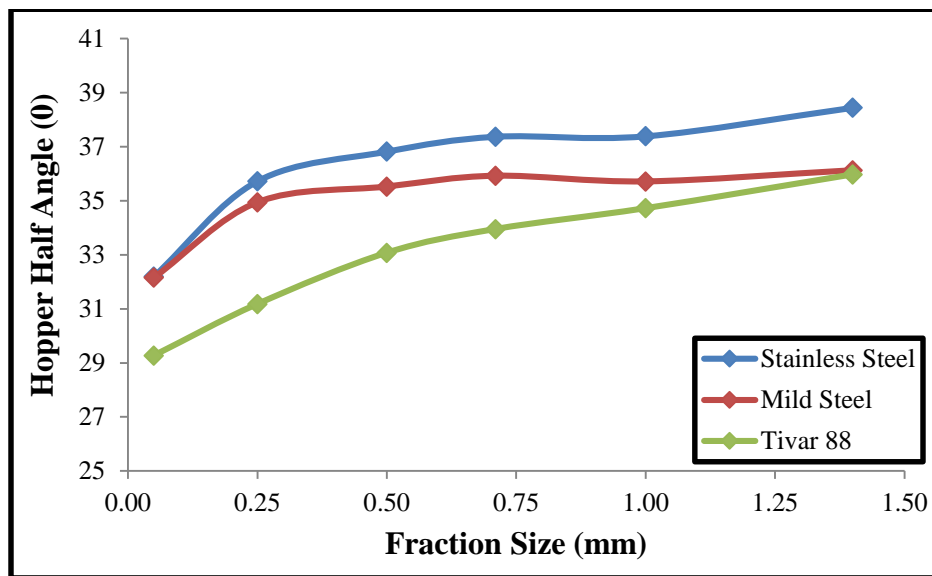


**Figure 4.8: Effect of fraction size on hopper half angle at the 4.78% moisture level.**

Figure 4.9 illustrates angles of wall friction versus hopper half angles obtained for the fractionated ground loblolly pine. The hopper half angle decreased with increase in angle of wall friction. The angles of wall friction recorded for stainless steel and mild steel had a wider spread of hopper half angles while tivar 88 had a small variation in its hopper half angle. The variation in

the hopper half angles for the three surfaces is attributable to the particle size and moisture effect on their angles of wall friction.

Jenike (1970) also designed a chart (Figure 2.7) showing the combination of the angle of wall friction and the hopper half angle. The chart indicates allowable hopper half angles for mass flow or funnel flow for given values of wall friction angles. The highest hopper half angle for the fractionated loblolly pine was  $38.44^{\circ}$  and the highest angle of wall friction recorded was  $24.8^{\circ}$ . Using the design chart provided by Jenike, the combination of these two data shows that mass flow pattern will exist during discharge of ground loblolly pine from a storage silo. Therefore, the hopper design was based on mass flow pattern.

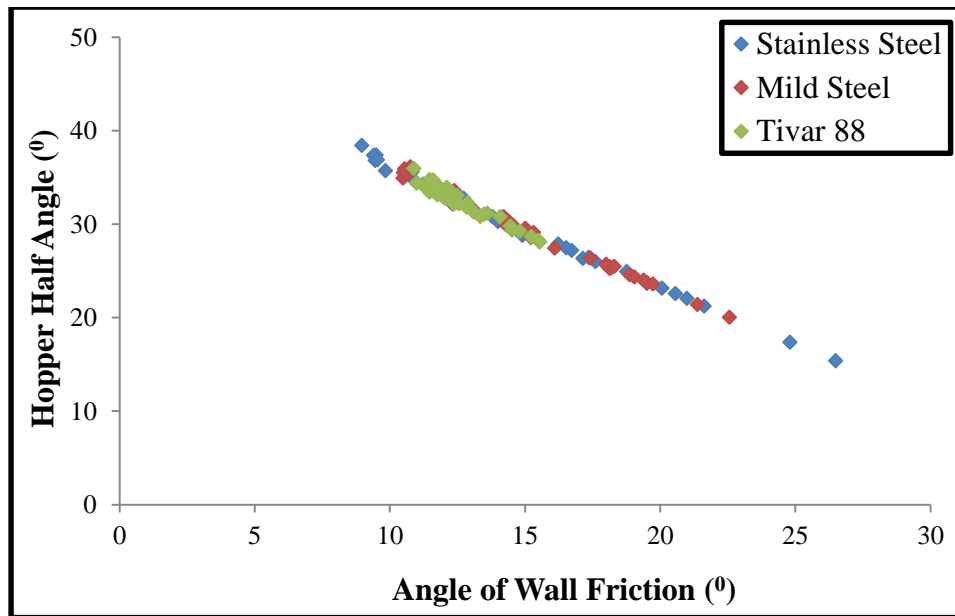


**Figure 4.9: Plot of hopper half angles and wall friction angle of ground loblolly pine.**

The intersection of the flow function and the flow factor lines are used in estimating the critical applied stress. Generally, it is assumed that the flow function and flow factor lines will intersect in order to obtain the critical applied stress. However, the flow function lines for the

fractions lie below the flow factor lines (Figure 4.10) resulting in no critical applied stress. This result implies that the applied stress exceeds the unconfined yield strength of the fraction.

The calculation of the minimum hopper outlet size was therefore not on the basis of cohesive arching but rather to prevent formation of mechanical arching. Purutyan and Barnam (2001) stated that in estimating the minimum hopper outlet size designed to ensure mass flow and prevent mechanical arching; the hopper outlet size should be at least six to eight times bigger than the largest particle diameter of the material. The minimum hopper outlet sizes were estimated by multiplying the geometric mean diameter by 10. The actual outlet dimensions were then multiplied by 1.20 (20% greater) in order to ensure the desired flow rate (Table 4.9). As expected, the minimum hopper outlet size followed the trend of the geometric mean diameters and it varied between 1.20 and 28.56 mm with 1.40 mm fraction having the highest minimum hopper outlet sizes.

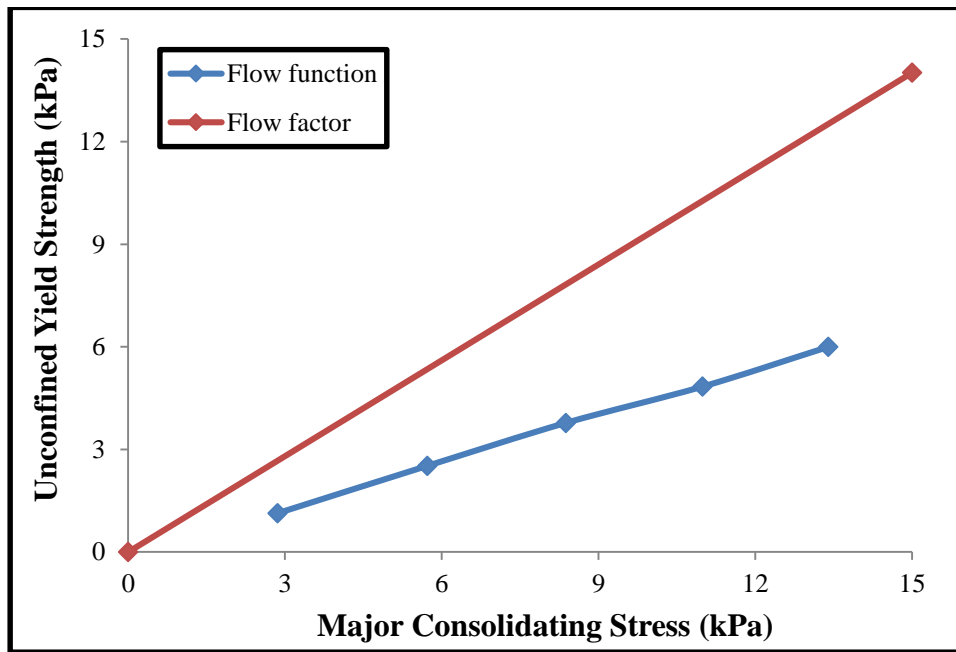


**Figure 4.10: Flow function and flow factor of fraction size 0.25 mm at 16.53% moisture content.**

The non- intersection of the flow function and flow factor lines (leading to design of hopper outlet size to prevent mechanical arching) is in contrast to the results obtained from the flow properties tests, which showed that fractionated ground loblolly pine was cohesive in nature. However, due to the small sizes obtained for the hopper outlets, there is tendency for cohesive arching to occur at the hopper outlet. Even though the hopper outlet sizes were calculated to prevent mechanical arching, the selection of the hopper outlet sizes must be large enough to prevent formation of cohesive arch as well.

#### **4.4.6 Silo wall loads**

Table 4.10 presents the estimated vertical and wall pressure exerted on the cylindrical section and also the initial fill and flow induced pressure exerted on hopper section of the designed silo with a height of 30.48 m (100 feet) and diameter of 15.24 m (50 feet). The wall pressure acting on the cylindrical section of the silo varied between 9.35 and 45.42 kPa while the vertical pressure ranged between 15.34 and 48.91 kPa. The pressures acting on the cylindrical and hopper section of the silo increased with increase in fraction size and decrease in moisture content (Figure 4.11 & 4.12). These results imply that during storage of ground loblolly pine in a storage bin, a large quantity of big particles at lower moisture content will exert more pressure on the cylindrical section of the silo wall.

**Table 4.10: Silo wall loads of fractionated ground loblolly pine.**

Screen Size (mm)	Moisture Content (%)	Cylindrical Section		Hopper section	
		Wall Pressure (kPa)	Vertical Pressure (kPa)	Initial Fill Load(kPa)	Flow Induced Pressure (kPa)
<b>0.05</b>	<b>4.78</b>	21.71	25.07	25.07	41.07
	<b>8.69</b>	18.46	22.59	22.59	36.39
	<b>16.53</b>	14.64	18.87	18.87	30.40
	<b>22.21</b>	9.35	15.34	15.34	24.71
<b>0.25</b>	<b>4.78</b>	28.58	31.33	31.33	50.46
	<b>8.69</b>	23.82	27.57	27.57	44.41
	<b>16.53</b>	19.20	23.02	23.02	37.08
	<b>22.21</b>	13.54	18.47	18.47	29.76
	<b>25.53</b>	10.32	16.16	16.16	26.03
<b>0.50</b>	<b>4.78</b>	32.50	35.35	35.35	56.95
	<b>8.69</b>	29.89	33.75	33.75	54.37
	<b>16.53</b>	21.63	25.82	25.82	41.59
	<b>22.21</b>	16.76	21.84	21.84	35.19
	<b>25.53</b>	13.38	19.25	19.25	31.02
<b>0.71</b>	<b>4.78</b>	39.33	42.72	42.72	68.82
	<b>8.69</b>	32.29	37.64	37.64	60.63
	<b>16.53</b>	24.50	29.52	29.52	47.56
	<b>22.21</b>	19.69	25.13	25.13	40.48
	<b>25.53</b>	16.05	22.73	22.73	36.61
<b>1.00</b>	<b>4.78</b>	41.95	45.67	45.67	73.57
	<b>8.69</b>	35.94	40.75	40.75	65.65
	<b>16.53</b>	27.00	32.67	32.67	52.64
	<b>22.21</b>	22.28	28.86	28.86	46.49
	<b>25.53</b>	19.84	27.45	27.45	44.22
<b>1.40</b>	<b>4.78</b>	45.42	48.91	48.91	78.79
	<b>8.69</b>	39.68	44.41	44.41	71.54
	<b>16.53</b>	28.69	34.55	34.55	55.65
	<b>22.21</b>	24.96	31.70	31.70	51.07
	<b>25.53</b>	23.38	31.33	31.33	50.47
<b>Raw</b>	<b>4.78</b>	42.09	45.86	45.86	73.87
	<b>8.69</b>	39.90	44.75	44.75	72.08
	<b>16.53</b>	25.14	31.72	31.72	51.10
	<b>22.21</b>	22.39	29.55	29.55	47.60
	<b>Raw</b>	20.58	28.84	28.84	46.46

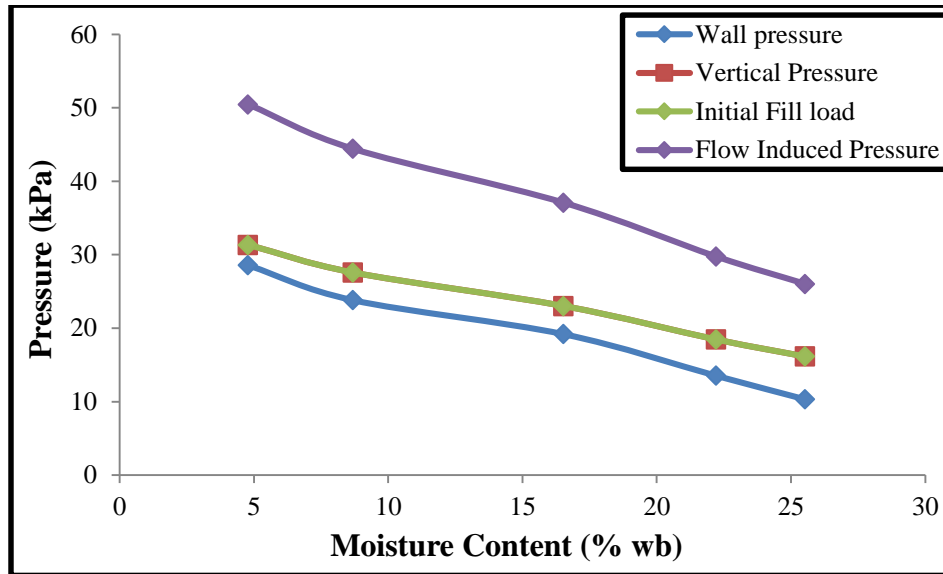


**Figure 4.11: Effect of moisture content on pressures acting on silo wall for 0.25 mm fraction at a wall height of 100 feet (30.48m).**

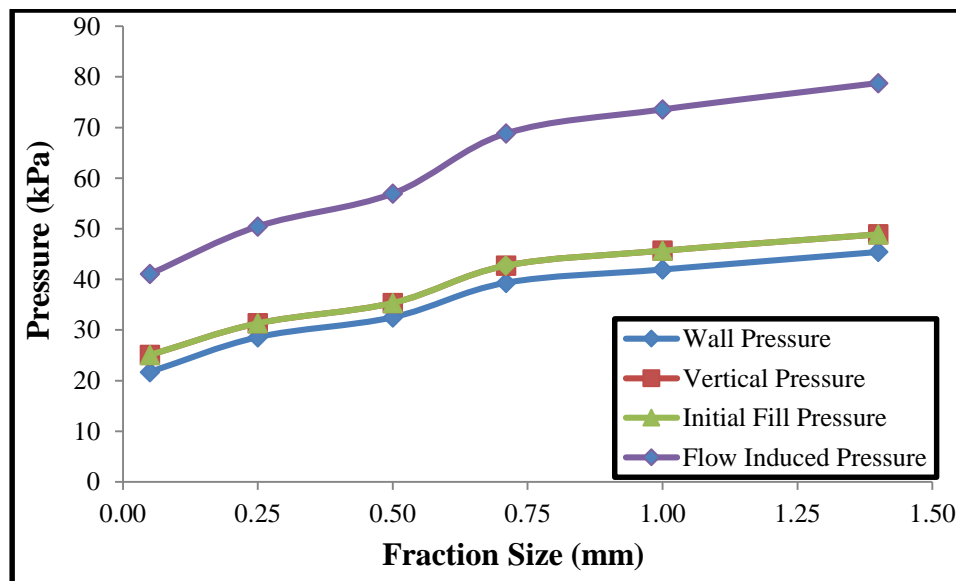
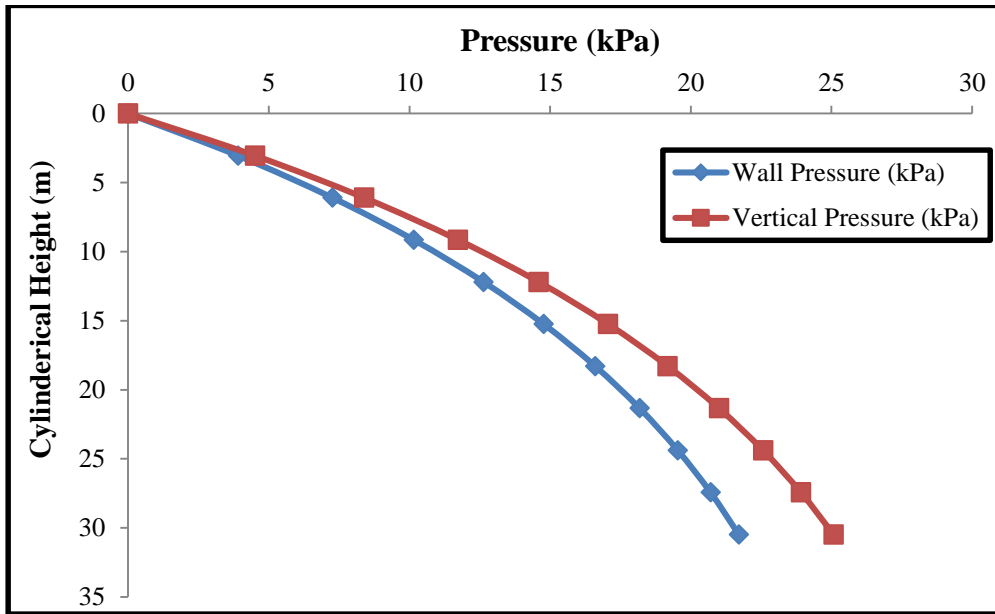


**Figure 4.12: Effect of particle size on pressures acting on the cylindrical and hopper section of the silo wall at a wall height of 100 feet (30.48m).**

Figure 4.13 illustrates the vertical and wall pressure versus the cylindrical height (from top of the silo to the bottom) for the 0.05 mm fractions at the 4.78 % moisture level. The vertical and the wall pressures exerted on the cylindrical section of the silo by the material increased with

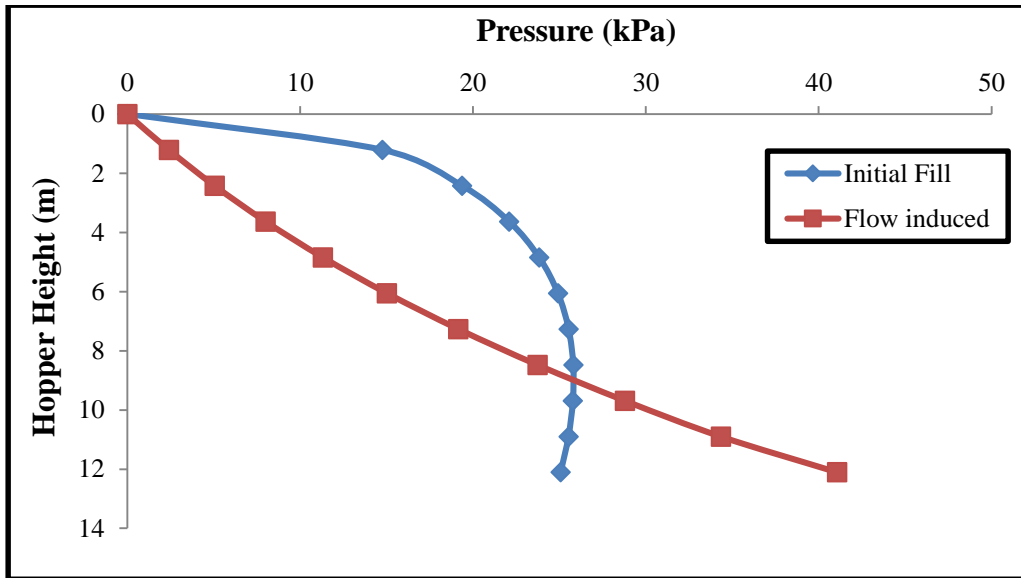
height. These pressures increased downward which indicated that there is a tendency for the silo to expand at the lower part of the silo due to the pressures exerted on the silo wall.

Figure 4.14 shows the change in the initial fill and flow induced pressures as the hopper height changes. The initial and flow induced pressures represent the pressures exerted on the hopper section of the silo when the silo is filled with bulk solid and during discharge respectively. The estimated initial fill and flow induced pressures for the fractionated ground loblolly pines are presented in Table 4.10. The initial fill loads varied between 15.34 and 48.91 kPa while the flow induced pressures varied between 24.71 and 78.79 kPa. The initial fill and flow induced pressures also increased with increase in fraction size and decrease in moisture content. The values obtained for the initial fill and flow induced pressures indicates the estimated peak pressures that can be attained when a silo of height 100 feet (30.48m) and diameter 50 feet (15.24m) is filled to capacity.



**Figure 4.13: Plot of vertical and wall pressure against cylindrical height for the 0.05 mm fraction at 4.78 % moisture level.**





**Figure 4.14: Plot of initial and flow induced loads against hopper height for the 0.05 mm fraction at 4.78 % moisture level.**

The initial fill and flow induced pressures increased as the hopper height increased. However, the initial fill pressure became constant at a certain hopper height. This shows that the pressure exerted on the hopper wall as the silo is filled with material reaches a maximum and remains constant at a certain hopper height.

#### 4.5 Conclusion

The design of a silo bin to allow easy flow of material represents important aspect of bulk solid handling. In this study, the flow properties of fractionated ground loblolly pine were quantified and a sensitivity analysis carried out on the silo design parameters. It was found that;

- The flowability of the fractions increased with increase in fraction size and decrease in moisture content. Dosing of large and small sized fractions resulted in reduced flowability. This result implied that the presence of small particles resulted in reduced flowability. Also, the wall friction properties were found to perform differently using three different wall

surfaces. Stainless steel and mild steel had better performance at lower moisture content while Tivar 88 surface had a good performance at higher moisture content.

- The hopper half angle (varied between  $15.37^{\circ}$  and  $38.44^{\circ}$ ) decreased with increase in moisture content and decrease in fraction size. The minimum hopper outlet sizes ranged from 1.20 to 28.56 mm. The vertical and wall normal pressures acting on the cylindrical section increased with increase in fraction size and decrease in moisture content. The initial fill and flow induced pressure also increased with increase in fraction size and decrease in moisture content.

## **Chapter 5: Summary and Recommendation**

### **5.1 Summary**

Particle size and moisture content contributed significantly to the physical and flow properties of ground loblolly pine. At varying fraction size and moisture content, the physical and flow properties of the fractionated ground loblolly pine was found to behave differently. The bulk and tap densities were found to increase with increase in fraction size while particle density was not significantly affected by fraction size. The porosity, Hausner ratio and compressibility of the fractions were also found to decrease with increase in the size of the fraction. Also, increased moisture content was found to significantly cause a reduction in the densities (bulk, tap and particle) and porosity while it had no significant effect on Hausner ratio and compressibility. Meanwhile, the flowability of the fraction increased with increase in fraction size and reduced moisture content. Dosing of large sized fraction and small sized fraction resulted in reduced flowability. This implies that the presence of small particles results in reduced flowability. Also, wall friction characteristics were found to perform differently. Stainless and mild steel had better performance at lower moisture content while Tivar 88 surface had a consistent and desirable results at different moisture content levels and across the particle sizes. The heating value of the fractions and volatile matter were not significant affected by fraction size. However, the ash content was found to increase with reduction in the size of the fraction. These compositional data are needed to design appropriate biomass conversion systems.

The sensitivity analysis indicated that the flow factor and flow function lines did not intersect and therefore a critical applied stress was not obtained. This implies that the design of the minimum hopper outlet size is to handle mechanical arching. This is in contrast to the flow properties test carried out on the fractions describing the loblolly fraction as a cohesive material.

However, the minimum discharge outlet sizes obtained for the fractions varied from 1.20 to 28.56 mm. This implies that with such minimum hopper outlet size, there is a tendency for cohesive arching to occur during material discharge. The vertical and wall normal pressures acting on the cylindrical section of the silo alongside the initial fill and flow induced pressures increased with increase in fraction size and decrease in moisture content. Also, the pressures increased as the height of the cylindrical and hopper sections increased.

The results obtained from this work shows that an increasing quantity of small sized fractions and moisture content will lead to typical flow problems associated with bulk materials. Therefore, in the design and selection of appropriate storage, handling and transport vessels for ground woody biomass (e.g loblolly pine), it is imperative to understand the proportion of varying sizes of fractions in the bulk material as this tends to significantly influence the physical and flow properties of ground loblolly pine. The design and selection of storage vessels should take into consideration the change in flow problems caused by particle size and moisture content especially in the estimation of hopper outlet size for mass flow in order to prevent cohesive and mechanical arching.

## **5.2 Recommendation and future works**

This work investigated the contribution of particle size and moisture content to the physical and flow properties of fractionated ground loblolly pine. In order to avoid flow problem during unloading of ground loblolly pine from storage vessels, ensuring large particles of sizes 1.40 mm and moisture content range of 4 – 10% (wb) will be appropriate. Also, in the selection of the type of wall lining material to be used for storage vessel, Tivar 88 surface will be desirable because of its low angle of wall friction at all moisture levels and particle sizes.

This research work focused mainly on characterization of the instantaneous physical and flow properties of the fractionated ground loblolly pine. Since there is a time difference between the storage of ground loblolly pine and when it is used, it is recommended that further analysis should be carried out on the effect of storage time (time consolidation) on the physical and flow properties of fractionated ground loblolly pine at different moisture content. Also, in the present study, a dosing experiment of two fractions was only carried out. Therefore, it is recommended that a dosing experiment involving the mixture of varying quantity of each fraction to determine the point at which flowability will change from easy flow to cohesive flow should be conducted.

## References

- Abdullah, E. C., and D. Geldart. 1999. The use of bulk density measurements as flowability indicators. *Powder Technology* 102(2): 151-165.
- Adapa, P. K., G. J. Schoenau, and E. A. Arinze. 2004. Fractionation of alfalfa into leaves and stems using a three pass rotary drum dryer. *Biosystems Engineering* 91(4): 455-463.
- Adapa, P., L. Tabil, G. Schoenau. 2009. Compaction characteristics of barley, canola, oat and wheat straw. *Biosystems Engineering* 104:335 – 344.
- Adapa, P.K., L.G. Tabil and G.J. Schoenau. 2011. Grinding performance and physical properties of non-treated and steam exploded barley, canola, oat and wheat straw. *Journal of Biomass and Bioenergy*, doi:10.1016/j.biombioe.2010.10.004, 35(2011), pp. 549-561.
- ASABE Standards. 2007. S269.4: Definition of methods for determining density, durability and moisture content, ASABE, St. Joseph, MI.
- ASABE Standards. 2008. S319.4: Method of determining and expressing fineness of feed materials by sieving, ASABE, St. Joseph, MI.
- ASABE Standards. 2011. S593.1: Terminology and Definitions for Biomass Production, Harvesting and Collection, Storage, Processing, Conversion and Utilization. ASABE, St. Joseph, MI 49085-9659.
- Austin, L.G. 2002. A treatment of impact breakage of particles. *Powder Technology* 126: 85-90.
- Bahram, H., M.H., Kianmehr, S.R Hassan-Beygi, I., Valaei and H., Alikhani. 2013. Characterizing of Flow Property for Wormy Compost by Using Newest Methods. *World Applied Sciences Journal* 25 (2): 306-313. ISSN 1818-4952.
- Barbosa-Canovas, G.V., E., Ortega-Rivas, P., Juliano, and H., Yan. 2005. Food Powders: Physical properties, processing and functionality. Kluwer Academic Publishers, New York, NY.
- Baker, J.B. and O.G., Langdon. 2013. *Pinus taeda* L.- Loblolly Pine. <http://forestry.about.com/library/silvics/blsilpintae.htm>. Accessed 08/20/2013.
- Benkovic, M. and I. Bauman. 2009. Flow properties of commercial infant formula powders. *World Academy of Science, Engineering and Technology* 30.
- Bernhart, M and O.O. Fasina. 2009. Physical properties and pyrolysis behavior of fractionated poultry litter. *Transactions of the ASABE* 52: 531–538.
- Bhadra, R., K. Muthukumarappan and K.A. Rosentrater. 2009. Flowability properties of commercial Distillers Dried Grains with Solubles (DDGS) *Cereal Chemistry* 86(2):170–180.

Biomass Research and Development Board (BRDB). 2010. Biofuel feedstock logistics: Recommendations for research and commercialization. [http://www.biomassboard.gov/pdfs/biomass\\_logistics\\_2011\\_web.pdf](http://www.biomassboard.gov/pdfs/biomass_logistics_2011_web.pdf).

Bitra, V.S.P., A.R. Womac, N. Chevanan, P.I. Miu, C. Igathinathane, S. Sokhansanj, D.R. Smith. 2009. Direct mechanical energy measures of hammermill comminution of switchgrass, wheat straw, and corn stover and analysis of their particle size distributions. *Powder Technology* 193:32–45.

Bradley, M.S.A, R.J. Berry, R.J. Farnish. 2011. Methods for Design of Hoppers for Reliable Gravity Flow, for Pharmaceutical, Food, Mineral and Other Applications. [www.bulksolids.com](http://www.bulksolids.com).

Bravo-Osuna, I., C. Ferrero, M.R. Jiménez-Castellanos. 2007. Influence of moisture content on the mechanical properties of methyl methacrylate-starch copolymers. *European Journal of Pharmaceutics and Biopharmaceutics* 66: 63-72.

Brennan, J.G., J.R. Butters, N.D. Cowell, and A.E.V. Lilly. 1969. *Food engineering operations*. NY: American Elsevier Publishing Company.

Bridgewater, A.V. (Ed.), 2001. Progress in Thermochemical Biomass Conversion. Blackwell Science, Oxford, pp. 1468–1481.

Buma, T.J. 1971. Free fat in spray dried whole milk 5. Cohesion; determination, influence of particle size, moisture content and free-fat content. *Netherlands Milk and Dairy Journal* 25: 107-122.

Cagli, A.S., B.N. Deveci, C.H. Okutan, D.A.A. Sirkeci and E.Y. Teoman. 2007. Flow property measurement using the Jenike shear cell for 7 different bulk solids. *Proceedings of European Congress of Chemical Engineering (ECCE-6)*.

Carr, R.L. 1965. Evaluating flow properties of solids. *Chemical Engineering* 72:163-168.

CEN/TC 335-WG 2 N94 Final draft. 2003. Solid biofuels - Fuel Specifications and Classes, European Committee for Standardization (ed.), Brussels, Belgium.

Chen, P., Y. Zhulin, X. Shen, and Y. Zhang. 2012. Flow properties of three fuel powders. *Particuology*.10: 438– 443.

Chevananan, N., A.R., Womac, V.S.P., Bitra, D.C., Yoder and S., Sokhansanj. 2009. Flowability parameters for chopped switchgrass, wheat straw and corn stover. *Powder Technology* 193:79-86

Chundawat, S.P.S., B. Venkatesh and B.E. Dale. 2006. Effect of particle size based separation of milled corn stover on AFEX pretreatment and enzymatic digestibility. *Biotechnology and Bioengineering* 92: 219–231.

Colley, Z., Fasina, O.O., Bransby, D. and Lee Y.Y. 2006. Moisture effect on the physical characteristics of switchgrass pellets. *Transactions of the ASABE*. 49(6): 1845-1851.

Cunningham, K., K., Barry and T., Walkingstick. Managing loblolly pine stands ... from A to Z. Agriculture and Natural Resources FSA5023. <http://www.uaex.edu>. Accessed 02/12/2014.

Datta, R., 1981. Energy requirement for lignocellulose pretreatment processes. *Process Biochemistry* 16- 42.

Darby, R. 2001. Chemical Engineering Fluid Mechanics. 2<sup>nd</sup> Edition, Revised and Expanded. Marcel Dekker, Inc. 270 Madison Avenue, New York, NY 10016.

Deshpande, S.D., S. Bal and T.P. Ojha, 1993. Physical properties of soybean. *Journal of Agricultural Engineering Research* 56(2): 89-98.

Dilts, M. D. 2007. Application of the roller mill and hammer mill for biomass fractionation. MS thesis. Ames, Iowa: Iowa State University, Department of Agricultural Engineering.

Drzymala, Z., 1993. Industrial briquetting – fundamentals and methods. *Studies in Mechanical Engineering* Volume 13. PWN-Polish Scientific Publishers, Warszawa.

Duffy, S.P. and V.M. Puri. 1996. Flowability parameters and flow functions for confectionery sugar and detergent powder at two moisture contents. *Applied Engineering in Agriculture* 12(5): 601-606.

Emery, E., J. Oliver, T. Pugsley, J. Sharma and J. Zhou. 2009. Flowability of moist pharmaceutical powders. *Powder Technology* 189: 409-415.

Energy Independence and Security Act (EISA). 2007. Available online: <http://www.energy.wsu.edu/documents/EnergyIndependenceAndSecurityActOf2007.pdf> Accessed on 01/22/ 2014.

Energy Information Administration (EIA). 2008. Annual Energy Outlook 2008. Washington, DC: DOE Energy Information Administration. Available at: <http://www.eia.doe.gov/piaf/aeo/index.html>. Accessed on 05/07/2013.

Energy Information Administration. 2009. Annual energy review Tech. Rep. DOE/EIA-0384(2009) 2010. <http://www.eia.doe.gov/totalenergy/data/annual/pdf/aer.pdf>. Accessed on 05/07/2013.

Energy Information Administration (EIA). 2010. Monthly Energy Review. U.S Department of Energy. Accessed at <http://tonto.eia.doe.gov/FTP/mer/00351005.pdf> on 05/07/2013.

Energy Information Administration (EIA). 2013. Monthly Energy Review February. [www.eia.gov/totalenergy/data/monthly/pdf/sec1\\_7.pdf](http://www.eia.gov/totalenergy/data/monthly/pdf/sec1_7.pdf). Accessed on 01/22/ 2014.



- Enstad, G.G. 1981. A novel theory on the arching and doming in mass flow hoppers. Bergen: The Michelsen Institute. 172p.
- Farhat, A.A. and M. A. Quraishi. 2010. Inhibitive Performance of Gemini Surfactants as Corrosion Inhibitors for Mild Steel in Formic Acid. *Portugaliae Electrochimica Acta* 28(5): 321-335. DOI: 10.4152/pea.201005321.
- Fasina, O.O. and Sokhansanj, S. 1995. Modelling the bulk cooling of alfalfa pellets. *Drying Technology* 13: 1881-1904.
- Fasina, O.O. 2006. Flow and physical properties of switchgrass, peanut hull and poultry litter. *Trans. ASABE* 49:721–728.
- Fasina, O.O. 2007. Physical properties of peanut hull pellets. ASABE Paper No. 076161. St. Joseph, MI: ASABE.
- Fasina, O.O. 2008. Physical properties of peanut hull pellets. *Bioresource Technology* 99:1259–1266.
- Fayed, M.E., and T.S. Skocir. 1997. Mechanical Conveyors: Selection and Operation. Lancaster, Pa.: Technomic Publishing.
- Fitzpatrick, J.J., 2003. Food powder flowability. In: Onwulata, C. (Ed.), Encapsulated and Powdered Foods. Taylor and Francis Group, New York, NY, pp. 247–260.
- Fitzpatrick, J. J. 2005. Food powder flowability, In *Encapsuled and powdered foods*, C. Onwulata, Ed. Boca Raton: CRC Press, pp. 247-258.
- Fitzpatrick, J.J., T. Iqbal, C. Delaney, T. Twomey, and M.K. Keogh. 2004. Effect of powder properties on the flowability of milk powders with different fat contents. *Journal of Food Engineering* 64(4): 435–444.
- Fitzpatrick, J.J., S.A. Barringer, T. Iqbal. 2004. Flow property measurement of food powders and sensitivity of Jenike's hopper design methodology to the measured values. *Journal of Food Engineering* 61: 399–405.
- Fitzpatrick, J.J. and L. Ahrne. 2005. Food powder handling and processing: Industry problems, knowledge barriers and research opportunities. *Chem Eng Proc.* 44(2): 209–214.
- Fitzpatrick, J. J. 2007. Particle properties and the design of solid food particle processing operations. *Trans IChemE, Part C, Food and Bioproducts Processing.* 85(4):308–314.
- Freeman, R. 2007. Measuring the flow properties of consolidated, conditioned and aerated powders — A comparative study using a powder rheometer and a rotational shear cell. *Powder Technology* 174: 25–33.

- Ganesan, V., K.A. Rosentrater, K. Muthukumarappan. 2009. Physical and Flow Properties of Regular and Reduced Fat Distillers Dried Grains with Solubles (DDGS). *Food Bioprocess Technology* 2:156–166. DOI 10.1007/s11947-007-0026-x.
- García, R., C. Pizarro, A.G. Lavín and J.L. Bueno. 2012. Characterization of Spanish biomass wastes for energy use. *Bioresource Technology* 103: 249–258.
- Geldart, D., N. Harnby, and A.C. Wong. 1984. Fluidization of cohesive powder. *Powder Technology* 37: 25-37.
- Gil, M., I. Arauzo, E. Teruel, C. Bartolome. 2012. Milling and handling Cynara Cardunculus L. for use as solid biofuel: Experimental tests. *Biomass and Bioenergy* 41: 145-156.
- Gil, M., D. Schott, I. Arauzo, E. Teruel. 2013. Handling behavior of two milled biomass: SRF poplar and corn stover. *Fuel Processing Technology* 112: 76–85.
- Günen, A., M.S. Karakas, B. Kurt, A. Çalik. 2014. Corrosion behavior of borided AISI 304 austenitic stainless steel. *Anti-Corrosion Methods and Materials* 61(2): 112 – 119.
- Gray, K.A., L.S. Zhao and M. Emptage. 2006. Bioethanol. *Current Opinion in Chemical Biology* 10 (2): 141–146.
- Grafton, M.C.E., I.J. Yule, C.E. Davies, J.R. Jones. 2009. Comparative study of the cohesive properties of commercial agricultural crushed limestones of New Zealand. ASABE Paper number 096346.
- Greene, D., S. Baker, B. Mendell, A.H. Lang. 2011. Integrating woody biomass into the U.S. South wood supply chain. 34th Council on Forest Engineering, June 12-15, 2011, Quebec City (Quebec).
- Guo, Q., X. Chen, H. Liu. 2012. Experimental research on shape and size distribution of biomass particle. *Fuel*. 94:551-555.
- Hargreaves, K., M. Zielinska, and S. Cenkowski. 2010. Flowability of Distiller's Spent Grains Processed with Air and Superheated Steam Drying. ASABE Paper number MBSK10-503.
- Holdich, R.G. 2002. Fundamentals of Particle Technology. Midland Information Technology and Publishing, Leicestershire, UK. www.midlandit.co.uk. ISBN 0-9543881-0-0.
- Igathinathane, C., A.R. Womac, S. Sokhansanj, S. Narayan. 2009. Size reduction of high- and low-moisture corn stalks by linear knife grid system. *Biomass Bioenergy* 33: 547–557.
- Ileleji, K. and K. Rosentrater. 2008. On the physical properties of distillers dried grains with solubles (DDGS). ASABE Paper Number: 084576.
- Ileleji, K.E., K.S. Prakash, R.L. Strohshine and C.L. Clementson. 2007. An Investigation of

Particle Segregation in Corn Processed Dried Distillers Grains with Solubles (DDGS) induced by Three Handling Scenarios. *Bulk Solids & Powder - Science & Technology* 2: 84 – 94.

Iqbal, T and J.J. Fitzpatrick. 2006. Effect of storage conditions on the wall friction characteristics of three food powders. *Journal of Food Engineering* 72: 273–280.

Jannasch, R., Y. Quan, R. Samson. 2001. Final Report: A Process and energy analysis of pelletizing switchgrass. Resource efficient agricultural production (REAP-Canada), Ste. Anne de Bellevue, OC, Canada, Available at: <http://www.reap-canada.com/library.htm>.

Janssen, H.A. Getreidedruck in Silozellen, Z. Ver. Dt. Ing. 39 (1895), pp. 1045-1049.

Jenike, A. W. 1964. Storage and flow of solids. Bulletin No. 123. Bulletin of the University of Utah. Salt Lake City: Utah Engineering Station.

Jenike, A. W. 1970. Storage and flow of solids. Bulletin No. 123. Bulletin of the University of Utah. Salt Lake City: Utah Engineering Station. (Revised edition).

Jenkins, B.M., L.L., Baxter, T.R., Miles Jr., and T.R., Miles. 1998. Combustion properties of biomass. *Fuel Processing Technology* 54: 17–46.

Johanson, J. R. 1978. Know your material—How to predict and use the properties of bulk solids. *Chemical Engineering*.

Johanson, J.R. 2002. Troubleshooting bins, hoppers and feeders. *Chemical Engineering Progress* 24–36.

Kashaninejad, M., M. Ahmadi, A. Daraei, D. Chabra. 2008. Handling and frictional characteristics of soybean as a function of moisture content and variety. *Powder technology* 188: 1-8.

Kibar, H., T. Öztürk and B. Esen. 2010. The effect of moisture content on physical and mechanical properties of rice (*Oryza sativa* L.). *Spanish Journal of Agricultural Research* 8(3): 741-749.

Kirtay, E. 2011. Recent advances in production of hydrogen from biomass. *Energy Conversion Management* 52:1778-1789.

Knowlton, T.M., J.W. Carson, G.E. Klinzing and W.C. Yang. 1994. The importance of storage, transfer and collection. *Chemical Engineering Progress* 90(4): 44–54.

Krantz, M., H. Zhang, and J. Zhu. 2009. Characterization of powder flow: Static and dynamic testing. *Powder Technology*. 194: 239–245.

Kumar, P., D.M. Barrett, M.J. Delwiche, and P. Stroeve. 2009. Methods of pretreatment of lignocellulosic biomass for efficient hydrolysis and biofuel production. *Industrial and Engineering Chemistry Research* 48: 3713–3729.

Lam, P.S., S. Sokhansanj, X. Bi, S. Mani, A.R. Womac, M. Hoque, J. Peng, T. JayaShankar, L.J. Naimi, S. Narayan. 2007. Physical Characterization of Wet and Dry Wheat Straw and Switchgrass – Bulk and Specific Density. Paper No. 076058. ASABE, St. Joseph, Michigan.

Lam, P.S., S. Sokhansanj, X. Bi, C.J. Lim, L.J. Naimi, M. Hoque, S. Mani, A.R. Womac, X.P. Ye, S. Narayan. 2008. Bulk density of wet and dry wheat straw and switchgrass particles. *Applied Engineering in Agriculture* 24: 351–358.

Leaver, R. H. 1985. Pelleting dies: Characteristics and selection. *Sprout-Waldron Feed Pointers* 26:1-6.

Littlefield, B., O.O. Fasina, J. Shaw, S. Adhikari and B. Via. 2011. Physical and flow properties of pecan shells—Particle size and moisture effects. *Powder Technology* 212: 173–180.

Littlefield, B. 2010. Characterization of pecan shells for value-added applications. Master’s Thesis submitted to The Graduate School, Auburn University, Auburn, AL.

Liu, K.S. 2008. Particle size distribution of distillers dried grains with solubles (DDGS) and relationships to compositional and color properties. *Bioresource Technology* 99: 8421–8428.

Liu, L.X., I. Marziano, A.C. Bentham, J.D. Litster, E.T. White and T. Howes. 2008. Effect of particle properties on the flowability of ibuprofen powders. *International Journal of Pharmaceutics* 362: 109-117.

Lopo, P., 2002. The right grinding solution for you: roll, horizontal or vertical. *Feed Management* 53: 6–23.

MacBain, R. 1966. *Pelleting Animal Feed*. Arlington, Va.: American Feed Manufacturers Association.

Mani, S., L. Tabil, and S. Sokhansanj. 2004. Grinding performance and physical properties of wheat and barley straws, corn stover and switchgrass. *Biomass Bioenergy*. 27: 339-352.

Mani, S., L.G. Tabil, S. Sokhansanj. 2006. Effects of compressive force, particle size and moisture content on mechanical properties of biomass pellets from grasses. *Biomass Bioenergy*. 30:648–654.

Manickam, I.N. and S.R. Suresh. 2011. Effect of moisture content and particle size on bulk density, porosity, particle density and coefficient of friction of coir pith. *International Journal of Engineering Science and Technology* 3: 2596-2602. ISSN: 0975-5462.

Marinelli, J and J.W. Carson. 1992. Solve solids flow problems in bins, hoppers, and feeders. *Chemical Engineering Progress* 88:22-28.

Maynard, E. 2013. Ten steps to an effective bin design. *American Institute of Chemical Engineers (AIChE)*. [www.aiche.org/cep](http://www.aiche.org/cep).

McGlinchey, D. 2005. Bulk property characterization. In: McGlinchey, D. (Ed.), *Characterization of Bulk Solids*. CRC Press, New York, NY, pp. 48–84.

McKendry, P. 2002. Energy production from biomass (part 2): conversion technologies. *Bioresource Technology* 83(1):47-54.

McMullen, J., O.O. Fasina, C.W. Wood, Y. Feng. 2005. Storage and handling characteristics of pellets from poultry litter. *Applied Engineering in Agriculture* 21: 645-651.

Merrow, E. W. 1988. Estimating Startup Times for Solids-Processing Plants. *Chemical Engineering Journal*: 89.

Miao, Z., T.E. Grift, A.C. Hansena, and K.C. Ting. 2011. Energy requirement for comminution of biomass in relation to particle physical properties. *Industrial Crops and Products* 33:504–513.

Miu P.I., R. Alvin, C. Igathinathane, and S. Sokhansanj. 2006. Analysis of biomass comminution and Separation, Processes in Rotary Equipment – A Review, ASABE paper no. 066169. St. Joseph, Mich.: ASABE.

Moriarty, P. and D. Honnery. 2008. Low-mobility: the future of transport. *Futures*. 40 (10): 865–872.

Molenda, M., M.D. Montross, J. Horabik, and I.J. Ross. 2002. Mechanical properties of corn and soybean meal. *Transactions of ASAE* 45(6): 1929-1936.

Munsell, J.F. and T.R. Fox. 2010. An analysis of the feasibility for increasing woody biomass production from pine plantations in the southern United States. *Biomass Bioenergy*. 34(12):1631-1642.

Naimi, L.J., S. Sokhansanj, S. Mani, et al. 2006. Cost and performance of woody biomass size reduction for energy production. CSBE/SCGAB Paper No. 06-107. 13p.

Newman, A.W. 1995. Micromeritics. In: Brittain, H.G. (Ed.), *Physical Characterization of Pharmaceutical Solids*. Marcel Dekker Inc., New York, NY, pp. 253–280.

Nimkar, P.M. and P.K. Chattopadhyay, 2001. Some physical properties of green gram. *Journal of Agricultural Engineering Research* 80(2): 183-189.

Nokhodchi, A. 2005. An overview of the effect of moisture on compaction and compression. *Pharmaceutical Technology* 46-66.

OECD/IEA. 2010. Sustainable Production of Second-Generation Biofuels: Potential and perspectives in major economies and developing countries. *Information paper*. Anselm Eisentraut.

- Opalinski, I., M. Chutkowski, M. Stasiak. 2012. Characterising moist food-powder flowability using Jenike shear tester. *Journal of Food Engineering* 108:51-58.
- Ortega-Rivas, E. 2003. Review and research trends in food powder processing. *Powder Handling and Processing* 15(1): 18-25.
- Ortega-Rivas, E. 2009. Bulk properties of food particulate materials: an appraisal of their characterisation and relevance in processing. *Food Bioprocess Technology* 2:28–44. DOI 10.1007/s11947-008-0107-5.
- Ozbay N., A.E. Putun, B.B. Uzun and E. Putun. 2001. Biocrude from biomass: pyrolysis of cotton seed cake. *Renewable Energy* 24:615-625.
- Pabis, S., Jayas, D.S., Cenkowski, S., 1998. Grain Drying: Theory and Practice. John Wiley & Sons, Inc., New York, NY.
- Peleg, M. 1977. Flowability of food powders and methods for its evaluation— A review. *Journal of Food Process Engineering* 1:303-328.
- Peleg, M., C.H. Manheim, and N. Passy. 1973. Flow properties of some food powders. *Journal of Food Science* 38(6): 959–963.
- Peleg, M. and M.R. Moreyra. 1979. Effect of moisture on the stress relaxation pattern of compacted powders. *Powder Technology* 23(2): 277–279.
- Perlack, R. D and B. J. Stokes. 2011. U.S. Billion-Ton Update: Biomass supply for a bioenergy and bioproducts industry. Tech. Rep. ORNL/TM-2011/224, Oak Ridge National Laboratory. [http://www1.eere.energy.gov/biomass/pdfs/billion ton update.pdf](http://www1.eere.energy.gov/biomass/pdfs/billion_ton_update.pdf). p.227.
- Prescott, J.K., D.A. Ploof, and J.W. Carson. 1999. Developing a better understanding of wall friction. *Powder Handling and Processing*. 19–26.
- Prescott, J. K., and R.A. Barnum. 2000. On powder flowability. *Pharmaceutical Technology* 60-84.
- Probst, K. V., R. P. K. Ambrose, R. L. Pinto, R. Bali, P. Krishnakumar, K. E. Ileleji. 2013. The effect of moisture content on the grinding performance of corn and corncobs by hammermilling. *Transactions of the ASABE* 56(3): 1025-1033.
- Puri, V. M. 2002. Characterizing powder flowability. *Chemical Processing* 65(1): 39-42.
- Purutyan, H., B.H. Pittenger, and J.W. Carson. 1998. Solve solids handling problems by retrofitting. *Chemical Engineering Progress*. 27–39.
- Purutyan, H., R. Barnum and M. Schimmelpfennig. 2001. Fuel handling consideration when switching to PRB coal. *Power* 53- 64. [www.platts.com/engineering](http://www.platts.com/engineering).

- Ramavath, P., M. Swathi, M. Buchi Suresh, R. Johnson. 2013. Flow properties of spray dried alumina granules using powder flow analysis technique. *Advanced Powder Technology* 24: 667-673.
- Ranney, J. W., J. L. Trimble, L. L. Wright and R. D. Perlack. 1985. Short-rotation woody crops production research in the south. In: *Proceedings of the 3rd Southern Biomass Energy Research Conference*, Gainesville, Fla, USA.
- Rennie, P.R, X.D. Chen, C. Hargreaves, A.R. Mackereth. 1999. A study of the cohesion of dairy powders. *Journal of Food Engineering* 39: 277-284.
- Rhodes, M. 1998. Introduction to particle technology. John Wiley and Sons, New York, 320 pp.
- Roberts, A. W. 1994. Developments in silo design for the safe and efficient storage and handling of grain. Proceedings of the 6th International Working Conference on Stored-Product Protection.
- Rosentrater, K.C., D. Subramanian, P.G. Krishnan. 2006. Fractionation techniques to concentrate nutrient streams in distillers grains. ASABE Meeting Presentation Paper Number: 066166.
- Rotter, J.M. 2001. Guide for the economic design of circular metal silos. Spon Press, Taylor and Francis group, London and New York. 235p.
- Rupar, K. and M. Sanati. 2004. The release of terpenes during storage of biomass. *Biomass and Bioenergy* 28(1): 29–34.
- SAS. 2010. SAS Users' Guide. SAS Institute Inc., Cary, NC.
- Saxena, R.C., D.K. Adhikari, and H.B. Goyal. 2009. Biomass-based energy fuel through biochemical routes: A review. *Renewable and Sustainable Energy Reviews* 13:167–178.
- Schell, D.J., and C. Harwood. 1994. Milling of lignocellulosic biomass: results of pilot scale testing. *Applied Biochemistry and Biotech* 45(46): 159–168.
- Schwedes, J. 2003. Review on testers for measuring flow properties of bulk solids. *Granular Matter*. 5:1-43.
- Schulze, D. 1996. Measuring powder flowability: A comparison of test methods. *Powder Bulk Engineering* 45–61.
- Schulze, D. 2006. Storage of powders and bulk solids in silos. Available at <http://www.dietmerschulze.de/storagepr.html>. Dietmar Schulze: Wolfenbüttel, Germany.
- Schulze, D. 2008. Powders and bulk solids: behavior, characterization, storage and flow. ISBN 978-3-540-73767-4 Springer Berlin Heidelberg New York. p 42.

- Shamlou, P. A. 1988. Handling of bulk solids—theory and practice. London, UK: Butterworths.
- Simmons, B. A., D. Loque, and H. W. Blanch. 2008. Next-generation biomass feedstocks for biofuel production. *Genome Biology* 9(12):9.
- Sokhansanj, S. and J. Fenton. 2006. Cost benefit of biomass supply and pre-processing, BIOCAP research integration program synthesis paper. Ottawa, Canada: BIOCAP Canada Foundation.
- Sokhansanj, S. and J.R. Hess. 2009. Biomass Supply Logistics and Infrastructure. *Biofuels Methods in Molecular Biology*. 58:1-25.
- Teunou, E. and J.J. Fitzpatrick. 1999. Effect of relative humidity and temperature on food powder flowability. *Journal of Food Engineering* 42:109–116.
- Teunou, E., J.J., Fitzpatrick, and E.C., Synnott. 1999. Characterization of food powder flowability. *Journal of Food Engineering* 39:31–37.
- Thomson, F.M. 1997. Storage and flow of particulate solids. In Fayed, M.E. and Otten, L. Handbook of Powder Science and Technology, Chapman and Hall, New York, pp. 389-436
- The United States Pharmacopeia (USP). 1995. *The National Formulary, USP23/NF18*; United States Pharmacopeial Convention, Inc.: Rockville, MD, USA.
- The United States Pharmacopeia. 2011. Bulk Density and Tapped Density of Powders. The United States Pharmacopeia Convention, Inc.: Rockville, MD, USA.
- Tomas, J. and D. Schubert. 1979. Particle characterization. Proc. of Partec 79, Nuremberg, Germany. 301-319.
- Tumuluru, J.S., L.G. Tabil, Y. Song, K.L. Iroba and V. Meda. 2014. Grinding energy and physical properties of chopped and hammer-milled barley, wheat, oat, and canola straws. *Biomass and Bioenergy* 60: 58-67.
- US Department of Energy. 1993. Assessment of costs and benefits of flexible and alternative fuel use in the US transportation sector. In: Evaluation of a Wood-to-Ethanol Process. Technical Report No. 11, DOE/EP-0004. US Department of Energy, Washington, DC.
- U.S. Energy Information Administration (EIA). 2014. Monthly Energy Review, February. [www.eia.gov/totalenergy/data/monthly/pdf/mer.pdf](http://www.eia.gov/totalenergy/data/monthly/pdf/mer.pdf).
- van der Stelt, M.J.C., H. Gerhauser, J.H.A. Kiel, K.J. Ptasinski. 2011. Biomass upgrading by torrefaction for the production of biofuels: A review. *Biomass Bioenergy*. 35: 3748-3762
- Velan, B. 2012. Selecting in-plant bulk handling systems and equipment. [www.bulk-solids-handling.com](http://www.bulk-solids-handling.com).



Verlinden, A. 2000. Experimental assessment of shear testers for measuring flow properties of bulk solids, PhD-Thesis, Univ. of Bradford, UK.

Weber, M.W., D.K. Hoffman and C.M. Hrenya .2004. Discrete particle simulations of cohesive granular flow using a square-well potential. *Granular Matter* 6(4): 239-254

Wei, L., L.O. Pordesimo, C. Igathinathane, and W.D. Batchelor. 2009. Process engineering evaluation of ethanol production from wood through bioprocessing and chemical catalysis. *Biomass Bioenergy* 33:255–266.

Werther, J., M. Saenger, E.U. Hartge, T. Ogada, and Z. Siagi. 2000. Combustion of agricultural residues. *Prog. Energ. Combust.* 26:1-27.

Williams, T. M., and C. A. Gresham. 2006. Biomass accumulation in rapidly growing loblolly pine and sweetgum. *Biomass and Bioenergy* 30(4):370-377.

White, E.M. 2010. Woody biomass for bioenergy and biofuels in the United States—a briefing paper. *General Technical Report PNW-GTR-825*. 45 p.

White, P. 2013. Biomass Energy. <http://pdsblogs.org/chargerapes713/tag/renewables/>. Accessed 11/01/2013

Womac, A. 2005. Integrated size reduction and separation to pre-fractionated biomass. In: Proceedings of the DOE/USDA Biomass Feedstock Gate Review Meeting.

Woodcock, C. R. and J. S. Mason. 1987. Bulk Solids Handling: An Introduction to the Practice and Technology. New York, N. Y.: Chapman and Hall

World Health Organization. 2012. S.3.6. Bulk density and tapped density of powders. Final text for addition to The International Pharmacopoeia. Document QAS/11.450 FINAL. March 2012

Wu, M.R., D.L. Schott, G. Lodewijks. 2011. Physical properties of solid biomass. *Biomass and Bioenergy* 35: 2093-2105

Yang, W., S. Sokhansanj, W.J. Crerer and S. Rohani. 1996. Size and shape related characteristics of alfalfa grind. *Canadian Agricultural Engineering* 38: 201– 205.

Zhang, M., X. X. Song, Z. J. Pei, and D. H. Wang. 2010. Effects of mechanical comminution on enzymatic conversion of cellulosic biomass in biofuel manufacturing: a review. In: *Proceedings of the ASME International Conference on Manufacturing Science and Engineering*, Erie, Pa, USA. Zhu, J. Y., G.S. Wang, X.J. Pan and R. Gleisner. 2009. Specific surface to evaluate the efficiencies of milling and pretreatment of wood for enzymatic saccharification. *Chemical Engineering Science* 64:474–485.

Zhou, B., K. Ileleji, and G. Ejeta. 2008. Physical property relationships of bulk corn stover particles. *Transaction of the ASABE*. 51(2): 581-590.

Zhou, J. and K. Komvopoulos. 2005. Wear Mechanisms of Untreated and Gamma Irradiated Ultra-High Molecular Weight Polyethylene for Total Joint Replacements. *Journal of Tribology* 127: 273-279.

Zulfiqar, M., B. Moghtaderi, T.F. Wall. 2006. Flow properties of biomass and coal blends. *Fuel Processing Technology* 87: 281–288.

## Appendix A

**Table A.1: Symbols and Nomenclatures**

Symbols	Nomenclature	Unit
$\rho_p$	Particle Density	kg/m <sup>3</sup>
$\rho_b$	Bulk Density	kg/m <sup>3</sup>
$\rho_T$	Tap Density	kg/m <sup>3</sup>
$FF$	Flow function	-
$FI$	Flow index	-
$\varphi_w$	Angle of wall friction	Degree
$\delta$	Angle of internal friction	Degree
$\alpha$	Hopper half angle	Degree
$\beta$	Characteristic of the material/wall relationship	Degree
$D_{min}$	Minimum hopper outlet size	m
$H(\alpha)$	Empirical factor depend on shape of hopper and hopper angle	-
$\sigma_c$	Critical applied stress	Pa
$P_w$	Wall pressure on the cylindrical portion of the silo	Pa
$P_v$	Vertical pressure on the cylindrical portion of the silo	Pa
$g$	Acceleration due gravity	m/s <sup>2</sup>
$\mu_h$	Hopper wall friction coefficient	-
$K$	Pressure coefficient	-
$H$	Height of the cylindrical portion of the silo	m
$\mu$	Wall friction coefficient for the hopper	-
$P_{nf}$	Normal pressure on hopper wall while filling	Pa
$P_{vf}$	Mean vertical stress in the silo at the transition after filling	Pa
$P_{ne}$	Normal pressure on hopper wall while emptying	Pa
$P_{ve}$	Mean vertical stress in the silo at the transition after emptying	Pa
$ff$	Flow factor	-

## ANOVA results

**Table B.1: ANOVA result of particle size and moisture effect on particle density of fractionated ground loblolly pine**

---

The GLM Procedure

Dependent Variable: PD

Source	DF	Sum of Squares	Mean Square	F Value	Pr > F
Model	33	83672.22520	2535.52198	57.95	<.0001
Error	68	2975.26000	43.75382		
Corrected Total	101	86647.48520			

R-Square	Coeff Var	Root MSE	PD Mean
0.965662	0.457950	6.614667	1444.407

Source	DF	SS	Mean Square	F Value	Pr > F
PS	6	9909.45586	1651.57598	37.75	<.0001
MC	4	62010.71172	15502.67793	354.32	<.0001
PS*MC	23	11752.05762	510.95903	11.68	<.0001

---

**Table B.2: ANOVA result of particle size and moisture effect on bulk density of fractionated ground loblolly pine**

---

The GLM Procedure

Dependent Variable: BD

Source	DF	Sum of Squares	Mean Square	F Value	Pr > F
Model	33	189319.0971	5736.9423	1164.84	<.0001
Error	68	334.9062	4.9251		
Corrected Total	101	189654.0033			

R-Square	Coeff Var	Root MSE	BD Mean
0.998234	1.064513	2.219255	208.4761

Source	DF	SS	Mean Square	F Value	Pr > F
PS	6	148915.5648	24819.2608	5039.35	<.0001
MC	4	37276.7487	9319.1872	1892.19	<.0001
PS*MC	23	3126.7836	135.9471	27.60	<.0001

---

**Table B.3: ANOVA result of particle size and moisture effect on tap density of fractionated ground loblolly pine**

The GLM Procedure						
Dependent Variable: TD						
Source	DF	Sum of Squares	Mean Square	F Value	Pr > F	
Model	33	153584.7941	4654.0847	469.55	<.0001	
Error	68	674.0000	9.9118			
Corrected Total	101	154258.7941				
	R-Square	Coeff Var	Root MSE	TD Mean		
	0.995631	1.141295	3.148296	275.8529		
Source	DF	SS	Mean Square	F Value	Pr > F	
PS	6	100864.2775	16810.7129	1696.04	<.0001	
MC	4	48920.4694	12230.1174	1233.90	<.0001	
PS*MC	23	3800.0472	165.2194	16.67	<.0001	

**Table B.4: ANOVA result of particle size and moisture effect on compressibility of fractionated ground loblolly pine**

The GLM Procedure						
Dependent Variable: Compressibility						
Source	DF	Sum of Squares	Mean Square	F Value	Pr > F	
Model	33	3837.140392	116.276982	36.41	<.0001	
Error	68	217.173333	3.193725			
Corrected Total	101	4054.313725				
	R-Square	Coeff Var	Root MSE	Compressibility Mean		
	0.946434	7.382317	1.787100	24.20784		
Source	DF	SS	Mean Square	F Value	Pr > F	
PS	6	3029.655059	504.942510	158.10	<.0001	
MC	4	429.032254	107.258063	33.58	<.0001	
PS*MC	23	378.453079	16.454482	5.15	<.0001	

**Table B.5: ANOVA result of particle size and moisture effect on Hausner ratio of fractionated ground loblolly pine**

---

The GLM Procedure

Dependent Variable: HR

Source	DF	Sum of Squares	Mean Square	F Value	Pr > F
Model	33	1.38885502	0.04208652	38.91	<.0001
Error	68	0.07354733	0.00108158		
Corrected Total	101	1.46240235			
	R-Square	Coeff Var	Root MSE	HR Mean	
	0.949708	2.474156	0.032887	1.329235	
Source	DF	SS	Mean Square	F Value	Pr > F
PS	6	1.07234157	0.17872359	165.24	<.0001
MC	4	0.15379908	0.03844977	35.55	<.0001
PS*MC	23	0.16271437	0.00707454	6.54	<.0001

---

**Table B.6: ANOVA result of particle size and moisture effect on porosity of fractionated ground loblolly pine**

---

The GLM Procedure

Dependent Variable: Porosity

Source	DF	Sum of Squares	Mean Square	F Value	Pr > F
Model	33	0.09110681	0.00276081	1003.67	<.0001
Error	68	0.00018705	0.00000275		
Corrected Total	101	0.09129386			
	R-Square	Coeff Var	Root MSE	Porosity Mean	
	0.997951	0.193844	0.001659	0.855599	
Source	DF	SS	Mean Square	F Value	Pr > F
PS	6	0.07559100	0.01259850	4580.06	<.0001
MC	4	0.01367591	0.00341898	1242.94	<.0001
PS*MC	23	0.00183990	0.00008000	29.08	<.0001

---

**Table B.7: ANOVA result of particle size and moisture effect on angle of internal friction of fractionated ground loblolly pine**

---

The GLM Procedure

Dependent Variable: Internal\_friction

Source	DF	Sum of Squares	Mean Square	F Value	Pr > F
Model	33	4909.529588	148.773624	69.32	<.0001
Error	476	1021.613333	2.146246		
Corrected Total	509	5931.142922			
	R-Square	Coeff Var	Root MSE	Internal_friction Mean	
	0.827754	3.117284	1.465007	46.99627	
Source	DF	SS	Mean Square	F Value	Pr > F
Particle_size	6	2380.074955	396.679159	184.82	<.0001
Moisture	4	2191.393605	547.848401	255.26	<.0001
Particle_si*Moisture	23	338.061029	14.698306	6.85	<.0001

---

**Table B.8: ANOVA result of particle size and moisture effect on cohesion of fractionated ground loblolly pine**

---

The GLM Procedure

Dependent Variable: Cohesion

Source	DF	Sum of Squares	Mean Square	F Value	Pr > F
Model	33	16.79996855	0.50908996	4.07	<.0001
Error	476	59.48413173	0.12496666		
Corrected Total	509	76.28410028			
	R-Square	Coeff Var	Root MSE	Cohesion Mean	
	0.220229	50.26351	0.353506	0.703306	
Source	DF	SS	Mean Square	F Value	Pr > F
Particle_size	6	13.96265015	2.32710836	18.62	<.0001
Moisture	4	1.33298185	0.33324546	2.67	0.0318
Particle_si*Moisture	23	1.50433655	0.06540594	0.52	0.9681

---

**Table B.9-1: ANOVA result of particle size and moisture effect on angle of wall friction of fractionated ground loblolly pine using stainless steel**

---

The GLM Procedure

Dependent Variable: Stainless

Source	DF	Sum of Squares	Mean Square	F Value	Pr > F
Model	33	52568.53652	1592.98596	417.67	<.0001
Error	2516	9595.99760	3.81399		
Corrected Total	2549	62164.53412			
	R-Square	Coeff Var	Root MSE	Stainless Mean	
	0.845635	12.85727	1.952944	15.18941	
Source	DF	SS	Mean Square	F Value	Pr > F
Particle_size	6	3182.27183	530.37864	139.06	<.0001
Moisture	4	46157.07183	11539.26796	3025.51	<.0001
Particle_si*Moisture	23	3229.19286	140.39969	36.81	<.0001

---

**Table B.9-2: ANOVA result of particle size and moisture effect on angle of wall friction of fractionated ground loblolly pine using mild steel**

---

The GLM Procedure

Dependent Variable: Mildsteel

Source	DF	Sum of Squares	Mean Square	F Value	Pr > F
Model	33	30789.45774	933.01387	350.22	<.0001
Error	2516	6702.77707	2.66406		
Corrected Total	2549	37492.23481			
	R-Square	Coeff Var	Root MSE	Mildsteel Mean	
	0.821222	10.70273	1.632195	15.25027	
Source	DF	SS	Mean Square	F Value	Pr > F
Particle_size	6	532.79849	88.79975	33.33	<.0001
Moisture	4	28973.33199	7243.33300	2718.91	<.0001
Particle_si*Moisture	23	1283.32725	55.79684	20.94	<.0001

---



**Table B.9-3: ANOVA result of particle size and moisture effect on angle of wall friction of fractionated ground loblolly pine using Tivar 88 surface**

The GLM Procedure					
Dependent Variable: TIVAR					
Source	DF	Sum of Squares	Mean Square	F Value	Pr > F
Model	33	4169.265400	126.341376	57.05	<.0001
Error	2516	5572.281067	2.214738		
Corrected Total	2549	9741.546467			
	R-Square	Coeff Var	Root MSE	TIVAR Mean	
	0.427988	11.65509	1.488200	12.76867	
Source	DF	SS	Mean Square	F Value	Pr > F
Particle_size	6	3206.808280	534.468047	241.32	<.0001
Moisture	4	260.570614	65.142653	29.41	<.0001
Particle_si*Moisture	23	701.886506	30.516805	13.78	<.0001

**Table B.10: ANOVA result of particle size effect on volatile matter (% db) of fractionated ground loblolly pine**

The GLM Procedure					
Dependent Variable: matter					
Source	DF	Sum of Squares	Mean Square	F Value	Pr > F
Model	5	17.57471921	3.51494384	1.24	0.3502
Error	12	34.04084058	2.83673671		
Corrected Total	17	51.61555979			
	R-Square	Coeff Var	Root MSE	matter Mean	
	0.340493	1.964800	1.684261	85.72176	
Source	DF	SS	Mean Square	F Value	Pr > F
size	5	17.57471921	3.51494384	1.24	0.3502

**Table B.11: ANOVA result of particle size effect on energy content of fractionated ground loblolly pine**

---

The GLM Procedure

Dependent Variable: energy\_content

Source	DF	Sum of Squares	Mean Square	F Value	Pr > F
Model	5	1.08365667	0.21673133	1.28	0.3361
Error	12	2.03869333	0.16989111		
Corrected Total	17	3.12235000			
	R-Square	Coeff Var	Root MSE	Mean	
	0.347064	2.214783	0.412178	18.61033	
Source	DF	SS	Mean Square	F Value	Pr > F
sample	5	1.08365667	0.21673133	1.28	0.3361

---

**Table B.12: ANOVA result of particle size effect on ash content (% db) of fractionated ground loblolly pine**

---

The GLM Procedure

Dependent Variable: content

Source	DF	Sum of Squares	Mean Square	F Value	Pr > F
Model	5	12.55626822	2.51125364	286.03	<.0001
Error	12	0.10535626	0.00877969		
Corrected Total	17	12.66162447			
	R-Square	Coeff Var	Root MSE	content Mean	
	0.991679	10.83524	0.093700	0.864771	
Source	DF	Type I SS	Mean Square	F Value	Pr > F
size	5	12.55626822	2.51125364	286.03	<.0001

---

**Table B.13: Effect of wall surface on angle of wall friction at 4.78% moisture level.**

Screen size (mm)	Type of Wall Materials		
	Stainless steel	Mild steel	Tivar 88
<b>0.05</b>	12.30 <sup>[b]</sup> ± 1.28	12.33 <sup>[b]</sup> ± 1.10	14.80 <sup>[a]</sup> ± 1.71
<b>0.25</b>	9.83 <sup>[c]</sup> ± 0.52	10.48 <sup>[b]</sup> ± 0.45	13.61 <sup>[a]</sup> ± 1.09
<b>0.50</b>	9.45 <sup>[c]</sup> ± 0.50	10.50 <sup>[b]</sup> ± 0.39	12.48 <sup>[a]</sup> ± 0.87
<b>0.71</b>	9.39 <sup>[c]</sup> ± 0.49	10.54 <sup>[b]</sup> ± 0.35	12.10 <sup>[a]</sup> ± 0.98
<b>1.00</b>	9.49 <sup>[c]</sup> ± 0.50	10.81 <sup>[b]</sup> ± 0.36	11.59 <sup>[a]</sup> ± 0.87
<b>1.40</b>	8.96 <sup>[b]</sup> ± 0.38	10.76 <sup>[a]</sup> ± 0.31	10.88 <sup>[a]</sup> ± 0.96
<b>Raw</b>	9.53 <sup>[c]</sup> ± 0.53	10.55 <sup>[b]</sup> ± 0.37	11.75 <sup>[a]</sup> ± 0.90

Superscripts shows comparison of means using Tukey test at  $\alpha < 0.05$  significant level  
 Values across the row with the same letter are not significantly different

**Table B.14: Effect of wall surface on angle of wall friction at 8.69% moisture level.**

Screen size (mm)	Type of Wall Materials		
	Stainless steel	Mild steel	Tivar 88
<b>0.05</b>	14.9 <sup>[b]</sup> ± 2.05	16.10 <sup>[a]</sup> ± 2.63	15.54 <sup>[a,b]</sup> ± 2.25
<b>0.25</b>	12.39 <sup>[b]</sup> ± 1.27	13.11 <sup>[a]</sup> ± 1.21	13.48 <sup>[a]</sup> ± 1.31
<b>0.50</b>	11.24 <sup>[c]</sup> ± 0.90	12.09 <sup>[b]</sup> ± 0.72	12.87 <sup>[a]</sup> ± 1.07
<b>0.71</b>	12.72 <sup>[a]</sup> ± 1.48	12.17 <sup>[b]</sup> ± 0.71	12.32 <sup>[a,b]</sup> ± 1.03
<b>1.00</b>	11.44 <sup>[b]</sup> ± 1.00	12.43 <sup>[a]</sup> ± 0.76	11.72 <sup>[b]</sup> ± 0.97
<b>1.40</b>	10.82 <sup>[c]</sup> ± 0.97	12.38 <sup>[a]</sup> ± 0.59	11.47 <sup>[b]</sup> ± 1.15
<b>Raw</b>	10.92 <sup>[c]</sup> ± 1.27	12.16 <sup>[b]</sup> ± 0.92	14.07 <sup>[a]</sup> ± 1.35

Superscripts shows comparison of means using Tukey test at  $\alpha < 0.05$  significant level  
 Values across the row with the same letter are not significantly different

**Table B.15: Effect of wall surface on angle of wall friction at 16.53%moisture level.**

Screen size (mm)	Type of Wall Materials		
	Stainless steel	Mild steel	Tivar 88
<b>0.05</b>	17.14 <sup>[a]</sup> ± 2.75	15.22 <sup>[b]</sup> ± 1.72	14.52 <sup>[b]</sup> ±1.79
<b>0.25</b>	14.00 <sup>[a]</sup> ± 1.54	14.29 <sup>[a]</sup> ± 1.32	13.14 <sup>[b]</sup> ± 1.28
<b>0.50</b>	13.79 <sup>[b]</sup> ± 1.43	15.07 <sup>[a]</sup> ± 1.36	12.83 <sup>[c]</sup> ± 1.12
<b>0.71</b>	14.22 <sup>[b]</sup> ± 1.47	15.31 <sup>[a]</sup> ± 1.34	12.01 <sup>[c]</sup> ± 1.05
<b>1.00</b>	14.40 <sup>[b]</sup> ± 1.38	15.01 <sup>[a]</sup> ± 1.34	11.24 <sup>[c]</sup> ± 0.99
<b>1.40</b>	14.18 <sup>[a]</sup> ± 1.31	14.22 <sup>[a]</sup> ± 1.14	11.61 <sup>[b]</sup> ± 1.02
<b>Raw</b>	16.23 <sup>[c]</sup> ± 2.21	14.53 <sup>[b]</sup> ± 1.30	12.17 <sup>[a]</sup> ± 1.30

Superscripts shows comparison of means using Tukey test at  $\alpha < 0.05$  significant level  
 Values across the row with the same letter are not significantly different

**Table B.16: Effect of wall surface on angle of wall friction at 22.21% moisture level.**

Screen size (mm)	Type of Wall Materials		
	Stainless steel	Mild steel	Tivar 88
<b>0.05</b>	26.49 <sup>[a]</sup> ± 4.61	21.38 <sup>[b]</sup> ± 3.15	15.50 <sup>[c]</sup> ± 2.64
<b>0.25</b>	19.50 <sup>[a]</sup> ± 2.64	18.12 <sup>[b]</sup> ± 2.08	13.33 <sup>[c]</sup> ± 1.70
<b>0.50</b>	17.60 <sup>[a]</sup> ± 1.96	18.18 <sup>[a]</sup> ± 1.70	12.36 <sup>[b]</sup> ± 1.35
<b>0.71</b>	16.72 <sup>[b]</sup> ± 1.73	17.42 <sup>[a]</sup> ± 1.58	12.02 <sup>[c]</sup> ± 1.58
<b>1.00</b>	17.35 <sup>[a]</sup> ± 1.83	17.99 <sup>[a]</sup> ± 1.53	12.81 <sup>[b]</sup> ± 1.89
<b>1.40</b>	16.52 <sup>[b]</sup> ± 1.65	18.00 <sup>[a]</sup> ± 1.42	12.44 <sup>[c]</sup> ± 1.74
<b>Raw</b>	18.13 <sup>[b]</sup> ± 1.85	19.04 <sup>[a]</sup> ± 1.77	14.45 <sup>[c]</sup> ± 2.28

Superscripts shows comparison of means using Tukey test at  $\alpha < 0.05$  significant level  
 Values across the row with the same letter are not significantly different

**Table B.17: Effect of wall surface on angle of wall friction at 25.53% moisture level.**

Screen size (mm)	Type of Wall Materials		
	Stainless steel	Mild steel	Tivar 88
<b>0.25</b>	24.80 <sup>[a]</sup> ± 3.96	22.56 <sup>[b]</sup> ± 3.42	15.23 <sup>[c]</sup> ± 2.46
<b>0.50</b>	21.62 <sup>[a]</sup> ± 2.80	19.52 <sup>[b]</sup> ± 2.55	13.06 <sup>[c]</sup> ± 1.64
<b>0.71</b>	20.98 <sup>[a]</sup> ± 2.58	19.73 <sup>[b]</sup> ± 2.28	11.76 <sup>[c]</sup> ± 1.47
<b>1.00</b>	20.06 <sup>[a]</sup> ± 2.51	18.87 <sup>[b]</sup> ± 2.18	11.46 <sup>[c]</sup> ± 1.40
<b>1.40</b>	18.76 <sup>[a]</sup> ± 2.05	18.30 <sup>[a]</sup> ± 1.90	10.98 <sup>[b]</sup> ± 1.32
<b>Raw</b>	20.56 <sup>[a]</sup> ± 2.54	19.39 <sup>[b]</sup> ± 2.29	12.55 <sup>[c]</sup> ± 1.58

Superscripts shows comparison of means using Tukey test at  $\alpha < 0.05$  significant level  
 Values across the row with the same letter are not significantly different

## Appendix B: SAS codes for statistical analysis

```
/*Importing files for physical properties*/
proc import datafile = 'C:\Users\ojo0002\Dropbox\Final_arrangement.xlsx'
out = properties DBMS=EXCEL Replace;
Getnames= yes;
SCANTEXT=YES;
USEDATE=YES;
SCANTIME=YES;
Range = 'physical$A1:H103';
Run;

/*ANOVA test on physical properties using GLM*/
proc glm data = properties;
class ps mc;
model PD BD TD Compressibility HR Porosity= ps mc ps*mc;
means ps mc ps*mc/tukey;
run;

/*ANOVA test of particle size effect on physical properties using GLM*/
proc glm data = properties;
class ps mc;
model PD BD TD Compressibility HR Porosity= ps;
means ps/tukey;
by mc;
run;

/*Data sorting for effect of Moisture content on physical properties*/
proc sort data = properties
Out = sortedproperties;
by ps;
run;

/*ANOVA test of moisture content effect on physical properties using GLM*/
proc glm data = sortedproperties;
class ps mc;
model PD BD TD Compressibility HR Porosity= mc;
means mc/tukey;
by ps;
run;

/*Analysis for internal friction and cohesion*/
proc import datafile = 'C:\Users\ojo0002\Dropbox\Final_arrangement.xlsx'
out = cohesion DBMS=EXCEL Replace;
Getnames= yes;
SCANTEXT=YES;
USEDATE=YES;
SCANTIME=YES;
Range = 'Angleofinternalfriction$A1:d511';
Run;

/*General ANOVA test on internal friction and cohesion*/
proc glm data = cohesion;
class Particle_size Moisture;
model internal_friction Cohesion = Particle_size|Moisture;
```

```

means Particle_size|Moisture/tukey;
run;

/*Effect of particle size on internal friction and cohesion*/
proc glm data = cohesion;
class Particle_size Moisture;
model internal_friction Cohesion = Particle_size;
means Particle_size/tukey;
by moisture;
run;

/*Sorting data for effect of moisture content*/
proc sort data = cohesion
    Out = sortedcohesion;
    by Particle_size;
run;

/*Effect of moisture content on internal friction and cohesion*/
proc glm data = sortedcohesion;
class Particle_size Moisture;
model internal_friction Cohesion = Moisture;
means moisture/tukey;
by Particle_size;
run;

/*Analysis for wall friction*/
proc import datafile = 'C:\Users\ojo0002\Dropbox\Final_arrangement.xlsx'
out = WF DBMS=EXCEL Replace;
Getnames= yes;
SCANTEXT=YES;
USEDATE=YES;
SCANTIME=YES;
Range = 'Angleofwallfriction$A1:e2551';
Run;

/*General ANOVA test on angle of wall friction*/
proc glm data = WF;
class Particle_size Moisture;
model Stainless Mildsteel TIVAR =Particle_size|Moisture;
means Particle_size|Moisture/tukey;
run;

/*Effect of particle size on angle of wall friction*/
proc glm data = WF;
class Particle_size Moisture;
model Stainless Mildsteel TIVAR =Particle_size;
means Particle_size/tukey;
by Moisture;
run;

/*Sorting data for effect of moisture content on wall friction*/
proc sort data = WF
Out = sortedWF;
    by Particle_size;
run;
proc print data = sortedWF;run;

```

```

/*Effect of moisture content on angle of wall friction*/
proc glm data = sortedWF;
class Particle_size Moisture;
model Stainless Mildsteel TIVAR =Moisture;
means Moisture/tukey;
by Particle_size;
run;

/*Effect of wall material on angle of wall friction*/
proc import datafile = 'C:\Users\ojo0002\Dropbox\Final_arrangement.xlsx'
out = wall_type DBMS=EXCEL Replace;
Getnames= yes;
SCANTEXT=YES;
USEDATE=YES;
SCANTIME=YES;
Range = 'MC4.78$A2:f1352';
Run;

/*Sorting data for effect of wall material on wall friction*/
proc sort data = wall_type
Out = sortedwall_type;
by Particle_size;
run;

/*General ANOVA test on wall material*/
proc glm data = sortedwall_type;
class Particle_size material;
model MC5 MC9 MC15 MC20 = material;
means material/tukey;
by Particle_size;
run;

/*Volatile matter*/
data volatile;
input size matter;
datalines;
2.14 84.84118783
2.14 85.15598639
2.14 85.17072722
1.54 84.83283142
1.54 84.77222336
1.54 85.13296634
1.28 85.30450814
1.28 84.72281068
1.28 85.30450814
0.97 85.72084866
0.97 90.99627324
0.97 85.70658378
0.81 85.34423753
0.81 84.87114629
0.81 89.82996463
0.15 84.97309511
0.15 84.97309511
0.15 85.33875314
;
run;
proc glm data = volatile;

```



```

class size;
model matter = size;
means size/tukey;
run;

proc means data =volatile;
var matter;
class size;
run;

*Ash content of fraction;
data ash;
input size content;
datalines;
2.14 0.217727694
2.14 0.326916507
2.14 0.217080337
1.54 0.217944338
1.54 0.217511479
1.54 0.218596866
1.28 0.541742825
1.28 0.677109678
1.28 0.691328245
0.97 0.426178823
0.97 0.554948894
0.97 0.391909849
0.81 0.938467972
0.81 0.92103963
0.81 1.077430782
0.15 2.45407148
0.15 2.721530982
0.15 2.754333398
; run;
proc glm data = ash;
class size;
model content = size;
means size/tukey;
run;

proc means data =ash;
var content;
class size;
run;

/*Energy content*/
data energy;
input sample energy_content;
datalines;
1.40 18.101
1.40 18.514
1.40 18.618
1.00 18.614
1.00 18.623
1.00 18.798
0.71 18.532
0.71 18.663
0.71 18.710

```

```
0.50 18.802
0.50 17.149
0.50 18.816
0.25 18.639
0.25 18.559
0.25 18.710
0.24 19.019
0.24 19.081
0.24 19.038
;
run;
proc glm data = energy;
class sample;
model energy_content = sample;
means sample/tukey;
run;
```